Molecular and Elemental Mass Spectrometric Approaches for Monitoring Oxidation Processes in Proteins

Dissertation

zur Erlangung des akademischen Grades

doctor rerum naturalium

(Dr. rer. nat.)

im Fach Chemie

eingereicht an der

Mathematisch-Naturwissenschaftlichen Fakultät I

der Humboldt-Universität zu Berlin

von

Mona Moustafa Sharar, M.Sc. Chemie

Präsidentin der Humboldt-Universität zu Berlin

Prof. Dr.-Ing. Dr. Sabine Kunst

Dekan der Mathematisch-Naturwissenschaftlichen Fakultät

Prof. Dr. Elmar Kulke

Gutachter :

1. Prof. Dr. Michael W. Linscheid.
2. Prof. Dr. Maria Montes-Bayón.
3. PD Dr. Michael G. Weller.

Tag der mündlichen Prüfung: 04. Oktober 2017

Acknowledgement

When there are no words and thanks sufficient to count blessings, comes the thank of Allah. Foremost all thanks to Allah for granting me this success …

I am especially indebted to Prof. Dr. Ulrich Panne and Prof. Dr. Janina Kneipp for providing me a protected academic time to pursue the goals of my life career ...

I would like to acknowledge my supervisors Prof. Dr. Michael Linscheid and Prof. Dr. Maria Montes-Bayón for giving me the chance to fulfill my desire to obtain a PhD degree in Chemistry and for contributing to the completion of this project .Thank you for believing in me and for being a source of inspiration, wisdom and supervision. Your encouragement, continuous support, patience and guidance helped me in the research time and in the writing of this thesis. I would like to extend my gratitude to Prof. Dr. Michael Linscheid for giving me the chance to work under the international umbrella of his group and to be a part of Prof. Dr. Maria Montes-Bayón group in Oviedo/Spain. Special thanks goes for Dr. Diego Esteban-Fernández, Dr. Ahmed El-Khatib, Dr. Georg Kubsch, Angelika Woyda, Dr. Petra Esperling, Dr. Sebastian Beck, David Benda, René Becker, Sabrina Trog, Stefanie Ickert, Pablo Lores Lareo and all the team members in Germany, thanks for every single person worked hard to support the group and believed in sharing his time and experience.

I would like to express my special appreciation to Prof. Dr. Maria Montes-Bayón for hosting me in Oviedo/ Spain. Thank you for allowing me to be a part of your team, for the knowledge you transferred to me and for making me feel that I'm in my second homeland. My deepest appreciation is directed to Prof. Dr. Elisa Blanco González, Prof. Dr. Jörg Bettmer, Mario Corte Rodriguez, Javier Alonso-García, Jenifer García, Roberto Álvarez-Fernández García, Dr. Tamara Iglesias, Dani Fernández and Nere Fernández, I could never ask for a better family, thank you for everything...

A very special gratitude goes out to Mrs. Katharina Schultens for her support that made my career goals work actively and for being a source of strength in all the hard times. I am deeply grateful for SALSA (School of Analytical sciences in Adlershof) team for their continuous work and support. Special thanks goes for Mrs. Katharina Gliege, thank you for your hard work and assistance .I would like to extend my gratitude for Prof. Dr. Ilko Bald for his supervision during the summer school and his administrative help.

My deepest appreciation goes to Prof. Dr. Michael Weller, Prof. Dr. Rüdiger Tiemann and prof. Dr. Christian Hackenberger for being in my exam committee. Thank you for giving me from your time and experience, your valuable comments will enrich my work and add significant values to my knowledge.

Thanks to my family and every single one of my friends in Jordan, Spain and Berlin, words are not enough to thank you for lighting my way and helping me through hard moments.

Finally, this research would not have been possible without the financial support of the DFG (German Research Foundation).I acknowledge SALSA graduate program and BAM (Bundesanstalt fur Materialforschung und -prufung) for funding through the scholarship.

Summary

Oxidative transformation of cysteine thiol group into different functional groups is considered a significant posttranslational modification (PTM) of great importance to pathological and physiological processes. Cysteine sulfenic acid residue (SA) is the transient state for thiol group oxidation; it can react with free thiols to form disulfide bonds or can be further oxidized with reactive oxygen species (ROS) to form sulfinic and sulfonic acids.

As any disturbance in the cellular reduction-oxidation (redox) balance is correlated to age-related diseases such as cancer and Alzheimer's disease, the detection of SA transient state formed a sensor for such redox-mediated events that reveals the status of the biological system and in turn can prevent further oxidative damage of cells and tissues. Whereas only any small change in the quantity of proteins, as well as the formed PTMs, can provide deeper insights into the status of the biological system, quantitative analysis should be carried out to reveal the status of the system as qualitative analysis is not sufficient in this regard.

On the other hand, the technological advances, in particular the separation techniques and mass spectrometry (MS), allowed the development of several approaches for the comprehensive assessment of proteome analysis. Liquid chromatography (LC) techniques and LC coupled to MS has emerged as a feasible alternative for qualitative characterization of complex mixtures, whereas the development of the soft ionization techniques such as electrospray (ESI) allowed MS to cover most of the qualitative and quantitative aspects of the proteomic studies along with the element- selective inductively coupled plasma mass spectrometry (ICP-MS) that can be emerged to have reliable and less complex quantitative data.

Herein, we provide a new strategy for the highly sensitive and specific detection of SA using alkyne β-ketoester (KE) previously linked to a lanthanide (Ln)-containing chelator (Ln-DOTA, where DOTA is 1,4,7,10-tetraazacyclododecane-1,4,7,10- tetraacetic acid). As a proof of concept, SA was generated by hydrogen peroxide (H_2O_2) in different peptide sequences to mimic the oxidative events produced in living cells by ROS and was detected by the prepared compound Ln-DOTA-KE. Molecular mass spectrometry (ESI-MS) and ICP-MS have been used to monitor the formation of SA linked to Ln-DOTA-KE.

The developed strategy has been further applied to the determination of SA-induced formation in human serum by using affinity chromatography for purification of albumin followed by ICP-MS to monitor the formed SA linked to Ln-DOTA-KE in combination with isotope dilution analysis (IDA) for the absolute quantification. Quantitative results showed levels of oxidative damage regarding SA formation in human serum up to 40% of the albumin present.

Zusammenfassung

Molekular und Element Massenspektrometrische Ansätze zur Untersuchung von Oxidation Prozessen in Proteinen

Die oxidative Transformation der Thiol-Gruppe des Cysteins in verschiedene andere funktionelle Gruppen wird als sehr wichtige posttranslationale Modifikation (PTM) angesehen, mit weitreichenden Auswirkungen in physiologischen und pathologischen Vorgängen. Cysteinsulfensäure (SA) ist eine Zwischenstufe der Thiol-Oxidation: Sie kann entweder mit freien Thiolen reagieren, um Disulfide zu bilden oder durch reaktive Sauerstoffspezies (reactiveoxygenspecies, ROS) weiter oxidiert werden.

Jede Störung des zellulären Redox-Haushalts wird mit altersbedingten Erkrankungen wie Krebs oder Alzheimer Verbinndung gebracht, daher stellt die Überwachung des SA-Spiegels einen vielversprechenden Wegdar, den Status dieses Redox-Haushalts festzustellen und so mögliche oxidative Schäden zu vermeiden. Da bereits kleinste Änderungen der Proteinmengen und PTMs tiefe Einblicke in den Zustand des biologischen Systems liefern können, ist eine quantitative Bestimmung von großer Bedeutung.

Technologische Fortschritte im Bereich der Trennungsmethoden und Massenspektrometrie (MS) erlaubten die Entwicklung umfassender Möglichkeiten in der Protein-Analytik. Flüssigkeitschromatographie gekoppelt mit Massenspektrometrie (LC-MS) stellt eine praktikable Möglichkeit der qualitativen Untersuchung komplexer Mischungen dar. Die Entwicklung weicher Ionisationsmethoden wie Elektronenspray-Ionisation (ESI) ermöglicht darüber hinaus, mit Massenspektrometrie die meisten qualitativen und quantitativen Aspekte der Proteomik abzudecken. Kombiniert mit elementspezifischer Massenspektrometrie mit induktiv gekoppeltem Plasma (ICP-MS) können weniger komplexe und gut reproduzierbare Daten gesammelt werden.

In dieser Arbeit wurde eine neue, hochsensitive und selektive Methode zur Detektion von SA entwickelt. Dafür wurde ein Alkin-β-Ketoester (KE) an einen Lanthanid-haltigen (Ln) Chelatkomplex (1,4,7,10-Tetraazacyclododecane-1,4,7,10- tetraacetat, DOTA) gebunden. Zum Nachweis des Funktionsprinzips wurden, mittels H_2O_2, Sulfensäuren in verschiedenen Peptidsequenzen erzeugt, um die in biologischen Systemen durch ROS hervorgerufenen Oxidationen nachzustellen. Diese Sulfensäuren wurden anschließend durch den Ln-DOTA-KE-Komplex gebunden. Die Bildung dieser SA-Ln-DOTA-KE-Einheit wurde mittels ESI-MS und ICP-MS nachverfolgt.

Die entwickelte Methode wurde weiterhin auf die Bestimmung von SA-Bildung in humanem Serum angewandt, humanes Serumalbumin wurde angereichert via Affinitätschromatographie. ICP-MS diente erneut der Bestimmung der SA-Ln-DOTA-KE-Einheit, durch Kombination mit einer Isotopenverdünnungsanalyse (IDA) wurde eine absolute Quantifizierung durchgeführt. Die Ergebnisse zeigen oxidative Schäden bis zu 40 % des vorhandenen Albumins.

List of Figures

List of Tables

Index

1. Introduction

1.1. Proteomics: an overview

1.1.1. Proteomics

The suffix -*omics* has found great popularity in biological research and is given to any large-scale of study that addresses the objects in different fields such as genomics (genes), transcriptomics (mRNA), proteomics (proteins) and metabolomics (metabolites)[1].

Genomics is a field of science that is concerned with studying the genetic material; whereas a genome represents the complete set of DNA, genomics field is concerned with the structure, function, evolution and genome mapping. However, proteins, were found to be responsible for the variations in cellular structure and function as they continuously change in response to internal and external events, but in all human cells , except mutations and red blood cells, the same complete genome is present[2]. As a consequence, the study of genomes was found to be insufficient for studying the complexity and diversity of the biological system[3,4].

Therefore "The entire PROTEin complement expressed by a genOME", proteomics, was introduced in 1995 as a field that covers and investigates the entire set of proteins produced or modified in an organism or a system[5].

As the expression, regulation and post-translational modifications (PTMs) of proteins are responsible for the vast diversity in the structure and function of human cells and organs, the study of these dynamics became vital in order to have better understanding for the cellular events in normal and disease states and to help in the development of new treatment strategies[6].

The fatal Bovine Spongiform Encephalopathy (BSE) (mad cow disease) is a striking example on the involvement of protein structure in the development of disease states, where the infectious agent is a naturally occurring protein in a misfolded form called *Prion*. In 1997 the Noble Prize discovery in Medicine that was awarded to Stanley B. Prusiner addressed the entrance of prions to healthy organisms where they triggers the transformation of an existing protein to the misfolded form (Figure 1).The accumulation of this misfolded form of proteins was found to be responsible for the disruption of tissue structure and thus the fatal symptoms of the disease[7,8,9].

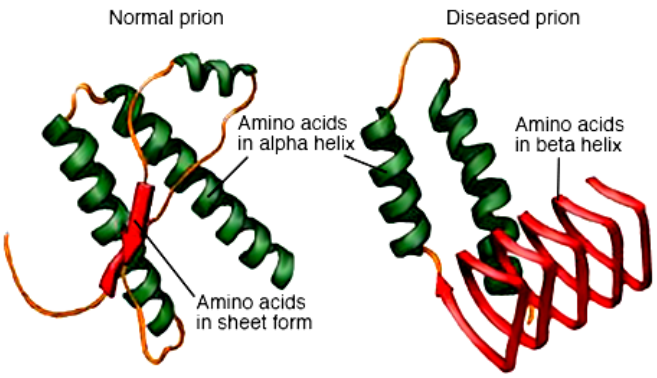

Figure 1.Normal and diseased "misfolded" prion protein. Prions are naturally occurring proteins in the brains of humans and animals. Normally, these proteins are harmless until they are misfolded. (Adapted from: Mayo Foundation for Medical Education and Research).

Therefore, proteomics provided an interdisciplinary domain that benefited in the study of the entire set of proteins that are produced or modified in the biological system and helped in understanding the proteome dynamic and complex nature resulting from PTMs and molecular interactions, where as a consequence different disease states can be explored and appropriate medications can be developed.

1.1.2. Significance of post-translational modifications (PTMs)

A significant difference between genomes and proteins is that post- translational modifications (PTMs) form a key mechanism for the increase in proteomic diversity. Human genome is estimated to include between 20,000 and 25,000 genes[10], while the total number of proteins in the human proteome is estimated to be over 1 million(Figure 2) [11].

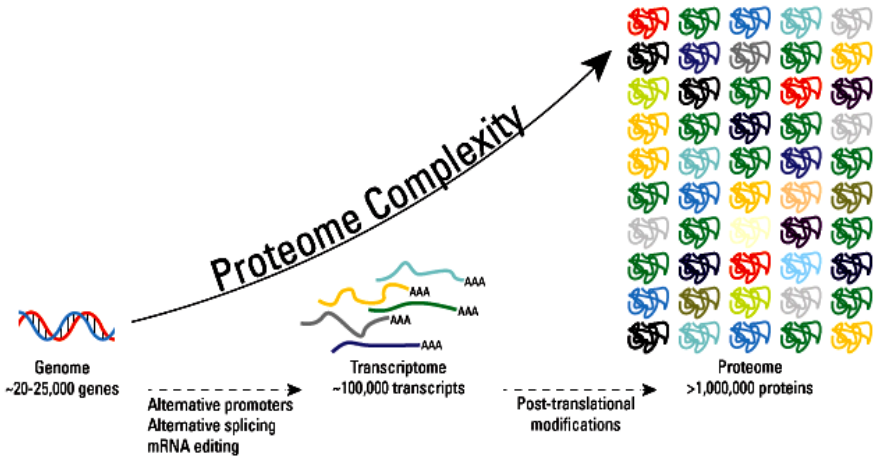

Figure 2.Proteome enormous complexity owing to post-translational modifications (PTMs). The proteome encompass over 1 million proteins forming exponential increase in complexity compared to genome~20-25,000 genes and transcriptome~100,000 transcripts. (Adapted from: Thermo Fisher Scientific).

PTMs increase the functional diversity by the covalent addition of different functional groups or proteins, these modifications, include for example, phosphorylation, methylation, disulfide bond formation and cysteine oxidation. These modifications on the amino acid residues in peptides and proteins alter their properties, which in turn, leading in turn to an enormous number of potential molecular states[12,13].

The importance of PTMs derived from their role in functional proteomics as they are involved in the different regulation activity, localization and interaction with other biological molecules including proteins, nucleic acids, lipids, and cofactors. Therefore, understanding, identifying and quantifying PTMs illustrate a major challenge in the study and the diagnose of cell biology[13]. PTMs detection is usually challenging as it is hindered by many factors including the stability of PTMs, lack of suitable methodologies, sample complexity, and low abundance of PTMs [14].

As numerous types of protein oxidative PTMs modifications were addressed in the biological system and were connected to different disease states, herein, cysteine oxidative modification and the formation, detection and quantification of cysteine sulfenic acid shall be intensively discussed as it was tackled in this work.

Sulfenation as PTM

Sulfur containing proteins are the most sensitive targets for oxidation. Methionine, cysteine, homocysteine and taurine are the most common sulfur- containing amino acids, but only methionine and cysteine are incorporated into proteins and they play an important role in the living organisms[15].

Cysteine and methionine residues (Figure 3) are sensitive to oxidation by almost all forms of reactive oxygen species (ROS). Therefore, these amino acids play a significant role in the antioxidative defense; where under mild conditions with the presence of reactive species host, cysteine residues form disulfide bridges and methionine residues are converted into methionine sulfoxide residues[16].

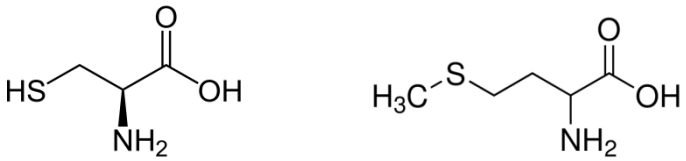

A **B**

Figure 3. Sulfur containing amino acids, A- Cysteine , sulfur atom appears on its side, and B- Methionine, sulfur atom attached to a methyl group.

However, the high reactivity for the sulfur atom in cysteine residue and it's capability on the covalent interactions with other thiols (-SH) and low molecular weight residues such as glutathione, have attributed several unique features for cysteine as having significant role in catalytic, regulatory, structure-stabilizing and cofactor-binding[17].

Additionally, cysteine thiol groups exist as thiolate anion ($Cys\text{-}S^-$) at physiological pH and are more susceptible to oxidation compared with the protonated cysteine thiol (Cys–SH) [18]. During redox signaling, ROS oxidizes the thiolate anion to the sulfenic form (Cys–SOH, SA), causing allosteric changes within the protein that alter its function, whereas higher levels of ROS further oxidize thiolate anions to sulfinic (SO_2H) or sulfonic (SO_3H) (Figure 4). Such oxidative modifications to cysteine can be involved in redox-based homeostasis and defense mechanisms [19,20], however, the excessive formation of such PTMs was connected to disease states (such as cancer, Alzheimer's and Parkinson's diseases)and cell damage[21,22].

Specifically, sulfenic acid (SA) formation is reversible where it can be reduced back with low molecular weight thiols such as glutathione or another cysteine residue. Thus, the short living SA can serve as a sensor that follows the initiation of changes in oxidation state where developing strategies for the fast and specific capture of SA group can provide an early marker for the cellular oxidative events[21].

As in this work protein oxidation is defined as the modification induced directly by ROS , and in turn these oxidative events serve as markers for assessing the oxidative stress *in vivo*, special consideration will be given to the term "oxidative stress".

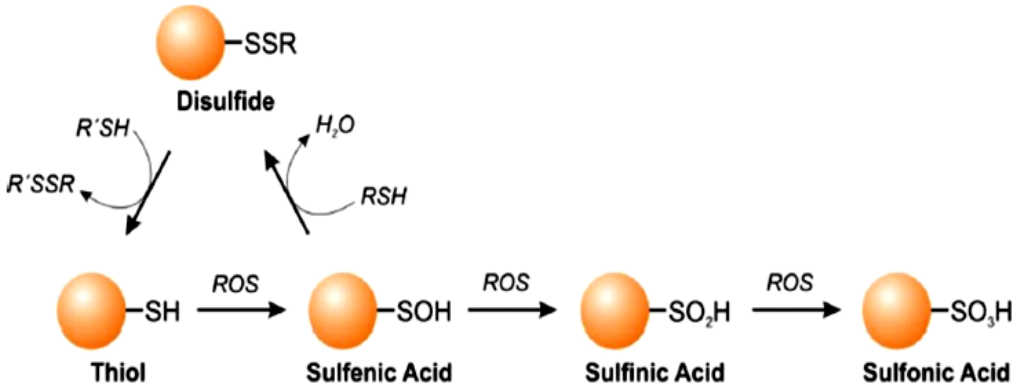

Figure 4.Oxidation of cysteine thiol group (-SH) via reactive oxygen species (ROS) leads to the formation of the short living sulfenic acid (SA) (-SOH) which can react to form more stable species, such as reacting with another free thiols (-SH) or glutathione (GSH), or can be further oxidized to sulfinic acid (-SO_2H) and sulfonic acid (-SO_3H).

Oxidative stress

Free radicals are chemical species that contain unpaired electron (s) [23,24]. The high reactivity of such electrons allowed them to be a part of chemical reactions with various cell components as lipids and proteins; where for most biological structures the damage of these free radicals is associated with the oxidative damage [25,26].

Being defined as the imbalance between the production of free radicals ($^{\cdot}O_2^{-}$, $^{\cdot}O_2^{-2}$, $^{\cdot}OH$) and the ability of the body to detoxify the harmful side effects of such oxidants, oxidative stress have been inducing many pathophysiological conditions in the body some of which include neurodegenerative diseases such as Parkinson's and Alzheimer's disease,

cancers, gene mutations, heart and blood vessel disorders and heart attack(Figure 5) [27].In most of biological systems, radicals of interest are usually referred to as reactive oxygen species (ROS), whereas most of the biologically significant free radicals are oxygen-centered [24,25].

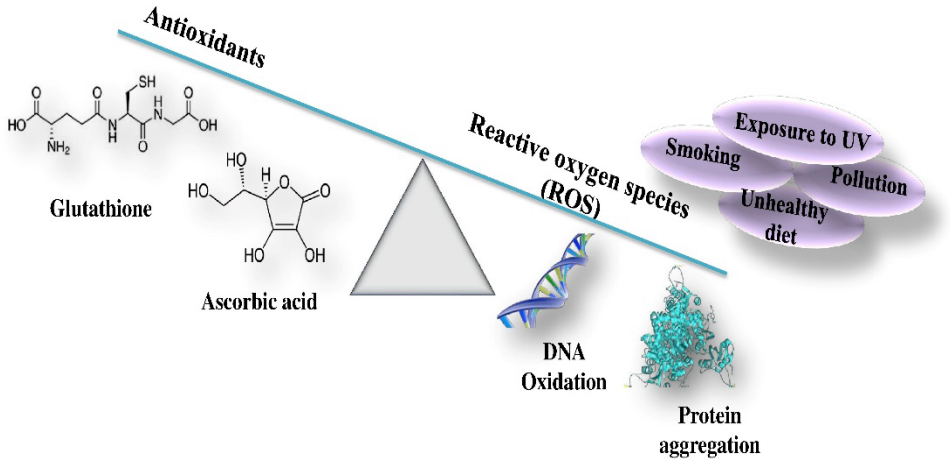

Figure 5. Oxidative stress is defined as the imbalance between the production of free radicals and the ability of the body to detoxify the harmful side effects of such oxidants. (Modified from[28]).

The existence of such alterations in the cellular reduction-oxidation (redox) balance have induced the organisms to evolve a number of strategies that counter the oxidative stress effects. Typical response involve the regulation of ROS scavengers, such as antioxidant proteins [29]. Therefore, the connection between ROS signaling and the oxidation of proteins provided a challenge for the development of new strategies to reveal the effect of such oxidants on the living organisms and connect it to the resultant disease states.

For example, Glutathione (GSH) is considered an important antioxidant as it is capable of preventing cells from the damage that can be caused by ROS. It is a linear tri-peptide composed of cysteine, glycine and glutamate (Figure 6), with the thiol group (SH) in

the cysteinyl portion which accounts for its strong electron-donating character and in turn is responsible for the antioxidant activity of glutathione.

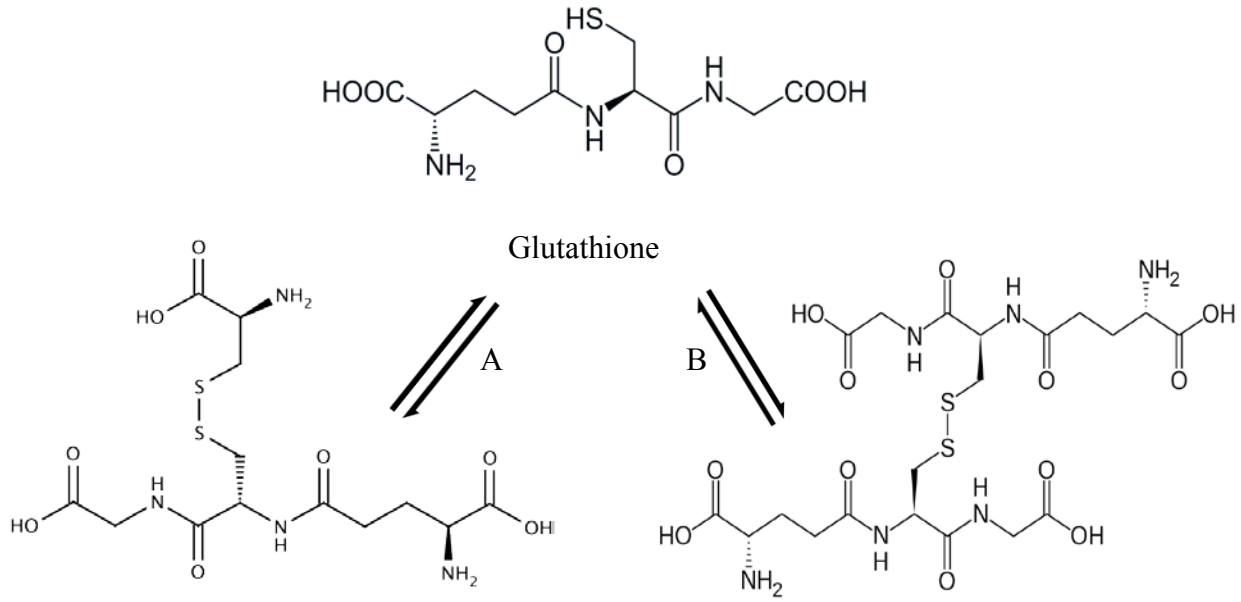

Figure 6. Glutathione is a linear tri-peptide composed of glutamic acid, cysteine, and glycine, respectively. It acts as an antioxidant against ROS where the sulfhydryl group (-SH) in cysteine forms a disulfide bridge with a cysteine amino acid (A) or with another present glutathione (B).

When the sulfhydryl groups lose their electrons, the molecule becomes oxidized and forms a disulfide bridge with another cysteine (Figure 6-A) or another glutathione (GSSG) (Figure 6-B) forming a reversible linkage that can be reduced back upon reduction [30]. Therefore, the antioxidant role of glutathione forms an important PTM that reveals and characterize the status of the biological system and protects the different residues present.

1.2. Proteomic approaches

For the separation and the determination of the molecular weight of proteins, sodium dodecyl sulphate polyacrylamide gel electrophoresis (SDS-PAGE) was the method of choice [31]. Several techniques were also established for biomolecules purification including size

exclusion chromatography (SEC) and affinity chromatography. Herein, we shall briefly discuss some of these invented methods.

1.2.1. Protein separation/purification techniques

Protein separation and purification techniques are based on a wide range of different chemical, physical and biological properties of the various protein molecules. Protein separation technique is a rapidly growing field, common examples on used methods for proteins separation include gel electrophoresis, ion exchange chromatography, affinity chromatography , size exclusion chromatography and high performance liquid chromatography[32].

Sodium dodecyl sulphate polyacrylamide gel electrophoresis (SDS-PAGE) - separation according to proteins molecular weight

Gel electrophoresis is a method of separation and analysis used with macromolecules such as DNA, RNA and proteins where charged molecules migrate through applied electric field. It is a process that enables the sorting of molecules based on their size and has a wide range of uses in the clinical and biochemistry, whereas several conditions and types of gel electrophoresis can be found[33,34].

One dimensional (1-D) sodium dodecyl sulphate polyacrylamide gel electrophoresis (SDS-PAGE) shall be discussed in more details as it was used in this work. Serving as a size selective sieve during separation, acrylamide gel was used to allow proteins to get separated, whereas smaller proteins travel more rapidly than larger proteins. Whereas the used polyacrylamide, serving as an anticonvective sieve, can cover protein size raging from 5- 250

KDa, the separation of proteins in gel electrophoresis is based on their size and shape. Therefore, comparing the separated proteins to the usual appearance patterns helps in the diagnosis of diseases[35].

Proteins in SDS-PAGE are separated in the presence of sodium dodecyl sulphate (SDS) and denaturating agents, which in turn denaturate the proteins resulting in their separation. The schematic of electrophoretic protein separation can be seen in Figure 7.

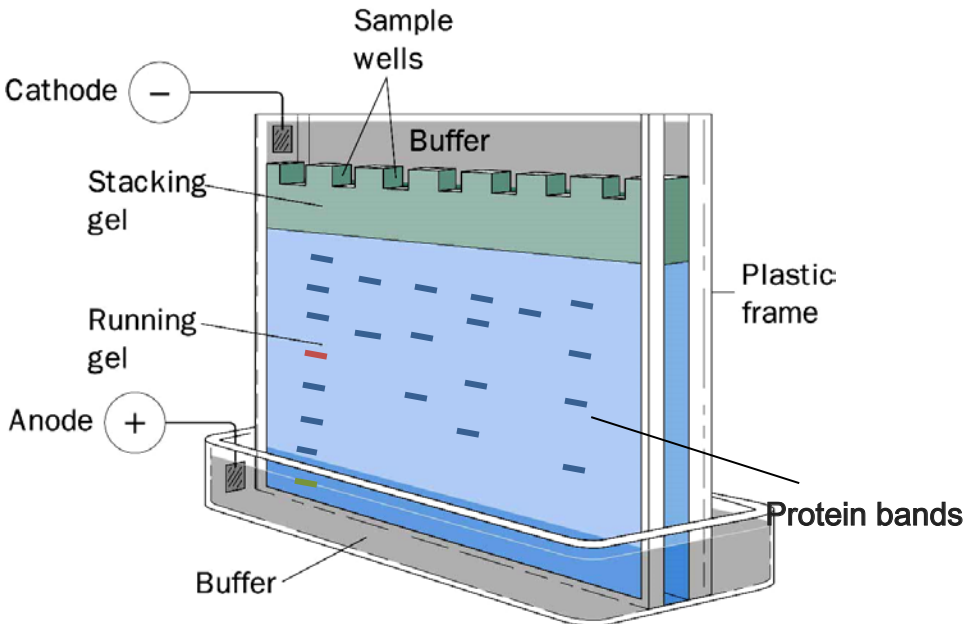

Figure 7.Schematic of electrophoretic protein separation in polyacrylamide gel.(Modified from: Southern Illinois University).

The used polyacrylamide gel is composed of acrylamide - bisacryl amide (*N*,*N*′-methylenebisacrylamide) sieving matrix (Figure 8) that is chemically inert and can be prepared in different pore sizes. Their polymerization reaction is a vinyl addition reaction that is catalyzed by the induced free radicals of APS (ammonium persulphate) initiated upon the addition of TEMED (*N*, *N*, *N*′, *N*′ -Tetramethylethylenediamine)[36].

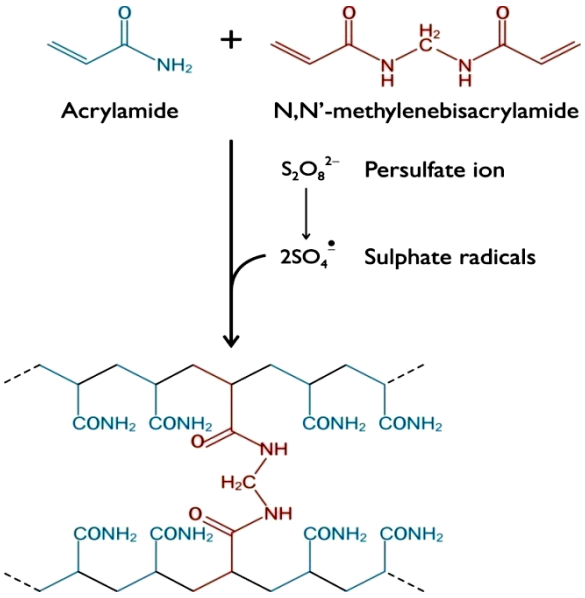

Figure 8.Polyacrylamide gel molecular structure. The sieving molecular network comes into being by a radical polymerization of acrylamide monomers and cross-linking *N*, *N'*-methylenebisacrylamide components. (Adapted from: [36]).

The discontinuous buffer system used (stacking pH 6.8 and resolving pH 8.8 gels) is included for a better resolution and to preconcentrate the proteins (united travelling time of proteins); where the stacking gel has lower concentration of acrylamide, and the used running buffer, and different pH. This used different buffer system control the charge state of glycine present in the running buffer upon applying power to the system[31].

As a consequence, proteins will be concentrated at the end of stacking gel zone where glycine would front accelerate leaving proteins to enter (all at a time) the concentrated running gel which will slow their motion according to their size, and the used concentration of the running gel as can be seen in Figure 9.

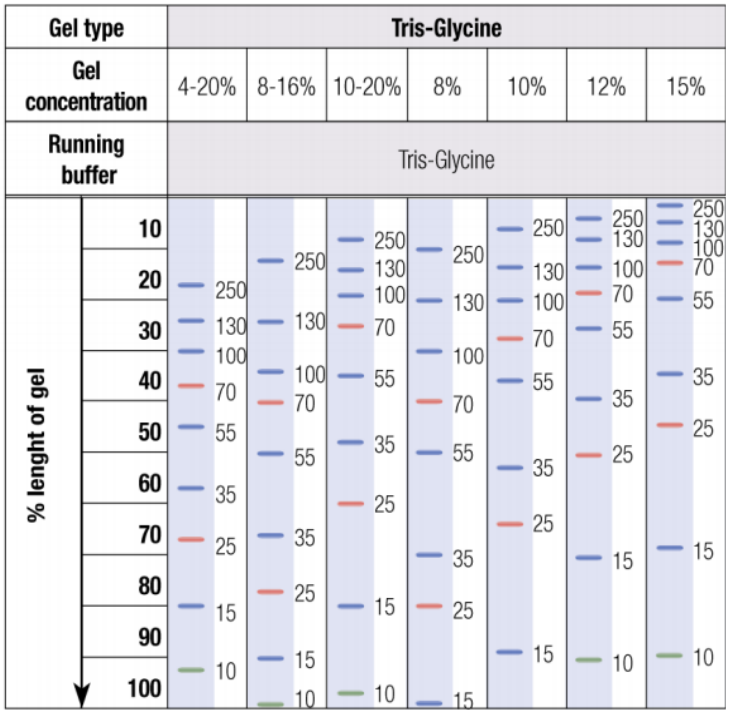

Figure 9. Migration patterns of prestained protein ladder where molecular sizes (KDa) migration patterns are shown.(Adapted from: BIO-RAD).

Size exclusion chromatography (SEC)- diameter of the molecule

Size exclusion chromatography (SEC) is an analytical technique for the size-based separation of biomolecules. The column is packed with porous material where upon the flow of dissolved molecules of various sizes the smaller dissolved molecules flow more slowly through the column; as they penetrate deep into the pores, while larger dissolved molecules flow quickly through the column[37].

The separation mechanism is schematically shown in Figure 10, where larger molecules elute sooner and smaller molecules elute later. As SEC is considered a fast and reliable method and requires less buffer, it is often used for the analysis and separation of wide variety of biomolecules. The type and length of the stationary phase packed in the

column play critical roles in influencing the resolution of separated biomolecules via SEC [38,39].

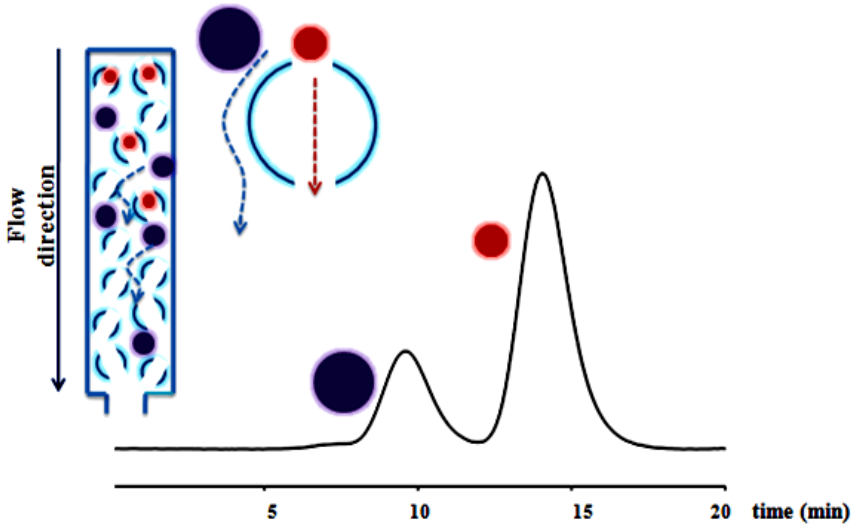

Figure 10.Schematic representation for the separation mechanism in size exclusion columns (SEC).

Several commercial types of SEC columns are available with different stationary phases, where their use count on the molecular weight and the conditions that should be used for biomolecules separation. Examples include superdex peptide 10/300 GL (10 mm inner diameter ×300 mm bed height) which separates peptides with fractionation range of 100 - 7000 peptides (100-10000 dextrans),superdex 75 10/300 GL column which separates proteins with fractionation range of 3 000- 70 000 Da globular protein (500 - 30 000 dextrans) and superdex 200 10/300 GL column which separates proteins with fractionation range of 10 000 and 600 000 Da globular protein (1000 - 100 000 dextrans). Typically, spherical composite of cross- linked agarose and dextran with mean bead size of 13 µm Figure 11.

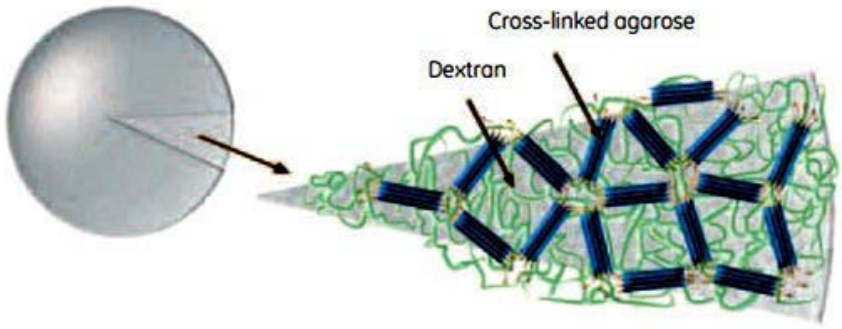

Figure 11. Schematic view through a bead of superdex section composed of dextran/cross-linked agarose matrix. Average particle size is 13 µm. (Adapted from: GE Healthcare).

Affinity chromatography(HiTrapTM Blue HP)-biospecific interaction

In affinity chromatography the separation relies on the specific and reversible binding of a desired protein to a matrix-bund ligand. The selectivity of affinity chromatography allows the desired molecule to be purified to specifically interact with the stationary phase in order to be separated from undesired molecules which will be eluting first as it would not interact with the stationary phase.

Undesired molecules are washed away with a buffer, while desired species are eluted upon passing eluting buffer of high salt concentration. Typically, agarose is usually used as a stationary phase [40]. HiTrap Blue HP column is an example (Figure 12) on a prepacked column used for affinity chromatography. It is particularly suitable for the isolation and purification of wide range of biomolecules including albumin. Albumin can be specifically removed from human serum with HiTrap Blue HP columns using a binding buffer of 50 mM KH_2PO_4 (pH 7.00) and elution buffer of 50 mM KH_2PO_4 + 1.5 M KCl (pH 7.00).

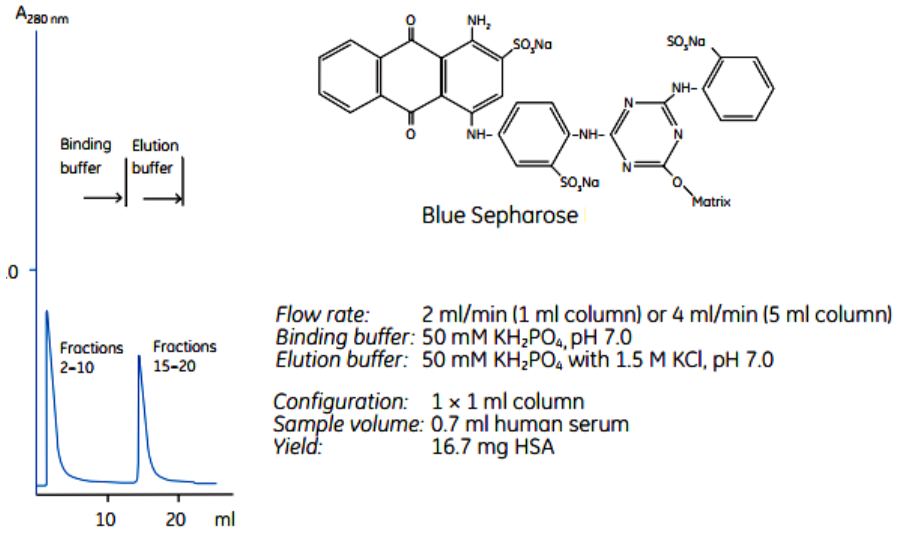

Figure 12. Scaled separation on HiTrap Blue HP column giving predictable and a quantitative reproducible yields of pure protein . Shown as well the partial structure of Blue Sepharose High Performance.(Adapted from: GE Healthcare).

The resulting chromatogram will show two separated peaks corresponding to plasma proteins (Figure 12 fractions 2-10) and albumin (Figure 12 fractions 15-20). The elution of the separated fractions depends on the configuration of the used column and on the injected sample volume. Partial structure of Blue Sepharose High Performance is shown in the inset of Figure 12 where the carbohydrate nature of the agarose base provides a hydrophilic and chemically favorable environment for coupling and the highly cross-linked structure of the 34 µm of the spherical matrix provides high chromatographic separation.

Cibacron Blue F3G-A is the covalently attached dye ligand to the Sepharose High Performance matrix via triazine part of the dye molecule, it provides an immobilized dye that shows certain structural similarities to some co-factors as $NADP^+$ which in turn enables it to bind strongly to a wide range of biomolecules and to provide chemical stability and continued re-use .

1.2.2. Ionization techniques in mass spectrometry for proteomics

Edman degradation was the traditional used tool for protein identification and sequencing [41,42] but it was subsequently replaced by mass spectrometry (MS) for being slow and relatively insensitive [43]. Driven by technical breakthroughs. MS revolutionized the analysis of proteins in the 1990s. The great and fast developments in MS field in terms of ionization techniques, speed, sensitivity and the potential for sequencing using a database provided great source for protein analysis [44].

Being a widely used analytical technique, MS ionizes molecules and sort their ions based on their mass-to-charge ratio (*m/z*), in other words; measuring the masses present within a sample. MS consists of two basic components: ionization source (ionizes molecules) and mass analyzer (measures masses of ionized molecules).

Wide variety of ionization sources, such as electrospray ionization (ESI) and inductively coupled plasma (ICP), and mass analyzers, such as Time-of-flight (TOF) and Quadrupole mass filter (Q) were invented and shall be briefly discussed in this section. In general, any mass analyzer can be coupled to any ionization source, where both should be considered upon purchasing decision forming important criteria for a properly executed MS experiment.

Ionization Sources

Ionization techniques can be classified into "soft" (i.e. non-fragmenting) and "hard" ionization techniques. Electrospray ionization (ESI) shall be discussed in this chapter as soft ionization whereas inductively coupled plasma (ICP) shall be introduced as the harsh one.

Electrospray ionization (ESI)

In 1989, the possibility of obtaining the mass spectrum of large biomolecules using electrospray ionization (ESI) was described [45]. Breakthroughs in MS development included the ESI-MS in 2002 when John Fenn received his Nobel prize for the development of this soft ionization method where a minimum of energy is retained by the analyte upon ionization. Therefore, ESI is a suitable technique for the analysis of small, large and non-volatile molecules.ESI can be coupled to a liquid chromatography system (HPLC) which made it a very well suited technique for proteomics studies[46,47].

ESI-MS is a liquid phase process that produces a fine mist of droplets at atmospheric pressure (Figure 13). The high potential difference applied between the capillary and the inlet of the MS generates a force that induces the liquid to form a cone from the capillary tip (Taylor cone) [48]. This formed cone results from the repulsive Coulomb forces between the like charges, where both the needle and the analyte have the same polarity.

This forces the spraying of charged droplets from the needle towards the oppositely charged cone at the inlet of the MS. As the droplets transverse between the needle tip and the cone, solvent evaporation takes place and the droplets shrink while having constant charge.

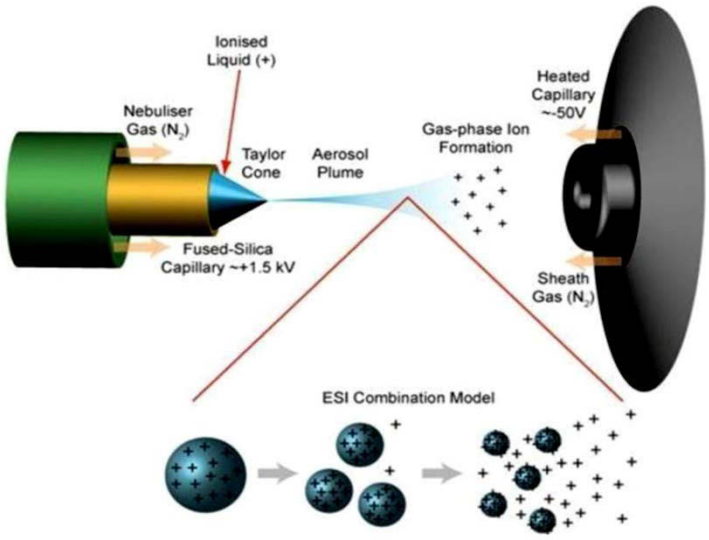

Figure 13. Schematic of electrospray ionization (ESI). (Source: Lamond Laboratory &Chromacademy).

Eventually, Rayleigh limit is reached where the surface tension can no longer sustain the charge where Coulomb explosion occurs forcing droplets to fission into smaller droplets. This process continues until nanometer-sized droplets are produced.

As mentioned before, this process works in both positive and negative ion modes and produces ions with a wide range of charge states (e.g., +1, +2, +3, …) making it amenable to high molecular weight species[49].

Polar molecules (such as biopolymers) and nitrogen- containing compounds (such as amino acids, peptides, and oligonucleotides) get ionized very well by ESI. Special attention should be given to the analyzed samples as the use of buffers and salts with ESI causes reduction in the vapor pressure which in turn reduces the signal.

Inductively coupled plasma (ICP)

In 1983, element-selective techniques based on inductively coupled plasma mass spectrometry (ICP-MS) were introduced [50], where it became a powerful technique whenever the elemental analysis is needed [51].

In ICP-MS, plasma (usually with argon) is used to generate gas-phase elemental ions. It operates at a temperature between 6 000 and 7 000 K, a temperature that no material can stand. In principle, all elements that have a first ionization potential below 15.75 eV, which is the first ionization potential of argon, can be ionized in an ICP. Therefore, all metals and most of the remaining semi- and non-metals (exceptions are C, H, N, O and F) can be determined [52,53].

In general, samples are introduced into the "nebulizer" of the ICP-MS (through a peristaltic pump) where it got mixed with argon forming a fine aerosol that passes through a "spray chamber" where large droplets are removed increasing by that the robustness of the plasma(Figure 14).

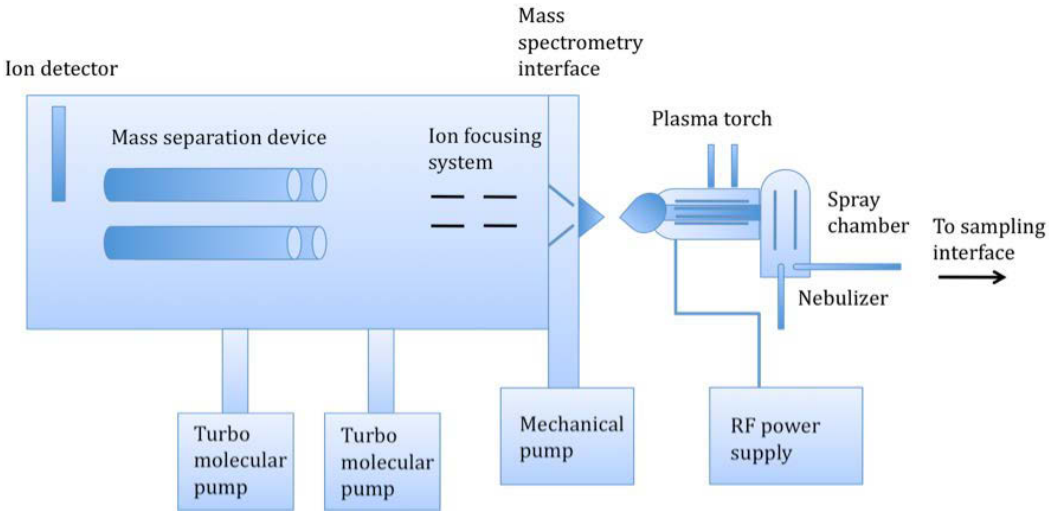

Figure 14.Schematic diagram for the basic components of an ICP-MS system. (Adapted from :[54]).

The small aerosol droplets are then transferred (RF power generator) to the plasma torch where the chemical bonds in the introduced samples get broken as the samples undergo successive volatilization, desolvatization, atomization and ionization (Figure 15) and in turn lose their structural information where only the total amount of the elements remain accessible.

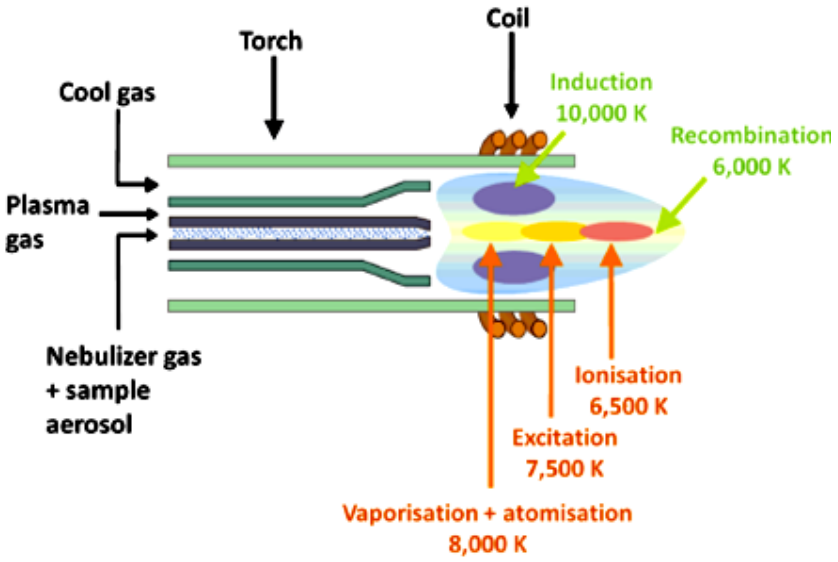

Figure 15.Design of an ICP torch. Three independent gas flows present which are introduced via different channels of the torch (Adapted from [55]).

As can be seen from the scheme of the ICP source (Figure 15), three independent gas flows present which are introduced via different channels of the torch. Through the inner channel the sample (for example via pneumatic nebulisation)is introduced where the typical flow rates are between 0.8 and 1.5 L min $^{-1}$, the second channel provides additional argon flow between 0.7 and 1.0 L min^{-1} for the generation of the plasma, whereas in the third outer channel Ar with flow rate of 15 L min $^{-1}$ is introduced to cool the torch system (which is manufactured from quartz due to the high thermal demands) [53].

Therefore, ICP-MS technique in considered independent from the molecular environment. The ions generated in the plasma are then extracted to the high vacuum region

to number of interface cones that helps in delivering high sensitivity across the mass range. Ions pass into a mass analyzer, as for example the quadrupole mass analyzer which in turn separates ions based on their *m/z* ratio [53].

ICP-MS advantages include the high sensitivity, multiplexing capability, minimal matrix effect, structure- independent response and a wide linear dynamic range. Moreover, ICP-MS can be used for the precise quantification when the isotopic dilution analysis (IDA) is performed [56].

ICP-MS own outstanding properties for elemental analysis, pg g^{-1} limits of detection for most elements can be obtained and multi-element analysis is possible beside the isotopic information. However, in the colder zone of the plasma recombination between ions can occur leading in turn to the formation of polyatomic species (Ar, O, N ...), where their presence can contribute to the signal of the analyte on a certain *m/z* ratio.

The combined use of ESI-MS and ICP-MS shall provide complementary results regarding structural and elemental information. The complementary use of these approaches provided significance improvement in proteomics field and the tackled the relative and absolute quantification which is considered essential to understand the different biological systems [57,58].

Mass analyzers

A mass analyzer is a component of the mass spectrometer which takes ions and separates them according to their mass-to-charge *m/z* ratio before they reach the detector. Several types of mass analyzers were invented such Time-of-Flight, Quadrupole, Magnetic sector, Quadrupole ion trap and Ion cyclotron resonance. Herein, we will briefly discuss two types of mass analyzers; Time-of-Flight and Quadrupole mass analyzers.

Time-of-Flight mass analyzer (TOF)

Time -of-Flight (TOF) instruments have significant role in modern mass spectrometry due to their speed, high accuracy (ppm) and compatibility to MALDI (Matrix assisted laser desorption/ionization) and ESI (Electrospray ionization). The TOF principle involves the acceleration of ions towards the detector (Figure 16), where the ions that exit the ionization source will be accelerated to the detector using the same voltage.

All ions will share the same kinetic energy (K.E.=$^1/_2$ m.v^2) so the velocity of the ion depends on its *m/z* ratio. The time that takes ions to reach the detector in a known distance is measured, and this time depends on the ions *m/z* ratio. An ion that has lower *m/z* ratio will travel faster than an ion with larger *m/z* ratio. In order to get higher mass accuracy, the prolongation for the flight path was invented where a number of turns can be chosen [59].

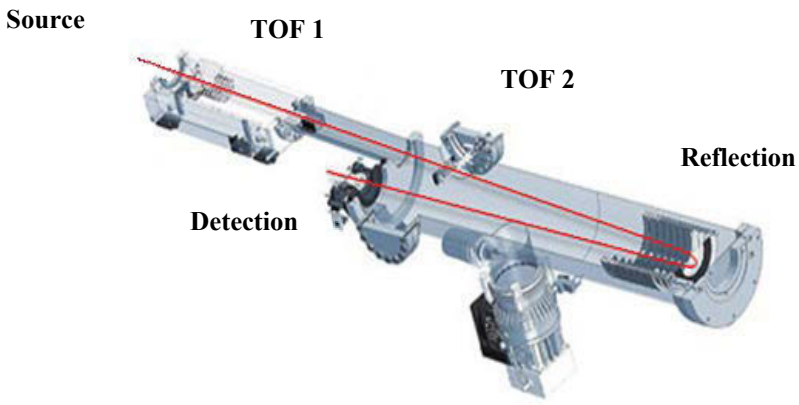

Figure 16.Schematic diagram for Time-of-Flight (TOF) mass analyzers. (Adapted from University of Kentucky, MS facility) .

Quadrupole mass analyzer (Q)

Quadrupole mass analyzer consists of four cylindrical rods that have been set in a parallel position to each other (Figure 17), and with the application of voltages (direct current, DC, and radio frequency, RF) they are responsible for filtering the ions based on their *m/z* ratio[60]. This simple working principle made the quadrupole mass analyzers the most commonly used analyzers as they can be switched rapidly between different *m/z* ratios allowing high scan speeds.

They can be combined with ICP as a triple quadrupole system (QQQ) Figure 17in an "On-mass" or "Mass-shift" methods for the removal of spectral interferences [61].In general, in both systems a collision cell is introduced in front of the first quadrupole (Q1) which can be filled with a gas at low pressure, where this cell can be a smaller quadrupole or similar device such as hexapole or octapole.

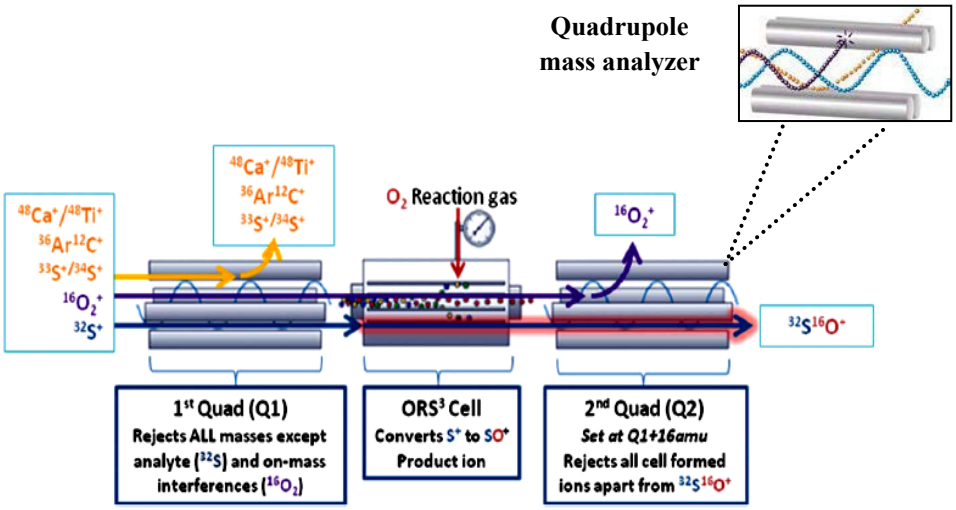

Figure 17.Schematic representation of the operating principle of ICP-QQQ system. (Modified from [62]).

For example in the "On-mass" methods, the introduced collision cell works with kinetic-energy discrimination; it is filled with a chemically inert gas (mostly He) and an additional energy barrier (around 2 V) is set between the collision cell and the quadrupole so that only the ions with a sufficient kinetic energy can overcome and got detected. According to this principle, as the polyatomic interferences consist of two or three atoms they will own larger cross section and therefore collide more often and suffer from a higher loss of their kinetic energy, where as a consequence their remaining kinetic energy would not be sufficient to allow them to enter the quadrupole.

For the "Mass-shift" method, oxygen will react with the present heteroatoms where an oxygen mass-shift will be produced (for example,$^{31}P^{16}O^{+}$ and $^{32}S^{16}O^{+}$) and measured, overcoming by that the polyatomic interferences that originate from N, O, H and C and make it possible in turn to measure the heteroatoms (such as sulfur and phosphorous) present in many proteins[63,62].

Basically, Q1 and Q2 function as mass filters ensuring that only targeted ions are measured so even if other matrices present, they will be rejected by the first quadrupole Q1.It

should be noted that an octopole-based reaction cell is located in between two quadrupole analyzers as seen in Figure 17.

1.3. Quantitative proteomics

As modern research calls for quantitative analysis, since the quantity of the protein is directly related to the condition within the biological system, several approaches have been developed to serve this demand .

The dynamics in quantitative proteomics (demonstrated in Figure 18) explain the gap between the number of proteins in any biological sample and the number of relatively quantified ones. Therefore, several approaches have been developed aiming to assess proteomes and achieve some information regarding the status of the system.

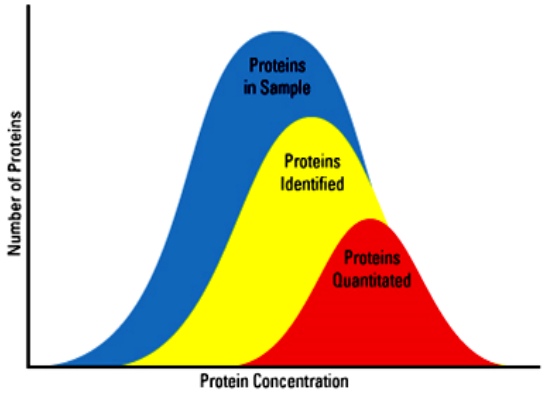

Figure 18.The complexity of proteome.(Adapted from [64]).

Isotopic labelling [65], metabolic labelling [66], enzymatic labelling [67] and chemical labelling [66] are some examples that illustrates the labelling strategies that have been developed and used for the labelling of different species.

Herein, and with the help of the previously discussed developed strategies for protein identification and quantification (such as SDS-PAGE and MS techniques) we will tackle one

type of chemical labelling namely " Metal-coded affinity tag (MeCAT) " labelling that is prepared to have certain specificity toward a certain residue.

1.3.1. Naturally occurring heteroatom tags

ESI-MS and ICP-MS have been widely used in the detection and quantification of different species , such as proteins, where they contain one or more metal ions coordination, forming a naturally occurring element label. Due to the presence of several residues, such as cysteine (-S) or histidine (-N), metals are usually coordinated forming metal-protein complexes that serve in a specific function such as detoxification of heavy metals, as the case of cysteine [68].

Herein, several studies will be addressed that deal with the different natural occurring elemental labels that have significant role in the biological system, such as phosphorus, sulfur and selenium. Studies on metallothioneines are also discussed, since they covalently incorporate element labels and are found in almost all cells. They form a family for small cysteine-rich proteins (20 cysteine residues) with strong complexing properties where up to 7 bivalent metal ion can be found [69].

Phosphorous

A wide spread post-translational modification (PTM) that represents important phenomena for the regulation of cellular processes is the reversible phosphorylation of proteins at serine, threonine and tyrosine residues [70]. Phosphorylation site analysis encounter several analytical challenges for being susceptible for suppression by other components during the analysis and due to the decrease of sensitivity of the peptide for the presence of phosphoryl groups as have been previously reported [71,72].

Utilizing elemental and molecular tools, phosphopeptides detection and identification have been carried out by using capillary liquid chromatography (μLC) that interfaced alternatively to ICP-MS for the detection of ^{31}P and ESI-MS to provide the corresponding molecular weight information [73]. Using this technique, tryptic digests for three phosphopeptides (ß- casein, activated human MAP kinase ERK1, and protein kinase A catalytic subunit) were successfully detected and identified with high selectivity [74].

Sulfur

Presenting another important naturally occurring elemental label, sulfur became an important detectable element by ICP-MS, as it is present in almost all peptides and proteins due to the sulfur- containing amino acids (cysteine and methionine) [15].

As an example, sulfur was used as a key element for the absolute quantification of Insulin (six cysteine residues per molecule) as a model analyte using thiamin as internal standard. μLC-ICP-MS, where the elution of sulfur containing analytes was recorded online with selective ^{32}S detection, and μLC-ESI-MS, for the identification of tryptic protein digests, were used complementary for the absolute quantification and characterization, respectively [75].

Selenium

Forming an essential trace element in human nutrition and being required for the activity of selenium- dependent enzymes [76,77], a study reported selenomethionine (SeMet) characterization and quantification using ESI-MS and ICP-MS in HEK 293 kidney cells. Proteins were screened and separated using LC-ICP-MS and the selenium- containing proteins were identified by peptide mapping using nLC-ESI-MS [78].

On the other hand, as the characterization and quantification of selenium provides a great output for the trace element speciation in complex systems [79]and is essential as well in food science, ESI-MS and ICP-MS were used complementary in selenium characterization in food such as in carrot [80], cereal crops [81], and mustard seeds [82].

Metallothioneines

Due to their multifunctional physiological behavior in different areas such as detoxification, storage, and transport of metals [69], several studies discussed the complementary use of ESI-MS and ICP-MS in the analysis of metallothioneins[83,84].

HPLC-ESI-MS and HPLC-ICP-MS were used to identify and quantify metallothionein isoforms and metal complexes in liver samples using [85,86].

For example, for the characterization of metal complexes with metallothionein isoforms in hepatic cytosols of Cd exposed crap, ESI-MS was used as a detector for the reverse phase RP-HPLC, this allowed the identification of two major peaks distinguished by RP-HPLC-ICP-MS. Mass spectra taken at the peak apices indicated the co-elution of different metal (Cd, Cu, Zn and Pb) complexes with metallothionein with each peak [86].

1.3.2. Chemical Labelling

As systematic identification and quantitative studies for several species and proteins in complex samples have been matter of study for scientists, different labelling strategies have been invented to permit insights to the absolute detection and quantification of any PTM or disease state in the biological system.

Labelling with chemical tags is a growing field that have many techniques and applications, herein we are reporting chemical tags using several elements as labels for different species that can be later get identified and analyzed by analytical techniques, or by the use of chelate chemistry (i.e. DTPA and DOTA) targeting specific residues.

Chemical Element Labels

Mercury

Molecular MS and elemental ICP-MS were used for the absolute quantification of sulfhydryl (-SH) groups in proteins using organic mercury ions CH_3Hg^+ labelling, where for being specific for -SH groups they end up in forming a simple 1:1 complex CH_3Hg^+ : -SH that was confirmed using ESI-MS and quantified *via* Hg determination using ICP-MS. Tested model proteins (bovine pancreatic ribonuclease A, lysozyme and insulin) showed absolute detection limits that reached to 0.6, 1.2 and 0.4 pmol, respectively [87].

Selenium

Reduced homocysteine was labelled and quantified using selenium- containing labelling agent called ebselen. Being reactive with -SH groups, ESI-MS/MS provided stoichiometry of the derivative of 1:1, and having selenium atom in the molecule the complementary use of ICP-MS revealed excellent features for the determination of selenium-derivatized reduced homocysteine in real samples [88].

Gallium

Selective detection of phosphopeptides was carried out using a metal tag, gallium-N,N-biscarboxymethyl lysine(Ga-LysNTA). Characterization of Ga-phosphopeptide complex has been done with linear ion trap (IT) ESI-MS and Fourier transform FT-MS, while LC-ICP-MS was used for the absolute quantification of the formed complex [89].

Chelate Chemistry

Chelating agents such as DTPA and DOTA are considered bi-functional agents that can harbor a metal ion and used for covalent interaction with a desired functional group. They have been widely used in several studies for the absolute detection and quantification of several resides. for example, complete characterization for a synthetic paramagnetic contrast agent (DTPA-PNA, metal-complexed DTPA-peptide nucleic acid) designed for magnetic resonance imaging (MRI) has been done using size exclusion SEC-ICP-MS and nESI-MS [90].

Novel activity-based element-tagged photo-cleavable biotinylated chemical "hub" was synthesized to orthogonally integrate ICP-MA and ESI-IT-MS. The synthesized chemical "hub" comprises four parts, each part has specificity toward specific residue [91].

In another approach, thiol residues were labelled in peptides and proteins following a two-step based strategy including *in situ* click chemistry reaction for quantification. Employed labels were found to be compatible with ESI-MS for identifying labelled peptides and protein, and with the ICP-MS for the quantitative analysis [92,93].

Meta- Coded Affinity Tag (MeCAT)

Several studies have been conducted with the use of a specific labelling ESI-MS and ICP-MS detectable reagent devised for proteomic analysis, namely metal coded affinity tag (MeCAT).

Due to their favorable electronic and coordination properties "Schiff bases" are common ligands in which the imine nitrogen is basic and exhibits pi-acceptor properties[94]. Containing a DOTA (Figure 19), MeCAT is a bi-functional chelating agent that harbor a metal - usually a lanthanide- and can be linked to several functional groups that target specific residues as for example -NH_2, amine groups, -SH cysteine thiol residues, and - SOH

cysteine sulfenic acids. MeCAT reagent was synthesized with amine reactive group N-hydroxysuccinimide (-NHS), where it was used for absolute quantification of proteolytic peptides and intact proteins from a complex biological system [95].

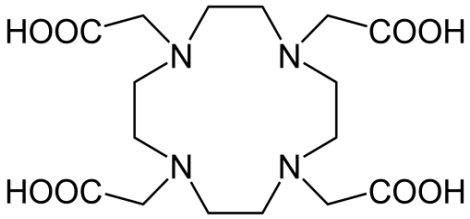

Figure 19.Structure of the chelating agent DOTA.

Cysteine reactive maleimide (Mal) or iodoacetamide (IA) were also coupled to DOTA forming specific chemical labelling reagent for -SH in peptide and proteins (Figure 20). Specific detection and quantification of synthetic model peptides, proteins and real samples have been successfully addressed using MeCAT-Mal/MeCAT-IA synthetic reagent[96].

Finally, dimedone was attached to DOTA for the specific labelling of cysteine sulfenic acid (SA) , where upon oxidation of cysteine thiol residues, MeCAT-dimedone can function for specific detection of SA[97].

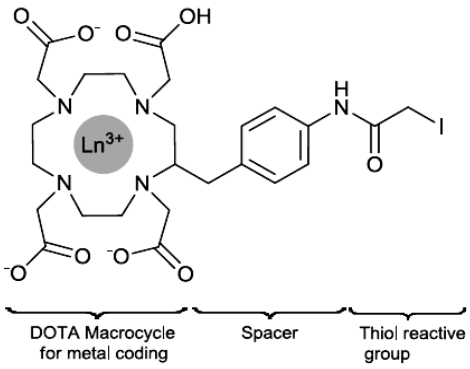

Figure 20. Structure of MeCAT specific for cystine thiol labelling due to the presence of Iodoacetamide functional group. (Adapted from [96]).

Lanthanides

Lanthanides (Ln) is a group of 14elements that can form stable complexes when metallated with many bi-functional chelating agents such as DOTA. All Ln form trivalent cations, Ln^{3+}, in solutions in which their chemistry is determined by the ionic radius that decreases from the lanthanum (La) to lutetium (Lu).

In brief, Ln complexes have attracted attention and found applications due to their luminescent properties arising from *f-f* transitions. Whereas the fluorescence of lanthanide salts is weak as the energy absorption of the metallic ion is low, the use of chelating agents with lanthanides in their most intense +3 oxidation state has been initiated. Ln adopt high coordination numbers usually between eight and nine and exhibit strong electromagnetic and light properties due to the presence of unpaired electrons in the *f*-orbitals[98].

Lanthanides have a high mass defect compared to other elements in the biomolecules, leading to an easier discrimination of the labelled species from unlabelled ones in MS[96,99]. Better multiplexing capabilities are achieved with the wide range of mono-, bi- and multi-isotopic lanthanides forming stable labels and allows quantification using isotopic dilution analysis (IDA). Thus, Ln presence allow the complementary use of ESI-MS and ICP-MS.

1.3.3. Isotopic dilution analysis (IDA)

Isotopic dilution analysis (IDA) is a method for the quantitative determination of chemical substances. IDA comprises the addition of known amounts of isotopically-enriched tracer/spike into the analyzed sample where upon mixing, the natural isotopic composition of the analyte gets changed (Figure 21) and it becomes possible to calculate the amount of the analyte present in the sample [100].

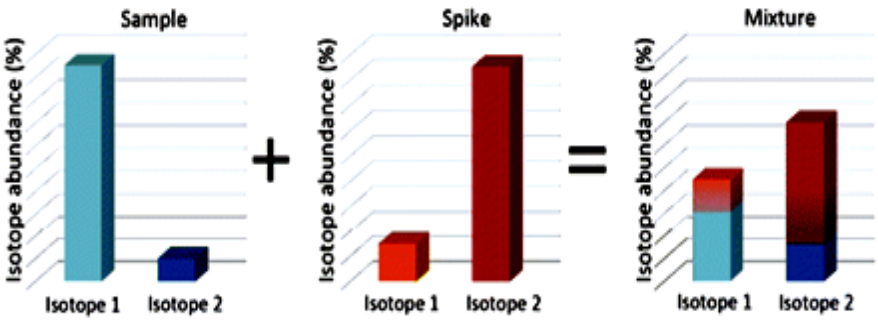

Figure 21.Basic principle of isotopic dilution analysis (IDA). As shown upon the addition enriched tracer to the sample changes in the natural isotopic composition of the analyte occurs making it possible to calculate the amount of the analyte present. (Adapted from [101]).

On-line isotopic dilution analysis is also possible where a direct flow of the tracer is mixed online with the sample to be analyzed in certain pre-calculated concentrations. The relationship between the number of components in the mixture and the isotope ratio can be expressed in the isotope dilution equation:

$$C_s = C_{sp} \cdot \frac{m_{sp}}{m_s} \cdot \frac{M_s}{M_{sp}} \cdot \frac{A^b_{Sp}}{A^a_S} \cdot \frac{(R_m - R_{sp})}{(1 - R_m R_s)}$$

m_{sp}, m_s: mass of the sample and the spike taken, respectively.

M_s, M_{sp}: atomic weight of the element in the sample and the spike, respectively.

$A^b{}_{sp}$: abundance of the enriched isotope b in the spike

$A^a{}_s$: abundance of the most abundant isotope a in the sample

R_m: isotope ratio (a/b) in the mixture

R_{sp}: isotope ratio (a/b) in the spike

R_s: isotope ratio (b/a) in the sample

The application of the IDA technique helps in determining the concentration of an element in a sample which in turn provides the desired quantitative analysis for the biological

system. During the last years, many examples for the use of IDA for the quantitative protein analysis have been published [102,103].

2. Aim and scope of work

Quantitative analysis of biological systems plays a significant role in modern analysis by forming a key for understanding the status of different studied systems. Therefore, highly sensitive analytical tools are required to quantify and address the changes and the status of the studied systems and eventually correlate between quantified concentrations and several diseases. The complementary use of molecular (ESI, electrospray ionization) and element (ICP, inductively coupled plasma) mass spectrometry (MS) has greatly contributed in the identification and quantification of different biological systems leading to a significant output with highly accurate quantitative results.

In the course of oxidative transformation of cysteine thiol groups into different functional groups, which is considered a significant posttranslational modification (PTM) of great importance to pathological and physiological processes, cysteine sulfenic acid residue (SA) is the transient state for thiol group oxidation where the detection of this short living SA formed a key to understand the different redox-mediated events.

SA can react with free thiols to form disulfide bonds or can be further oxidized with reactive oxygen/nitrogen species (ROS/RNS) to form sulfinic and sulfonic acids. The increment in ROS/RNS concentrations is correlated to age-related diseases such as cancer and Alzheimer´s disease, therefore SA form a transient state for different functional groups formation and serve as sensors for the presence of ROS/RNS.

As the detection of the short living SA shall provide closer insight into these redox-mediated events that alter the structure and function of peptides and proteins, herein, we provide a new strategy for the highly sensitive and specific detection of SA in peptides and

proteins. Since ketoesters (KE) have been reported to be specific for SA detection and to exhibit improved reactivity at physiological pH compared to other probes (such as dimedone), we have developed an MS and ICP-MS detectable compound for SA detection using KE.

In the prepared compound, alkyne β-ketoester (KE) is previously linked to a lanthanide (Ln)-containing chelator (Ln-DOTA, where DOTA is 1,4,7,10-tetraazacyclododecane-1,4,7,10- tetraacetic acid). SA was generated by hydrogen peroxide (H_2O_2) to mimic oxidative events produced in living cells by ROS and was detected by the prepared compound Ln-DOTA-KE.

Molecular MS (ESI-MS) and elemental MS (ICP-MS) have been used to monitor the formation of SA linked to Ln-DOTA-KE. Isotopic dilution analysis (IDA) was used for the absolute quantification of labelled SA in protein samples using an isotopically enriched Nd tracer.

3. Materials and methods

Purchased materials were used without any further purification. High-purity MilliQ water was used for samples preparation (Millipore, Bedford, USA). Argon for ICP-MS (purity 99.99%) was delivered by Alphagaz (Madrid, Spain). Azide–DOTA (1,4,7,10-tetraazacyclododecane-1,4,7-tris-acetic acid-10- (azidopropylethylacetamide)) was purchased from Macrocyclics (Dallas, US). TEAA (triethyl ammonium acetate) and TEAB (triethyl ammonium bicarbonate) were purchased from Fluka (Buchs, Switzerland).

Holmium(III) chloride hexahydrate, 99.9%, terbium(III) chloride hexahydrate, 99.9%, europium (III) chloride hexahydrate, 99.9%, neodymium (III) chloride hexahydrate, 99.99%, ytterbium (III) chloride hexahydrate, 99.99%, THPTA (tris (3- hydroxy propyl-triazolylmethyl) amine 95 %, TCEP (tris (2-carboxyethyl) phosphine hydrochloride) ≥98 %, TPP (triphenylphosphine),99% , methyl acetoacetate, 99% , propargyl alcohol , sodium ascorbate, ß-lactoglobulin from bovine milk (3908), human serum albumin standard (A1653) and human serum (ERM® certified reference serum proteins) were purchased from Sigma-Aldrich (Madrid, Spain).

Sodium acetate trihydrate 95%, hydrogen peroxide 30 %, THAM (tris (hydroxymethyl) amino methane), copper (II) sulfate pentahydrate, C18 Millipore Ziptips® for desalting and concentrating peptides, Amicon® Ultra centrifugal filter units and potassium dihydrogen phosphate were purchased from Merck KGaA (Darmstadt, Germany).

Three peptides with one cysteine unit were investigated (H- WWCNDGR- OH ≥ 95 %), (H-QNCDQFEK-OH ≥ 95 %), and (H-DDPHACYSTVFDK- OH), all obtained from Schafer- N (Copenhagen, Denmark).

Isotopically enriched (^{145}Nd) neodymium standard was purchased from Euriso-Top GmbH (Saarbrücken, Germany), the isotopic abundances were 0.59% ^{142}Nd, 0.45% ^{143}Nd, 2.61% ^{144}Nd, 86.57% ^{145}Nd, 9.44% ^{146}Nd, 0.22% ^{148}Nd, 0.11 ^{150}Nd**.** HiTrap™ Blue HP column was purchased from GE Healthcare (Uppsala, Sweden).

Instrumentation

Ln-DOTA-KE

Ln- DOTA purification was performed using an Agilent 1100 system equipped with a diode array detector. A Nucleosil® 100 A° C18 column (5 µm, 200 × 4.6 mm)(Phenomenex, Spain) was used, operating at a flow rate of 0.5 ml min^{-1}. The employed mobile phases were: phase A: 5% methanol, 0.1 % TFA (V/V) and phase B: 90% methanol, 0.1 % TFA (V/V).

Ln-DOTA-KE-peptide

Reactivity of peptides with the new MeCAT reagent, specific for SA labelling, was monitored by electrospray ionization time-of-flight instrument (ultra- high resolution Qq-TOF-MS, Bruker Impact II ™, Germany), and with inductively coupled plasma coupled to size exclusion chromatography (SEC-ICP-MS) (the ICP-MS is an Agilent 7700, Germany).

Used size-exclusion column was Superdex peptide HR 10/30 (GE Healthcare Bio-Sciences, Sweden), where the mobile phase was pumped using a chromatographic pump (Shimadzu LC-10AD, Shimadzu Corporation, Japan) with a flow rate of 0.6 ml min^{-1}, and the injection volume of samples was 20 µl using a six-way injection valve. The employed mobile phase was ammonium acetate (50 mmoll^{-1}, pH = 6.5) introduced into the ICP-MS through a concentric nebulizer in combination with a cyclonic spray chamber.

Ln-DOTA-KE-protein

HiTrap™ Blue HP column was used to purify albumin from human serum using an Agilent 1100 system equipped with a diode array detector. Employed binding buffer was 50 mM KH_2PO_4 (pH 7.00) and elution buffer was 50 mM KH_2PO_4 + 1.5 M KCl (pH 7.00).

To monitor signals, electrospray time-of-flight instrument (ultra- high- resolution double- quadrupole time- of- flight mass spectrometry; Impact II, Bruker, Germany) was used. Two different ICP-MS systems were used, the Agilent 7500 ce(Agilent Technologies, Kyoto, Japan) and the iCAP TQ ICP-MS (Thermo Fisher Scientific, Bremen, Germany).

Both systems were coupled on-line to size exclusion chromatography (SEC) using Superdex 200 10/300 GL column (GE Healthcare Bio-Sciences, Sweden) with a mobile phase containing ammonium acetate (50 mM, pH = 6.5). The mobile phase was pumped using a chromatographic pump (Shimadzu LC-10AD, Shimadzu Corporation, Japan) with a flow rate of 0.6 ml min^{-1}, and the injection volume of samples was 20 µl using a six-way peek injection valve.

3.1. Labelling peptides with alkyne ß-keto ester

Preliminary tests were conducted on KE in order to be able to identify optimum conditions for SA detection. Different peptide sequences (H-WWCNDGR-OH ≥ 95 %), (H-QNCDQFEK-OH ≥ 95 %), and (H-DDPHACYSTVFDK-OH) with one cysteine unit were tested. Peptides disulfide bridges were initially reduced with three fold excess of TCEP to thiol-disulfide units in THAM buffer pH = 8.4, for 1 h at 50 ° C [104].

Reduced peptides were then desalted and concentrated with zip-tips to remove the used reducing agent (TCEP). Oxidation for the concentrated peptides with five-fold excess of

hydrogen peroxide (H_2O_2) (5mM) to cysteine units was carried out. Finally, eight- fold excess of synthesized KE to cysteine was added to the mixture. Labelling reaction was carried out in THAM buffer (100 mM, pH= 8.4). The mixture was left for 3 h with gentle shaking at room temperature.

Synthesis of alkyne β -ketoester (KE)

Alkyne-β-ketoester(but-3-yn-1-yl 3-oxobutanoate) was synthesized in the organic department (Prof. Dr. Christoph Arenz group), where methyl acetoacetate (1g, 8.6 mmol) was dissolved in 40 ml dry toluene. Boric acid (53 mg, 0.86 mmol) and 3-butyn-1-ol (1g, 14.3 mmol) were added to the methyl acetoacetate/toluene solution. Reaction was kept under vacuum and was refluxed for 24 h. Solvents were removed under reduced pressure. The crude product was purified by flash column chromatography (SiO_2, hexane/ethyl acetate: 15/1) to obtain KE (950 mg, 73 % yield), as a pale yellow to colorless liquid where it was kept at -20° C in acetonitrile.

^{1}H NMR 300 MHZ (ppm, $CDCl_3$) :4.21 (2H, t J=6.8 Hz), 3.48 (2H, s), 2.59-2.54 (2H, dt J=6.8, 2.7 Hz), 2.29 (3H,s), 2.00(1H, t J=2.7). 13C NMR ($CDCl_3$, 75 MHZ): 200.22, 166.83, 79.70, 70.12, 62.99, 49.92, 30.16, 18.89. ESI-MS (6 mM sample): $(M+H)^+$ = *m/z* 155.02, $(M+Na)^+$ = 177.01. Calculated MW of $C_8H_{10}O_3$: 154.16 u [105,106].

3.2. Preparation of the labelling reagent (Ln-DOTA-KE)

Azide-DOTA metallation

Azide-DOTA metallation was carried out using ten-fold excess of lanthanide salts (Figure 22) ($YbCl_3.6H_2O$,$HoCl_3.6H_2O$, $TbCl_3.6H_2O$, $EuCl_3.6H_2O$ and $NdCl_3.6H_2O$). Azide-DOTA (8.39×10^{-3} mmol) was added to lanthanide solution (ten- fold excess of Ln dissolved in 110 mM sodium acetate buffer, pH= 6.20). The reaction was left for 2 h in darkness with gentle shaking. Ln-azide-DOTA solution was purified using the C_{18} column and monitoring the signals at 215 and 280 nm [104].

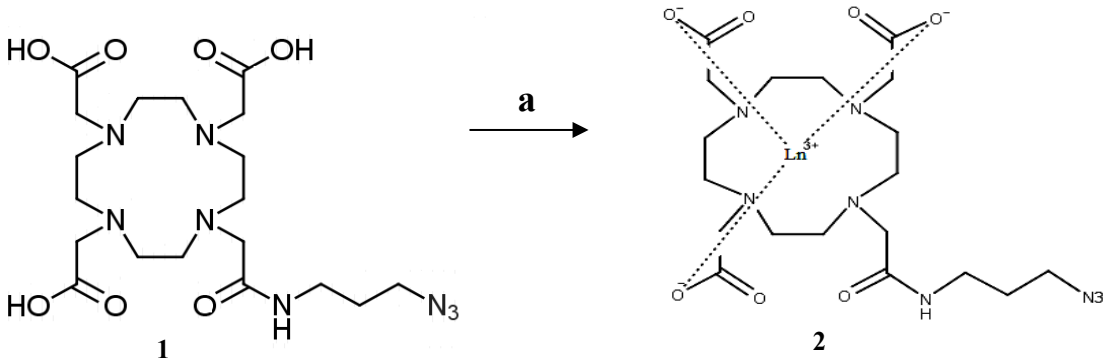

Figure 22.Azide- DOTA metallation where a) ten-fold excess of Ln dissolved in 110 mM sodium acetate buffer, pH 6.20. The reaction was left for 2 h in darkness with gentle shaking.

Copper-catalyzed azide-alkyne cycloaddition (CuAAC) of Ln-DOTA with KE

Copper catalyzed azide alkyne cycloaddition (CuAAC), click reaction, was carried out to perform the selective reaction between Ln- DOTA and synthesized KE (Figure 23).

The reaction was carried out according to the following order; KE **2** (4 mM) was mixed with TEAA buffer (100 mM, pH= 7.00). Two-fold excess of Ln-DOTA **1** (8 mM) to KE **2**was added. THPTA (500 µM) and copper (II) sulfate (100 µM) were premixed in 5:1 ratio and then added to the mixture. Finally sodium ascorbate (5 mM) was added. The reaction was carried out in 500 µl TEAA buffer, left in darkness for 1 h under sonication to yield compound **3**[107,108]. Compound **3** was purified using C_{18} column and monitored at 260 and 280 nm.

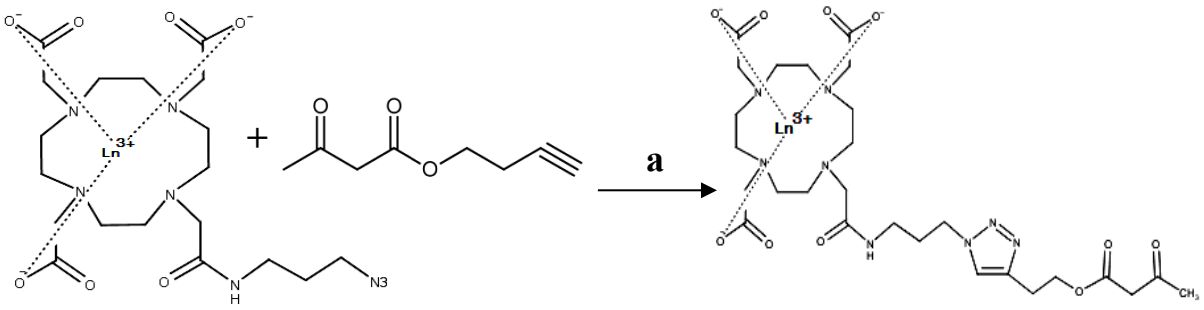

1 **2** **3**

Figure 23.Click reaction between KE and Ln-DOTA. a) azide: alkyne (2:1), THPTA: Cu(II) SO_4 (5:1), sodium ascorbate (5mM), TEAA (100 mM, pH =7), sonication in darkness, 1h.

3.3. Elemental labelling and mass spectrometry for the specific detection of sulfenic acid groups in model peptides: a proof of concept

Peptides labelling with Ln-DOTA-KE

The three different peptide sequences were oxidized and labelled with the purified Ln-DOTA KE (Figure 24). Previously optimized SA capture conditions with KE alone for the different peptides (mentioned in oxidation of peptides and labelling with KE) were used for SA labelling with the new reagent (Ln-DOTA-KE). In this case, comparable labelling efficiencies for SA with KE and Ln-DOTA-KE were observed.

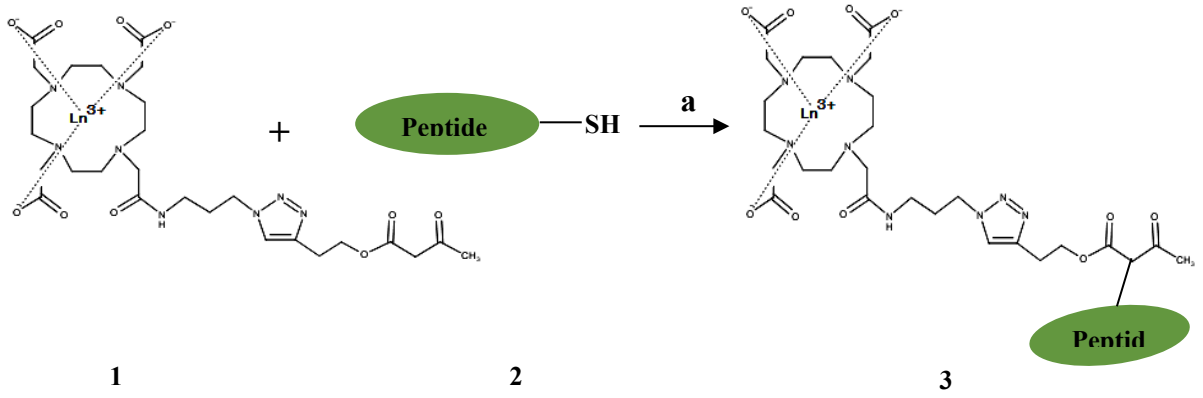

Figure 24. SA labelling with Ln-DOTA-KE a) hydrogen peroxide (H_2O_2) (5mM) (five-fold excess to cysteine), Ln-DOTA-KE (eight- fold excess to cysteine), THAM buffer 100 mM, pH= 8.4, 3h, shaking at room temperature.

3.4. Detection of sulfenic acid in intact proteins by mass spectrometric techniques: application to serum samples

Evaluation of SA labelling in ß-lactoglobulin

Ho-DOTA-KE was used to label ß-lactoglobulin (BLG) as protein model susceptible to be oxidized in the free cysteine to form SA. For this aim, BLG solution of 90µM was prepared in THAM buffer (pH = 8.4). For SA labelling in BLG, BLG was denaturated in 8 M urea and then oxidized with different excess ratios of hydrogen peroxide (H_2O_2) (5mM).

Finally, 30- fold excess of Ho-DOTA-KE to cysteine was added to the mixture. Labelling reaction was carried out in THAM buffer (100 mM, pH= 8.4). The mixture was left for 4 h with gentle shaking at room temperature. Labelling reaction was monitored with LC-ESI-MS and SEC-ICP-MS.

Evaluation of SA labelling in albumin standards and serum samples

Nd-DOTA-KE was used to label intact albumin first as protein models susceptible to be oxidized in the free cysteine to form SA. For this aim, an albumin solution of 90µM was prepared in THAM buffer (pH = 8.4). For SA labelling in human serum albumin (HSA), HSA was denaturated in 8 M urea and then oxidized with different excess ratios of hydrogen peroxide (H_2O_2) (5mM). Finally, 30- fold excess of Nd-DOTA-KE to cysteine was added to the mixture. Labelling reaction was carried out in THAM buffer (100 mM, pH= 8.4). The mixture was left for 4 h with gentle shaking at room temperature.

In the case of the serum sample, the protein was previously purified from the remaining proteins using affinity chromatography on a HiTrap™ Blue HP column and the signal was monitored at 280 nm. Collected albumin fractions were lyophilized and cleaned through 30KDa amicons in order to remove any traces of salts that might affect further labelling

reactions. Labelling of the oxidized HSA was conducted under the same conditions as carried out in the albumin standard. Labelling signal for albumin (Nd-DOTA-KE-SA) was monitored with LC-ESI-MS and SEC-ICP-MS.

Quantification of the labelled SA by IDA-SEC-ICP-MS

The isotopically enriched ^{145}Nd standard was used for post column isotope dilution analysis (ID-SEC-ICP-MS). For this aim, a continuous flow of the tracer (0.1 ml/min) was added and mixed with the column eluent using a T piece. The concentration of the spiked solution (^{145}Nd) was firstly estimated using a natural Nd standard solution. Further calibration using reverse ID-ICP-MS analysis was performed to measure the precise concentration of the spike solution [100].

Optimum ratio between Nd standard and spike was experimentally determined $(R_m)^{142}Nd/^{145}Nd$, [109] and 20 μL loop was used for introducing the sample of labelled SA with Nd-DOTA-KE. A 5ppb solution of ^{145}Nd prepared in 2% HNO_3 was finally used. All samples were precisely weighed using a four-digit analytical balance.

Protein electrophoresis

In order to test the purity of the labelled product, separation of the labelled human serum albumin was carried out by using sodium dodecyl sulphate- polyacrylamide gel electrophoresis (SDS-PAGE) according to the Laemmli gel system [31]. Proteins were separated by 10% SDS-PAGE under denaturating conditions (boiled for 1 min in 4x SDS sample buffer before loading into the gel) by using a Bio- Rad electrophoresis system.

4. Results and discussion

4.1. Alkyne ß-Keto ester reactivity

Once reactive oxygen species (ROS) are generated, thiols in cysteine residues (-SH) are targeted due to their low redox potential. Sulfur attributes strong nucleophilic character due to its large size which makes it readily polarizable beside the readily accessible lone pairs of electrons.

H_2O_2-mediated oxidation of cysteine residues within proteins is a well-known mechanism of redox signalling that can also conduct to further cell damage. Cysteine residue exist as a thiolate anion ($Cys–S^-$) at physiological pH and are more susceptible to oxidation compared with the protonated cysteine thiol (–SH) [18].

The nucleophilic attack of protein thiolate on the electrophilic H_2O_2 releases water and results in cysteine sulfenic acid (SA) (-SOH) formation. Several detection methods were invented for SA detection, exploiting whether the electrophilic or the nucleophilic character of the SA transient state (-SOH), by the use of different probes such as dimedone or activated halogenated compound such as 4-chloro-7nitrobenzo-2-oxa-1,3-diazole (NBD-Cl), respectively [97,105,110].

However, the vast majority of probes tackled the unique electrophilic character of sulfur in cysteine SA detection. Dimedone and alkyne ß-keto esters probes, owing active methylene groups, provided examples for the electrophilic character of SA, where SA residues act as electrophiles and react selectively with such probes (Figure 25). The rate of probes reactivity is based on the surrounding microenvironment of the protein [110].

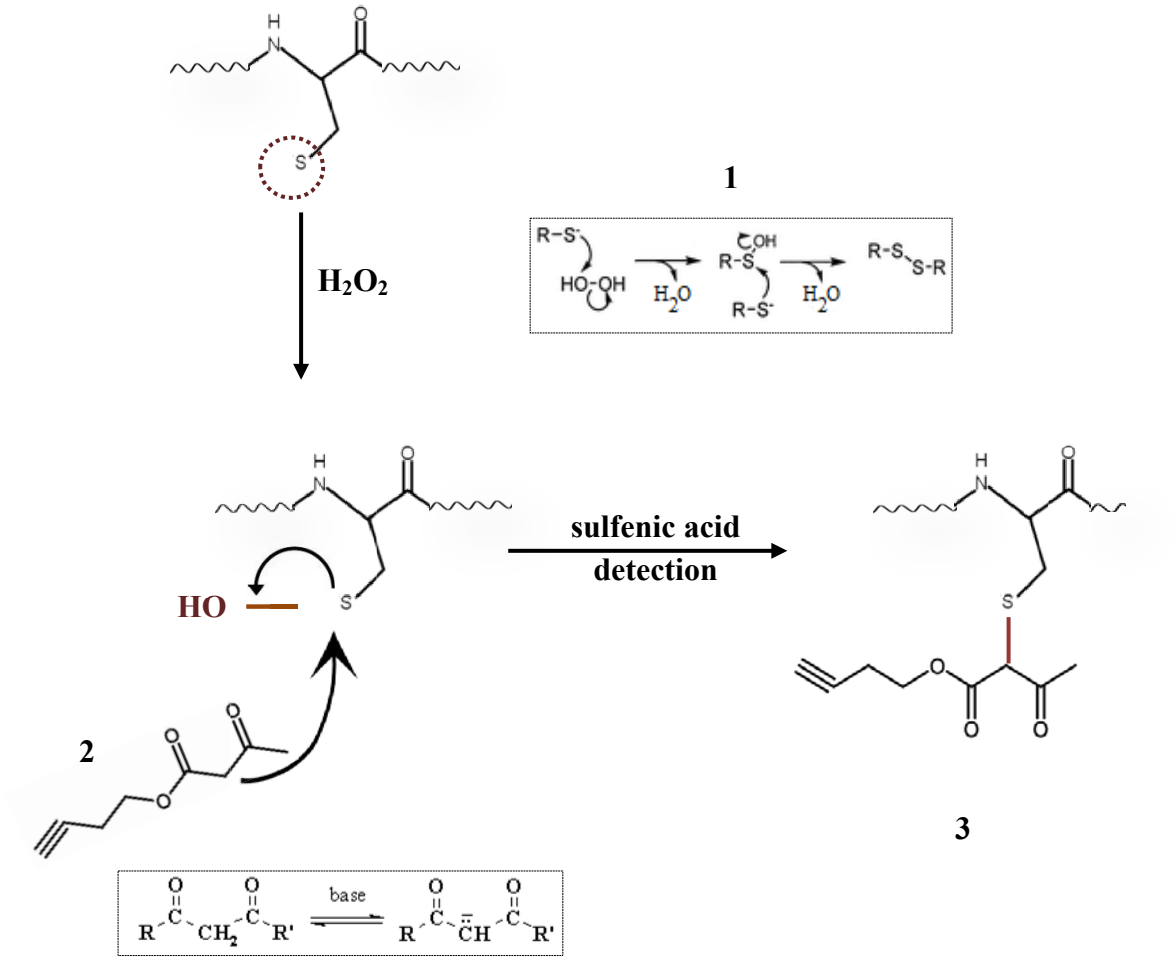

Figure 25. Nucleophilic attack of thiolate anion on electrophilic hydrogen peroxide (H_2O_2) releases water and results in the formation of sulfenic acid (SA) whereas SA formation is considered reversible as it can be reduced back with another thiol and form a disulfide bridge (1) . SA can act as an electrophile and reacts selectively with alkyne ß-keto ester (KE) (2) , therefore SA can be detected with the use of such probes (3).

4.2. Labelling peptides with alkyne ß-keto ester

Direct reactivity of alkyne ß-keto ester(KE) with different peptide sequences, each with one cysteine unit, was tested before labelling of SA with the new synthesized reagent Ln-DOTA-KE. The standard peptides studied were selected because of their presence within bovine serum albumin (BSA) or lysozyme sequences; they have one cysteine residue, and were successfully identified by ESI-MS [111].

To obtain efficient SA labelling, different preliminary tests were conducted for SA oxidation with different buffers and pH ranges, as well as different concentrations of KE with respect to thiol groups. As cysteine units are usually present in the form of disulfide bridges (-S-S-), three-fold excess of TCEP (reducing agent) per disulfide bond was used to pre-reduce the existing disulfide bridges back to the free thiol (-SH) form. Denaturation was achieved by heating the mixture at 50° C for 1 h. The reduced peptides were then desalted and concentrated with ziptips to remove the used reducing agent (TCEP). Then free cysteines were oxidized with H_2O_2, where the optimum oxidation conditions were found to include five- fold excess of H_2O_2 (5 mM) [97].

Also, different buffer solutions were evaluated as solvents for SA labelling with KE, including TEAB, TEAA and THAM buffers with pH ranging from 5.00- 8.50. High pH values were avoided (pH >8.50) as they can eventually cause degradation of DOTA in the synthesized reagent (Ln-DOTA-KE). Besides that, the use of high pH values can cause the formation of some adducts, such as the formation of iso-aspartate because of the presence of aspartic acid (D) and glycine(G) in the peptide sequence used (e.g. H- WW**C**NDGR- OH) (peptide structure can be seen in the Appendix Figure 1) . Low pH values (pH < 5.00) were

also avoided as they can affect the metallation of azide- DOTA. Effective labelling for SA was achieved with THAM buffer (pH range 8.00-8.40).

Different concentrations of KE were also tested, ranging between four-fold to ten-fold excess of KE with respect to thiol groups (-SH). The experiments were monitored at 1, 3, and 6h, with gentle shaking at room temperature. The results showed that eight- fold excess of KE with 3 h of gentle shaking at room temperature was enough for efficient labelling. The labelling reaction was monitored by LC- ESI-MS. As shown in Figure 26, SA was successfully labelled in three different peptide sequences with the synthesized KE .However, relatively high intensities for other oxidation products of cysteine (-S-S-)and over oxidized moieties ($-SO_2H$, $-SO_3H$) shown in the inset of Figure 26 were observed in all cases.

These species showed maximum intensities at retention times different from that of the labelled SA (see the insets) but the KE did not show any reactivity towards them or towards any other amino acid residue of the model peptides.

This is consistent with the reported selectivity of KE towards SA [105]. In addition, no signal corresponding to the unlabelled peptide with SA group was detected, which suggests a quantitative labelling reaction.

Labelling the second peptide sequence DDPHA**C**YSTVFDK (Figure 26-B) revealed the presence of relatively high levels of unlabelled sequences (-SH, -S-S-) and over oxidized moieties ($-SO_2H$ and $-SO_3H$). The presence of a high amount of -SH can be attributed to the hard accessibility to thiol groups (see Figure 27for the 3D structure of the peptide obtained by molecular modelling). This peptide can also lose the two aspartic acid units (DD), and this can lead to the formation of different adducts (peptide structure can be seen in the Appendix Figure 2).

For last peptide sequence, QN**C**DQFEK (Figure 26-C), we observed, together with the labelled product, a relatively high formation of the unlabelled and overoxidized species.

As previously reported for the other two peptides, no signal corresponding to the unlabelled peptide with the SA group was detected, which suggests a quantitative labelling reaction. It should be mentioned that N- terminal glutamine residue can readily cyclize to the pyroglutamyl derivative which might induce the loss of NH_3 (peptide structure can be seen in the Appendix Figure 3).

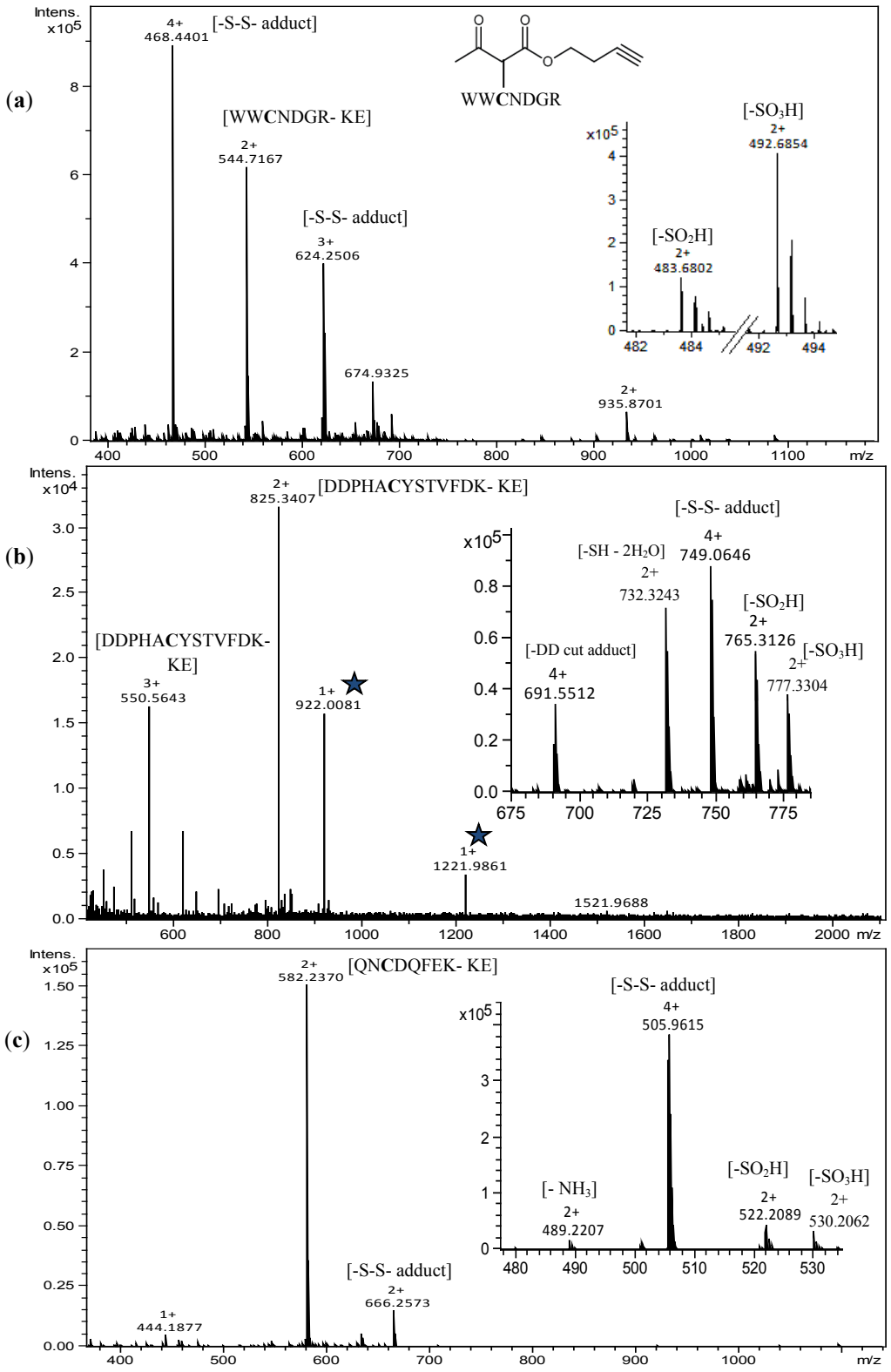

Figure 26. Mass spectrum obtained by ESI-q-TOF for (a) labelled SA in WWCNDGR with KE (expected *m/z*, 544.7163, z= 2), (b) labelled SA in DDPHACYSTVFDK with KE (expected *m/z*, 825.3430, z=2 and 550.5644, z=3), and (c) labelled SA in QNCDQFEK with KE (expected *m/z*, 582.2373, z=2). Note: calibration solution signal is indicated with a *star*.

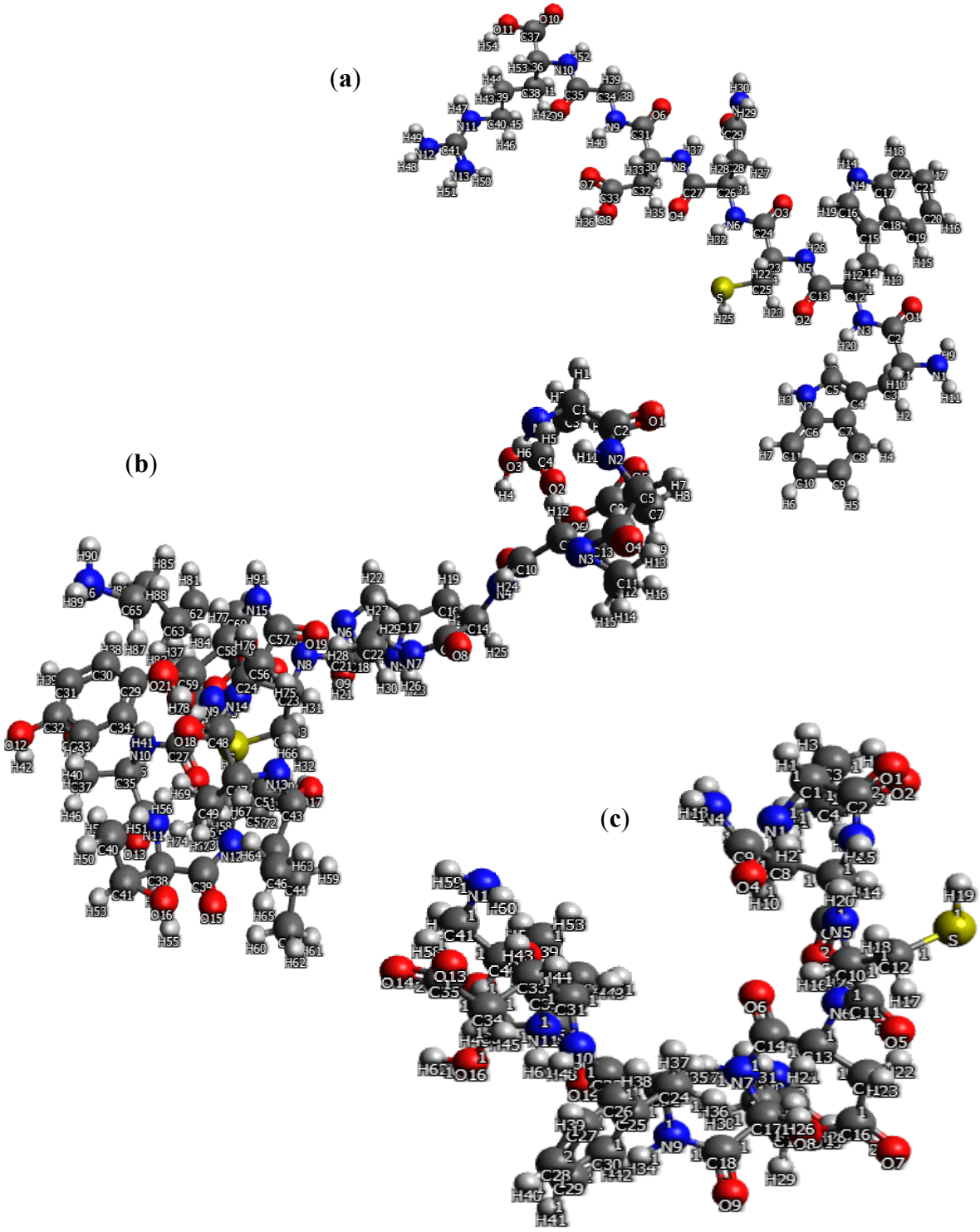

Figure 27.3D structure of (a) WWCNDGR peptide, (b) DDPHACYSTVFDK and (c) QNCDQFEK peptide. Thiol group (sulfur atom) is pointed out in yellow color. As can be seen in the two peptide sequences (a) WWCNDGR and (c) QNCDQFEK the thiol group is easily accessible, while in the longer peptide sequence (b) DDPHACYSTVFDK steric hindrance can reduce the accessibility to thiol group.

4.3. Preparation of the labelling reagent (Ln-DOTA-KE)

Azide-DOTA metallation

Azide- DOTA metallation was evaluated with five different Ln metals (Yb, Ho, Tb, Eu and Nd). Since the DOTA chelating agent is a macrocyclic compound that can hold a metal ion in the inner structure, the stability of the metal- containing species will be dependent on the "fitting" of the metal ion into the macrocyclic cavity. Thus, five different Ln metals (Yb, Ho, Tb, Eu and Nd) (with different ionic radii 86.8, 90.1, 92.3, 94.7 and 98.3 pm, respectively) that provide good sensitivities in the ICP-MS detection were selected [112,113].

For this aim, ten-fold excess of Ln salts was used to ensure efficient metallation of DOTA. As Ln ions show strong complexing behavior with some buffers, different buffers (TEAA, TEAB, ammonium and sodium acetate) with pH ranging from 6.00 to 9.00 were tested for metallation studies.

Sodium acetate buffer was selected for DOTA metallation in pH ranges between 6.00 and 7.00, as high pH values can cause faster decomposition for azide- DOTA and low pH values might induce the release of lanthanide metals from DOTA. Two hours of gentle shaking or incubation at 37˚C was enough for efficient metallation of azide-DOTA with all the Ln metals. Figure 28shows the ESI-MS spectra obtained for Ho and Tb- DOTA metallation. Figure 29shows the ESI-MS spectra obtained for Eu, Yb and Nd- DOTA metallation where the isotopic distributions for the used Ln can be clearly seen. The LC- ESI-MS results and mass errors for the obtained Ln-DOTA were calculated and are shown in Table 1-A.

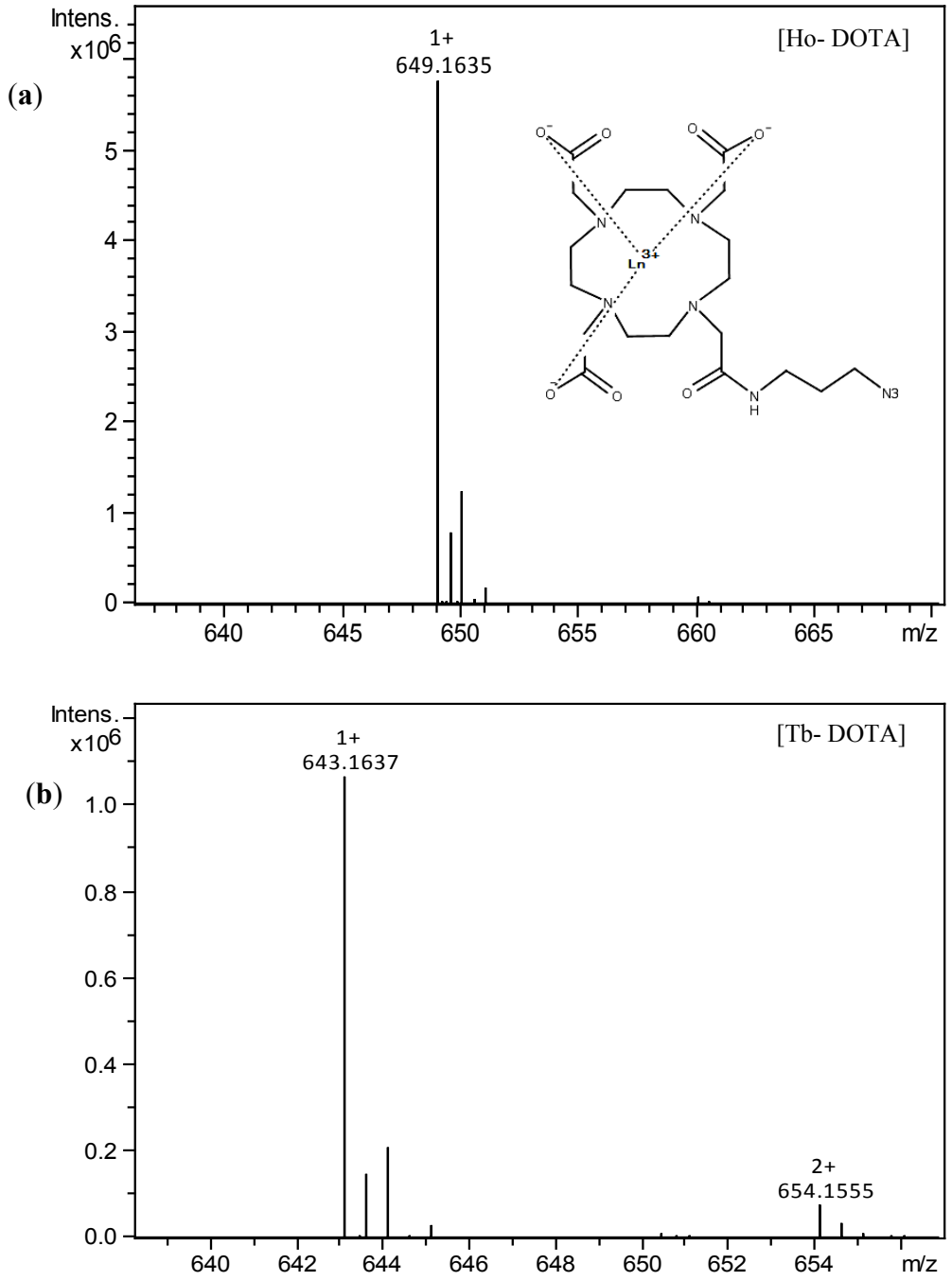

Figure 28. Mass spectrum obtained by ESI-q-TOF for metallated DOTA. The Ln metals used were a) ^{165}Ho (expected *m/z* Ho-DOTA 649.1691) and b) ^{159}Tb (expected *m/z* Tb-DOTA 643.1641).

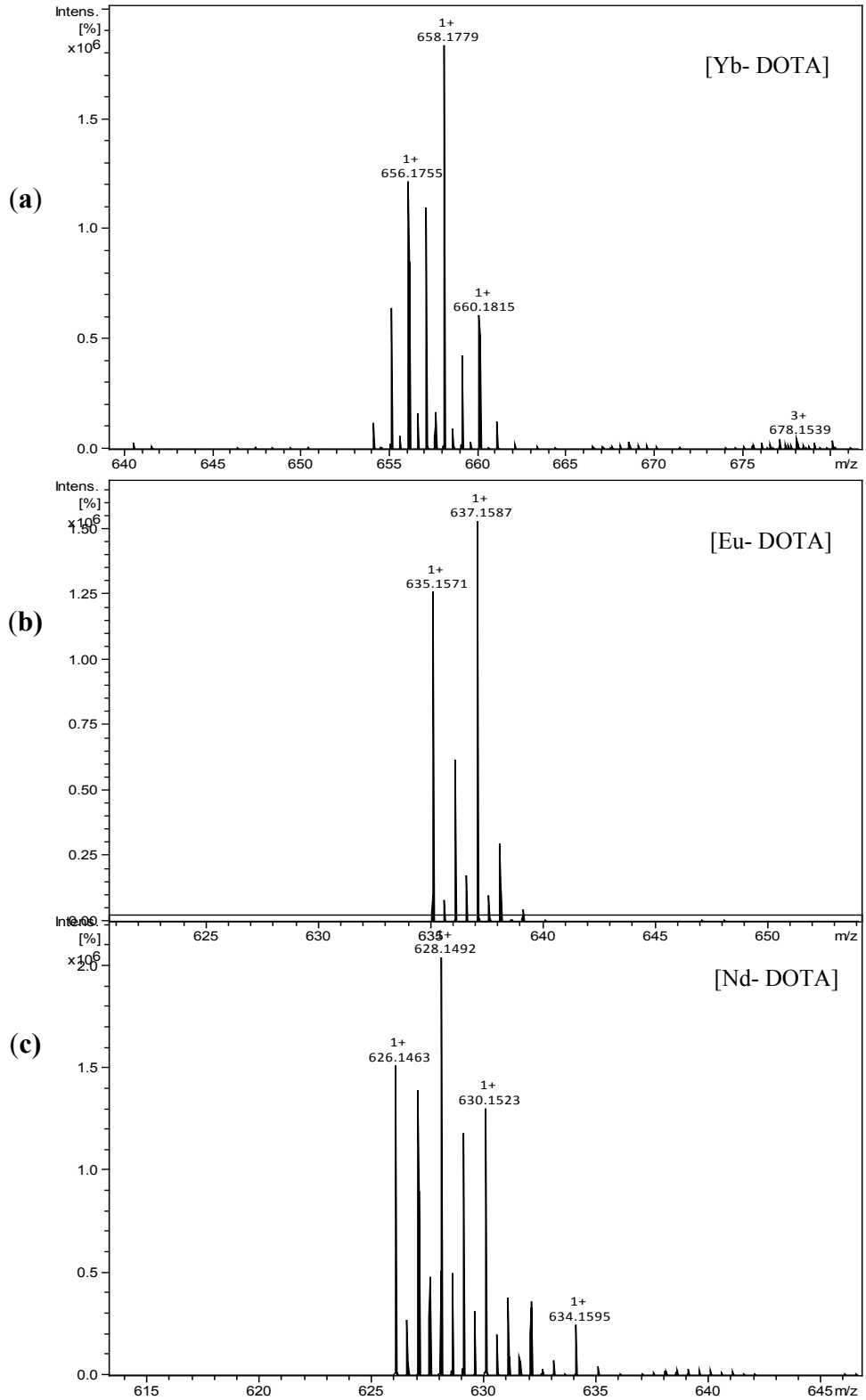

Figure 29. Mass spectrum obtained by ESI-q-TOF for metallated DOTA. The poly-isotopic Ln metals used were a) Yb (expected *m/z*^{172}Yb-DOTA 658.1779), b) Eu (expected *m/z*^{153}Eu-DOTA 637.1602) and c) Nd (expected *m/z*^{142}Nd-DOTA 628.1492).

Table 1. LC-ESI-MS results and mass errors for a) Ln containing DOTA (Ln-DOTA) and b) the product formed by click reaction ,CuAAC reaction , of Ln-DOTA and KE (Ln-DOTA-KE) .

a)	Formula Ln- DOTA	MW $[M+H]^+$ theoretical/ experimental	Δ M* (ppm)
	$C_{19}O_7N_8H_{31}Yb^+$	658.1779/658.1779	---
	$C_{19}O_7N_8H_{31}Ho^+$	649.1691/ 649.1635	-8.62
	$C_{19}O_7N_8H_{31}Tb^+$	643.1641/ 643.1637	-0.62
	$C_{19}O_7N_8H_{31}Eu^+$	637.1602/ 637.1587	-2.35
	$C_{19}O_7N_8H_{31}Nd^+$	628.1492/ 628.1492	---
b)	Formula Ln-DOTA-KE		
	$C_{27}O_{10}N_8H_{41}Yb^+$	812.2411/ 812.2418	0.86
	$C_{27}O_{10}N_8H_{41}Ho^+$	803.2321 / 803.2306	-1.86
	$C_{27}O_{10}N_8H_{41}Tb^+$	797.2271/ 797.2257	-1.75
	$C_{27}O_{10}N_8H_{41}Eu^+$	791.2233 / 791.2218	-1.89
	$C_{27}O_{10}N_8H_{41}Nd^+$	782.2124/ 782.2120	-0.51

* Δm = (mass error/ exact mass) $*10^6$

Copper-catalyzed azide-alkyne cycloaddition (CuAAC) of Ln-DOTA with KE

The selective reactivity of azides (azide- DOTA) and alkynes (alkyne ß-ketoester) motivated the preparation of Ln-DOTA-KE for the specific detection of sulfenic acid (SA). Huisgen's 1,3-dipolar cycloaddition of organic azides and alkynes results in the formation of 1,2,3-triazoles[114]. Uncatalyzed azide-alkyne cycloadditions are often slow even at elevated temperatures and produce mixtures of the regioisomers 1,4- and 1,5- disubstitutes 1,2,3-triazoles, whereas the discovery of copper(I)-catalyzed azide-alkyne cycloaddition (CuAAC) resulted in the regioselective 1,4-disubstituted triazole formation under mild conditions (Figure 30).

Therefore, being widely known as a selective reaction between azides and alkynes, Cu catalyzed reaction was carried out between azide-DOTA and alkyne KE. CuAAC requires the use of copper catalyst in its Cu (I) oxidation state. Cu(I) oxidation state is usually maintained by mixing the copper catalyst with an appropriate chelating agent. A major drawback for the use of Cu(I)is that it requires air-free techniques that can be difficult to perform [107,108].

Therefore, copper (II) sulphate ($CuSO_4$) was used instead, where it was reduced *in situ* with sodium ascorbate (reducing agent).THPTA was used as a water soluble ligand with copper. As the performance of the ligand (THPTA) with the catalyst (Cu) was found to be sensitive to the catalyst concentration, an excess of THPTA ligand was recommended [108]. Efficient reactions were obtained with a 5:1 ratio of THPTA: Cu.

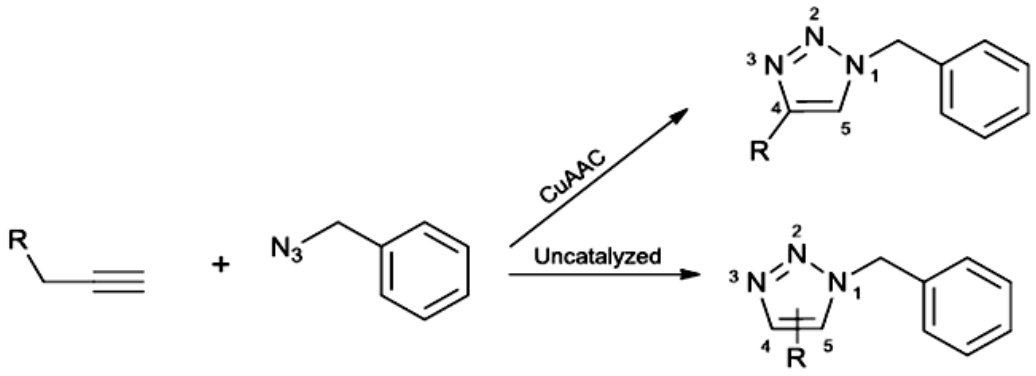

Figure 30. The effect of using Copper catalyst on the Huisgen 1,3-cycloaddition reaction. CuAAC: Copper(I)-catalyzed azide-alkyne cycloaddition.

The presence of high Cu and sodium ascorbate concentrations was found to mediate destructive side reactions as it can mediate ROS and ascorbate byproducts generation [115]. However, the use of five equivalents of THPTA ligand was sufficient to accelerate the decomposition of the formed ROS. For the used THPTA: Cu ratio (5:1), 2.5 mM of sodium ascorbate was enough to enhance the CuAAC reaction and avoid the harmful effects resulting from the presence of high Cu-sodium ascorbate concentrations[116,117].

CuAAC reaction was found to be sensitive for the nature of the used solvent, therefore regarding buffer selection, THAM buffer was avoided as it can be competitive and inhibitory ligand for Cu. Being compatible with CuAAC reaction, TEAA buffer was used (100 mM,

pH= 7.00) [107].As the ligand performance (THPTA: Cu) can be inhibited in the presence of an excess of alkyne (KE), KE concentration was kept below 5mM. Two-fold excess of azide(Ln -DOTA) with respect to alkyne groups was used, azide: alkyne 2:1 ratio, to obtain an efficient CuAAC reaction [107,108].

In addition, CuAAC reaction was carried out according to a specific order of chemicals addition. In the first place KE was mixed with TEAA buffer (100 mM, pH= 7.00) and then two-fold excess of Ln- DOTA to KE was added. After that THPTA and copper (II) sulfate were premixed in 5:1 ratio and then added to the mixture. Finally sodium ascorbate was added to start the reaction. One hour of sonication was enough to complete the CuAAC reaction. CuAAC reaction was kept protected from light to maintain the efficiency of sodium ascorbate [107,108].

LC-ESI-MS was used to monitor the product of the click reaction. The efficiency of the CuAAC reaction was tested with all the metallated DOTA from previous section. Figure 31 shows the ESI- MS spectra corresponding to the click reaction with Ho and Tb. Figure 32shows the ESI- MS spectra corresponding to the click reaction with Yb, Eu and Nd. Table 1-B shows the mass accuracy for the product of the click reaction which seems to be adequate in all metallated Ln. Ln-DOTA-KE was then purified for further use in SA detection.

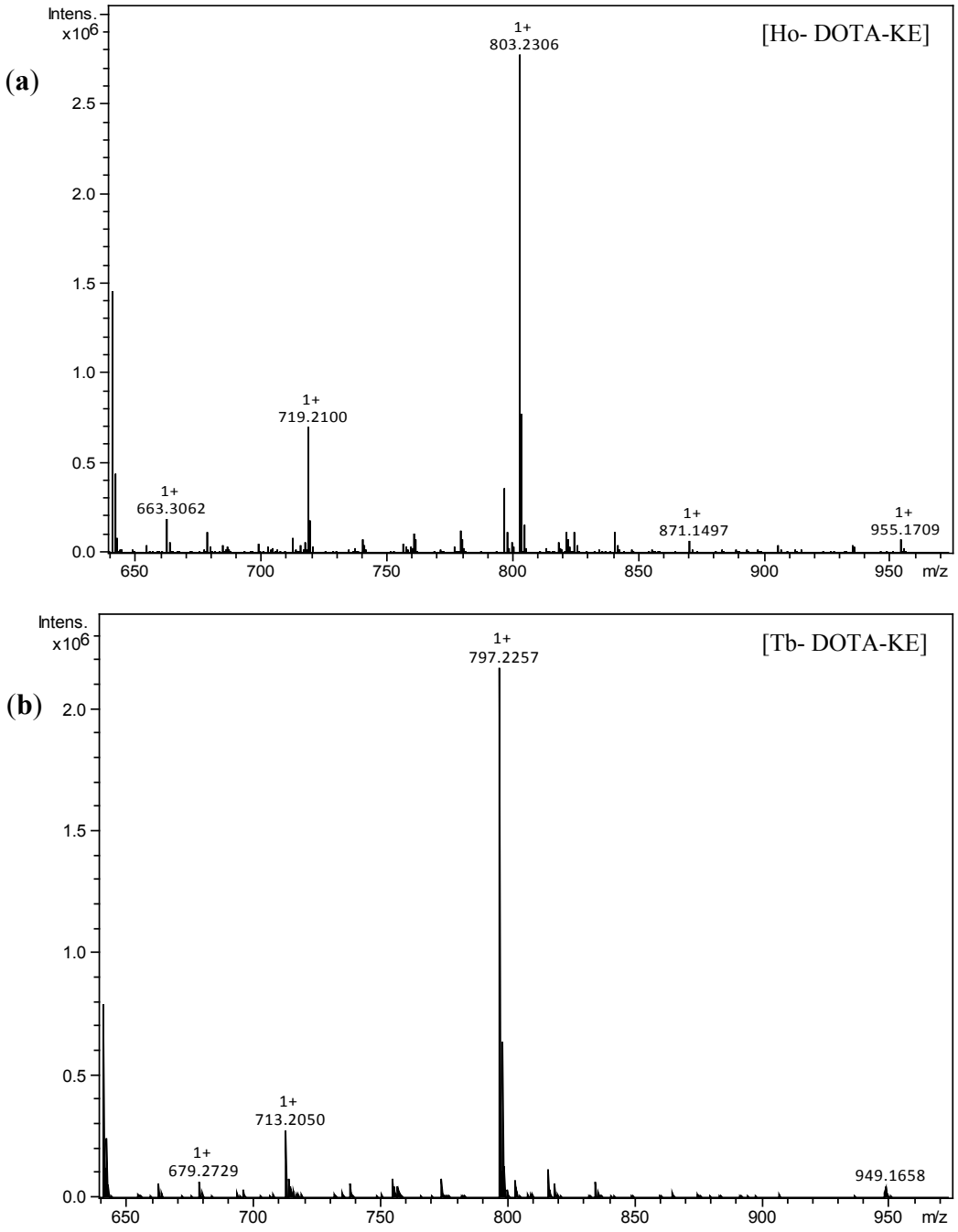

Figure 31. Mass spectrum obtained by ESI-q-TOF mass spectrometry for Ln-DOTA-KE. The Ln metals used were a) ^{165} Ho (expected *m/z* Ho-DOTA-KE 803.2321) and b) ^{159} Tb(expected *m/z* Tb-DOTA-KE 797.2271).

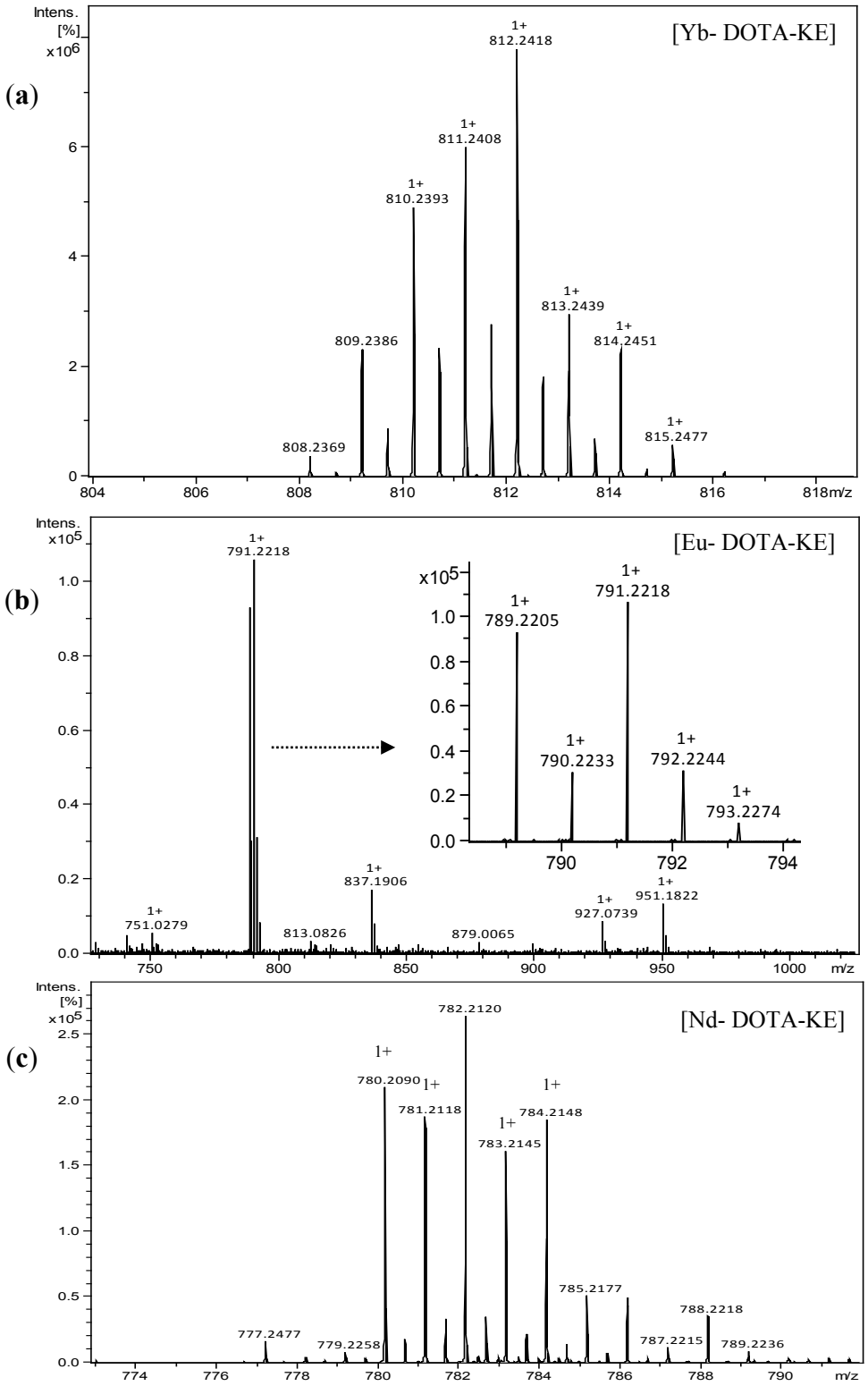

Figure 32.Mass spectrum obtained by ESI-q-TOF mass spectrometry for Ln-DOTA-KE. The poly-isotopic Ln metals used were a) Yb (expected *m/z*^{172}Yb-DOTA-KE 812.2411) , b) Eu (expected *m/z*^{153}Eu-DOTA-KE 791.2233) and c) Nd (expected *m/z*^{142}Nd-DOTA-KE 782.2124).

Although all the lanthanides have been successfully evaluated in this study by SEC-ICP-MS although, for simplicity, only the results of Ho-DOTA-KE and Nd-DOTA-KE are shown in Figure 33. These chromatographic profiles show the signals Ln-DOTA and Ln-DOTA-KE using two different SEC columns (which will be eventually used for the purification of labelled peptides and proteins) to monitor the elution time of the labelling reagent Ln-DOA-KE.

Figure 33-A shows Ho-DOTA (blue) and Ho-DOTA-KE (black) using ICP-MS monitoring Ho signal with SEC superdex peptide column, whereas Figure 33-B shows Nd-DOTA (blue) and Nd-DOTA-KE (black) using ICP-MS monitoring Nd signal with SEC superdex 200 column.

As can be observed, the two species show different elution times, with a shift to lower retention times in the case of Ho-DOTA-KE and Nd-DOTA-KE. This shift is expected since after the click reaction KE is added to the Ln-DOTA increasing its molecular weight by 154 u. As earlier elution time in SEC is attributed to larger compounds, comparison between Ln- DOTA and Ln-DOTA-KE addresses, together with the ESI-MS data, the formation of Ln-DOTA-KE.

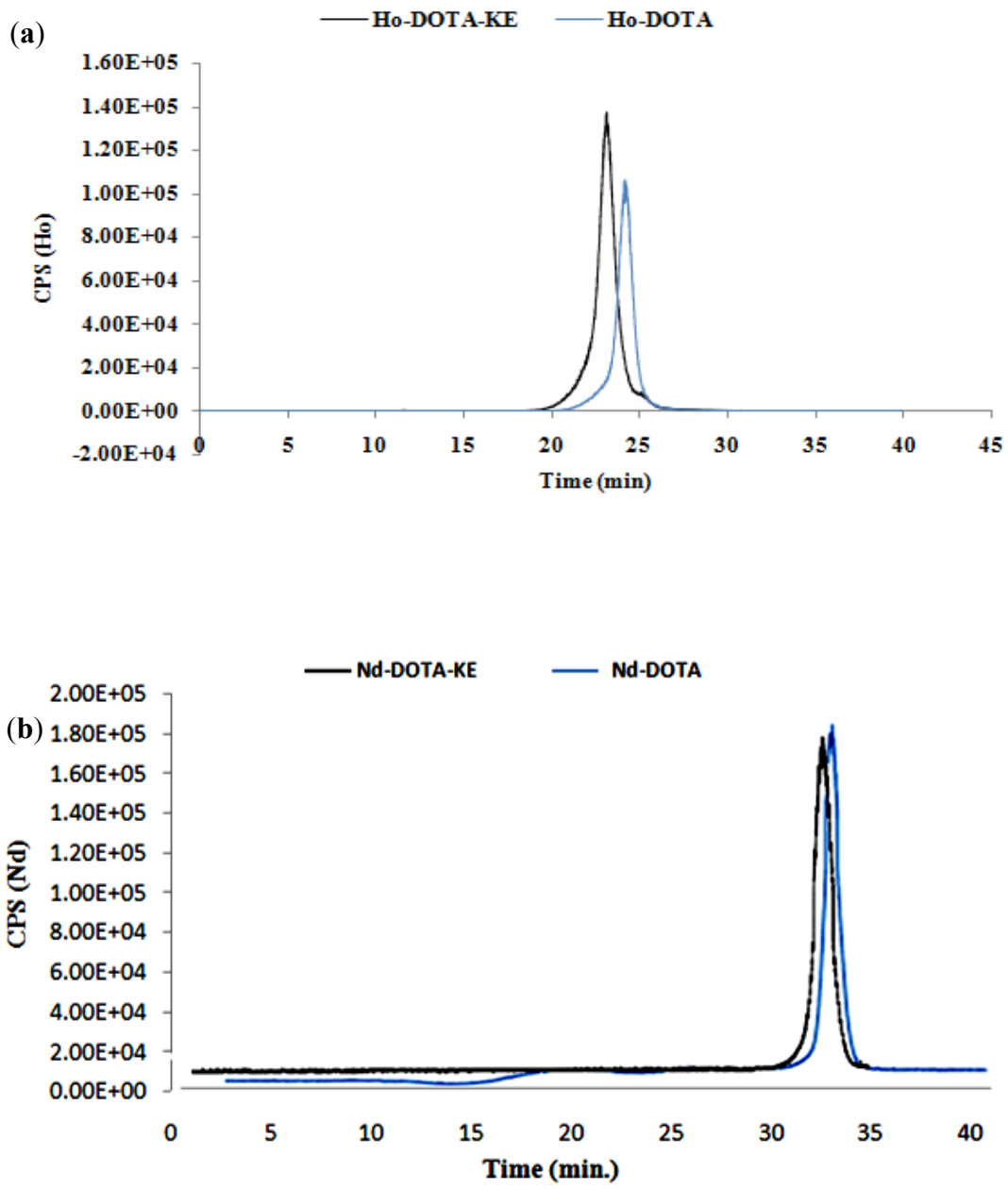

Figure 33. Chromatograms obtained by SEC-ICP-MS of a) Ho-DOTA and Ho-DOTA-KE using superdex peptide 10/300 GL column and b) Nd-DOTA and Nd-DOTA-KE using superdex 200 10/300 GL column. The isotopes monitored were ^{165}Ho and ^{142}Nd. Earlier elution is observed for Ho-DOTA-KE and Nd-DOTA-KE.

4.4. Elemental labelling and mass spectrometry for the specific detection of sulfenic acid groups in model peptides: a proof of concept

Peptides labelling with Ln-DOTA-KE

The previously optimized conditions for labelling the SA with KE were used with the new reagent Ln- DOTA- KE. Peptides were pre-reduced with three- fold excess of TCEP to cysteine disulfide bond for 1 h at 50° C. Reduced peptides were then desalted and concentrated with ziptips to remove the used reducing agent (TCEP). As Ln- DOTA- KE is to be used in this step, desalting is important to remove TCEP from the mixture as it can cause decomposition of the used azide- DOTA.

Then the concentrated peptides were oxidized with five-fold excess of H_2O_2 (5 mM) to cysteine units (as previously described), followed by the addition of eight-fold excess of Ln-DOTA-KE. The labelling reaction was performed in THAM buffer (100 mM, pH= 8.40). For the complete labelling reaction, the mixture was left for 3 h with gentle shaking at room temperature. The reaction product was monitored by LC-ESI-MS (Figure 34) and SEC-ICP-MS (Figure 35).

As can be observed, the ESI-MS signal for the labelled SA in WW**C**NDGR peptide sequence with Tb-DOTA-KE was obtained (Figure 34 A) at *m/z* 577.5306 (+3 ion). Regarding the over oxidized adducts, high sulfinic acid ($-SO_2H$) intensity was observed in Tb-DOTA-KE-WW**C**NDGR, where no sulfonic acid ($-SO_3H$) was found. As before, the presence of unlabeled SA in WW**C**NDGR was not observed in the mass spectra, exhibiting a complete labelling reaction.

The LC-ESI-MS results and mass errors for the obtained Tb-DOTA-KE-WW**C**NDGR were calculated and are shown in Table 2-A.Regarding the second peptide sequence

DDPHA**C**YSTVFDK, the results revealed the labelled product at *m/z* 766.9527 (+3 ion)and relatively higher intensities of sulfinic(- SO_2H) and sulfonic (-SO_3H) acids formation. The LC-ESI-MS results and mass errors for the obtained Ho-DOTA-KE-DDPHA**C**YSTVFDK were calculated and are shown in Table 2- B.

Finally, for the last tested peptide sequence QN**C**DQFEK, the labelled species showed *m/z* 907.3264 (+2 ion). Although the three peptide sequences were labelled according to the ESI-MS data, it is not possible to draw any conclusion on the labeling efficiency on the light of these results. Thus, the three sequences were analyzed by SEC-ICP-MS in order to extract semi-quantitative data (since no calibration curve was conducted).

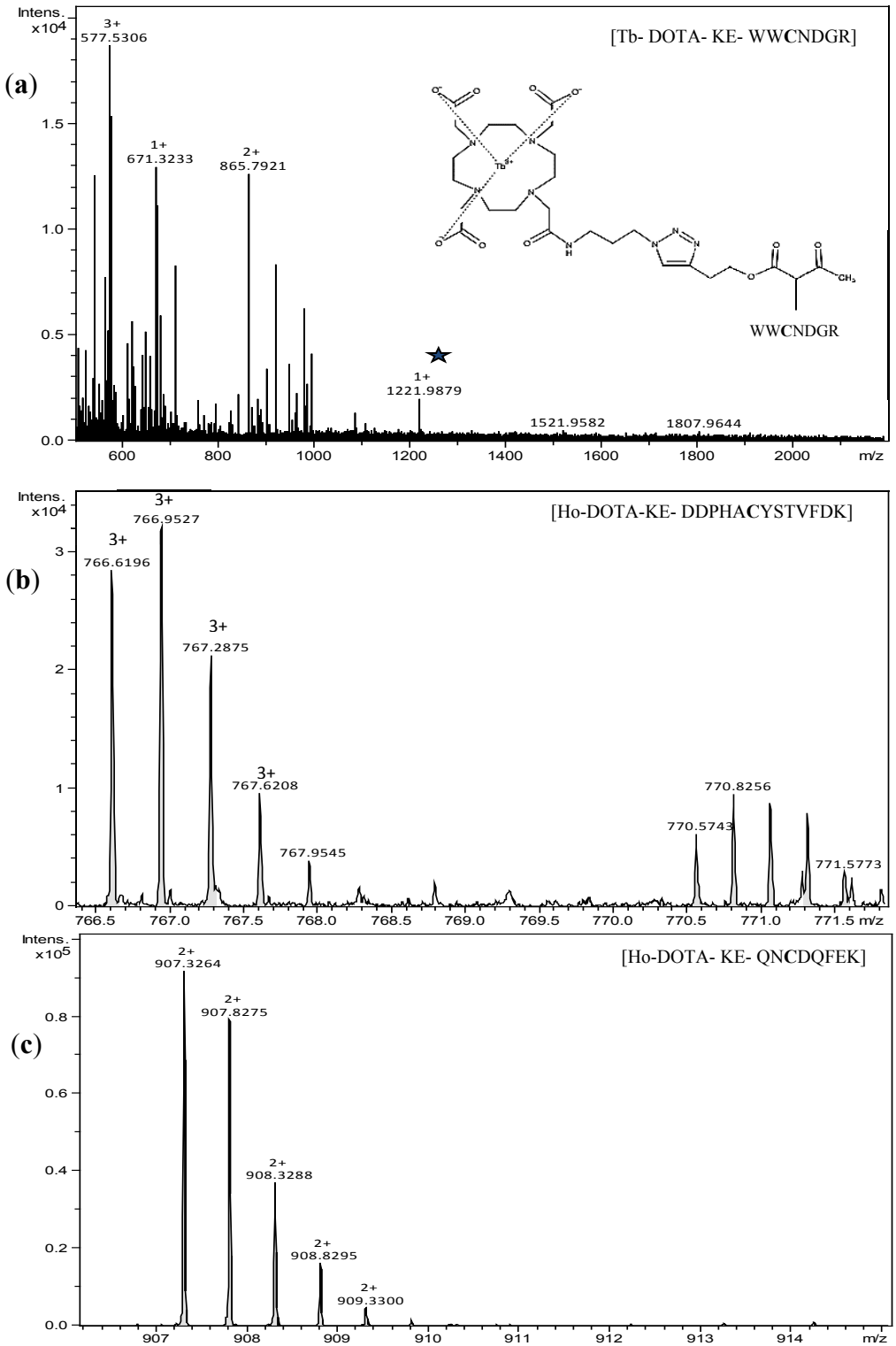

Figure 34.Mass spectrum obtained by ESI-q-TOF for a) Tb-DOTA-KE-WWCNDGR peptide (expected m/z,865.7948, z=2 and 577.5323, z=3), b) Ho-DOTA-KE-DDPHCYSTVFDK peptide (expected m/z,766.6184,z=3) and c) Ho-DOTA-KE-QNCDQFEK peptide (expected m/z, 907.3260,z=2). The ions from the calibration solution signal are indicated with a star.

Table 2. LC-ESI-MS results and mass errors for a) labelled peptide sequences with KE and b) for labelled peptide sequences with Ln-DOTA-KE .

a)	Peptide sequence	Labelled formula KE($C_8H_{10}O_3$)		MW $[M+nH]^{n+}$ theoretical/ experimental	Δ M* (ppm)
	WW**C**NDGR		+1	1088.4254/ 1088.4246	-0.73
	($C_{41}H_{53}N_{13}O_{11}S_1$)	$C_{49}H_{61}N_{13}O_{14}S_1$	+2	544.7163/ 544.7167	0.73
			+3	363.4799/ 363.4805	1.65
	DDPHA**C**YSTVFDK	$C_{73}H_{100}N_{16}O_{26}S1$	+2	825.3430/ 825.3407	-2.78
	($C_{65}H_{92}N_{16}O_{23}S_1$)		+3	550.5644/ 550.5643	-0.18
	QN**C**DQFEK	$C_{49}H_{70}N_{12}O_{19}S1$	+1	1163.4673/ 1163.4657	-1.37
	($C_{41}H_{62}N_{12}O_{16}S_1$)		+2	582.2373/ 582.2370	-0.51
b)		Labelled formula ($C_{27}O_{10}N_8H_{41}$.Ln)			
	WW**C**NDGR	$C_{68}H_{92}N_{21}O_{21}S_1$.Tb	+2	865.7948/ 865.7921	- 3.11
	($C_{41}H_{53}N_{13}O_{11}S_1$)		+3	577.5323/ 577.5306	- 2.94
	DDPHA**C**YSTVFDK	$C_{92}H_{131}N_{24}O_{33}S_1$.Ho	+2	1149.4239/ 1149.4232	-0.60
	($C_{65}H_{92}N_{16}O_{23}S_1$)		+3	766.6184/ 766.6196	1.56
	QNCD**C**QFEK	$C_{68}H_{101}N_{20}O_{26}S_1$.Ho	+2	907.3260/ 907.3264	0.44
	($C_{41}H_{62}N_{12}O_{16}S_1$)		+3	605.2198/ 605.2179	-3.13

* Δm = (mass error/ exact mass) $*10^6$

As an example, the comparative chromatogram of SA with Ho-DOTA-KE in DDPHA**C**YSTVFDK and QN**C**DQFEK peptide sequences by SEC-ICP-MS is shown in Figure 35 A and B, respectively. As expected, it is shown that the first elution is for the larger molecular weight, which is related to the SA peptide bound to the Ho-MeCAT-KE (~ 21 min) followed by the elution of the excess of the labelling reagent (~ 24 min).

The obtained signals indicated lower labeling efficiency (significantly lower peak area) for the DDPHA**C**YSTVFDK sequence which could be ascribed to the worse accessibility of the thiol group. The results indicate that SA detection can vary from one species to another, as tested peptide sequences showed different behavior upon oxidation and formation of SA. Different adducts can be formed for each sequence [118] and as all tested peptides present within BSA or lysozyme sequences [111] more complex data is expected upon *in vivo* application for SA detection.

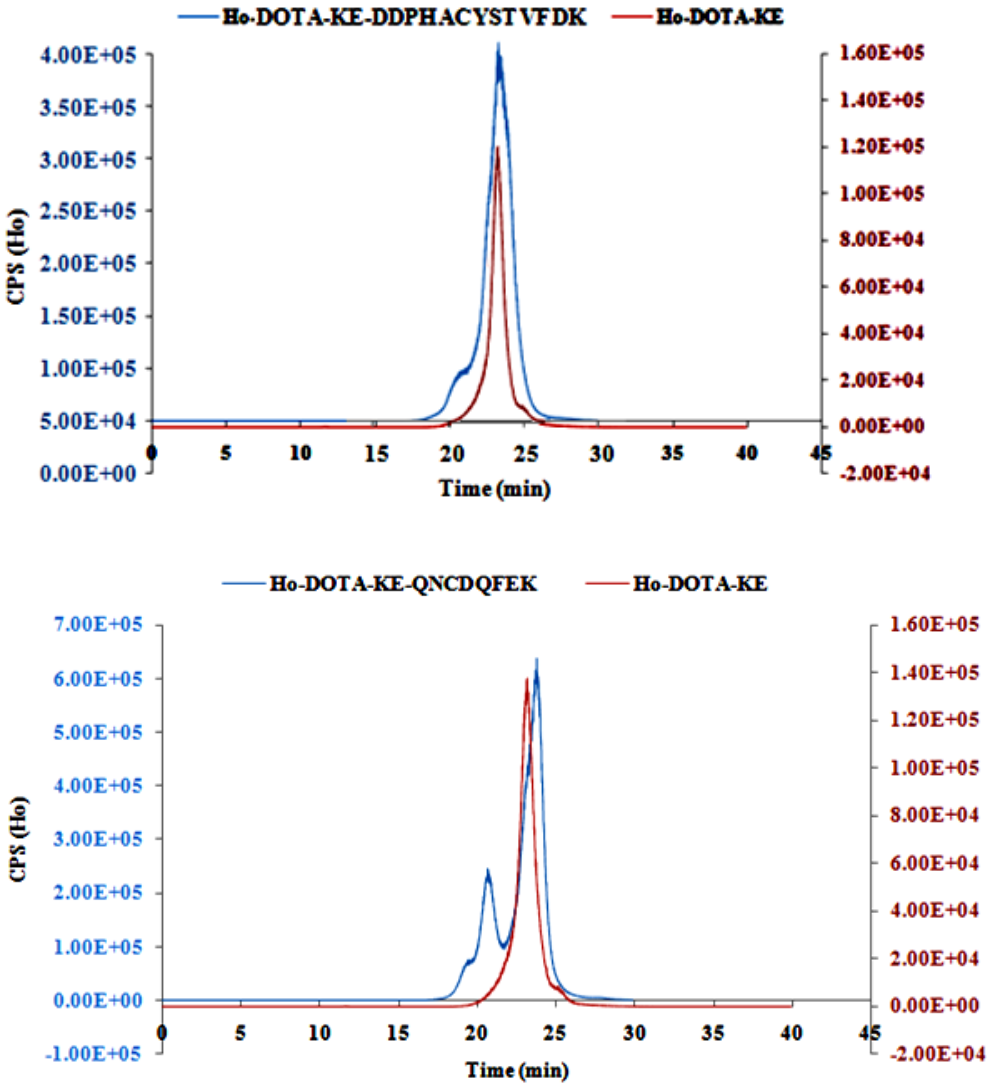

Figure 35. Chromatograms obtained by SEC-ICP-MS for a) Ho-DOTA-KE (red trace) and Ho-DOTA-KE-DDPHACYSTVFDK (blue trace) and b) Ho-DOTA-KE (red trace) and Ho-DOTA-KE-QNCDQFEK (blue trace). The isotope monitored was ^{165}Ho. Used column for separation Superdex peptide 10/300 GL.

4.5. Detection of sulfenic acid in intact proteins by mass spectrometric techniques

Evaluation of SA labelling in ß-lactoglobulin

Bovine ß-lactoglobulin(BLG) is one of the main protein components of cow's milk. It consists of 162 amino acid residues, five of which are cysteine residues;they form two disulfide bridges leaving one free cysteine residue (Cys-121). Three variants of BLG (labelled as A, B and C) commonly occur in cow's milk, whereas they vary in different identified sites [119]. Both (A and B) BLG variants undergo pH-independent conformational changes in the range pH 6.5 to pH 7.5 [120].

The commercial BLG was analyzed using ESI-MS to evaluate the different forms of the protein and potential post-translational modifications (PTMs). The ESI-MS spectrum (Figure 36) provided the multiple charge profile of BLG and the deconvolution of the spectrum resulted in a calculated molecular mass ranging from18264 Da to 18674 Da. This corresponds mainly to the A and B variants of BLG (18350 Da and 18264 Da, respectively) as can be identified from the 162 amino acid sequence of BLG (Appendix Figure 4).

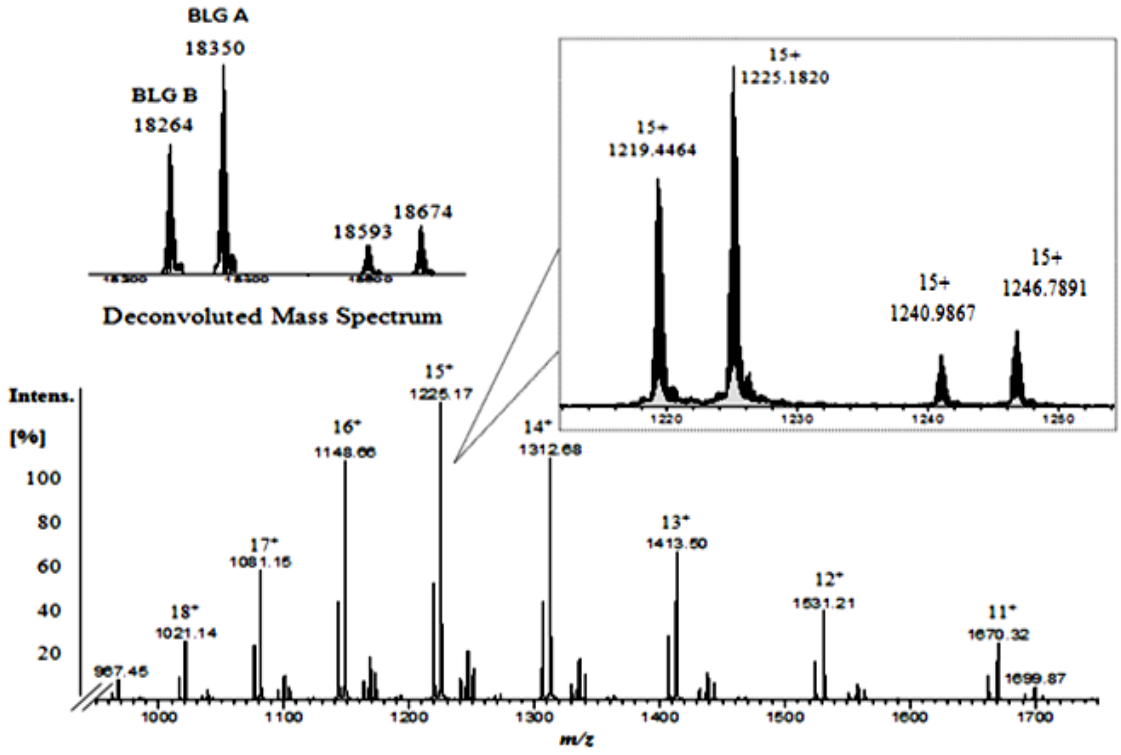

Figure 36. Mass spectrum obtained by ESI-q-TOF mass spectrometry for ß-lactoglobulin obtained from the commercial standard . The deconvoluted mass spectrum represents several variants for the BLG A and B and other commercial PTMs.

The labelling efficiency of the prepared Ln-DOTA-KE was tested with BLG for being relatively a small protein. Therefore, BLG solution of 90µM was prepared in THAM buffer (pH = 8.4). BLG was denaturated in 8 M urea and then oxidized with different excess ratios of hydrogen peroxide (H_2O_2) (5mM). Finally, 30- fold excess of Ho-DOTA-KE to cysteine was added to the mixture. Labelling reaction was carried out in THAM buffer (100 mM, pH= 8.4). The mixture was left for 4 h with gentle shaking at room temperature.

The labelling reaction was monitored with LC-ESI-MS and the results are shown in Figure 37. As can be observed, a mixture of labelled (marked with a *star*) and unlabelled BLG is obtained with a mass difference between both species corresponding to the molecular mass of the used labelling reagent (Ho-DOTA-KE-HSA)which has 801.21 u. Results are

summarized in Table 3. The deconvoluted mass spectrum showed high peak of native unlabelled BLG variants (from 18277 Da to 18753 Da) along the labelled BLG (19077 Da). Moreover, used labelling reagent (Ho-DOTA-KE) did not show any reactivity towards any amino acid residue other than SA.

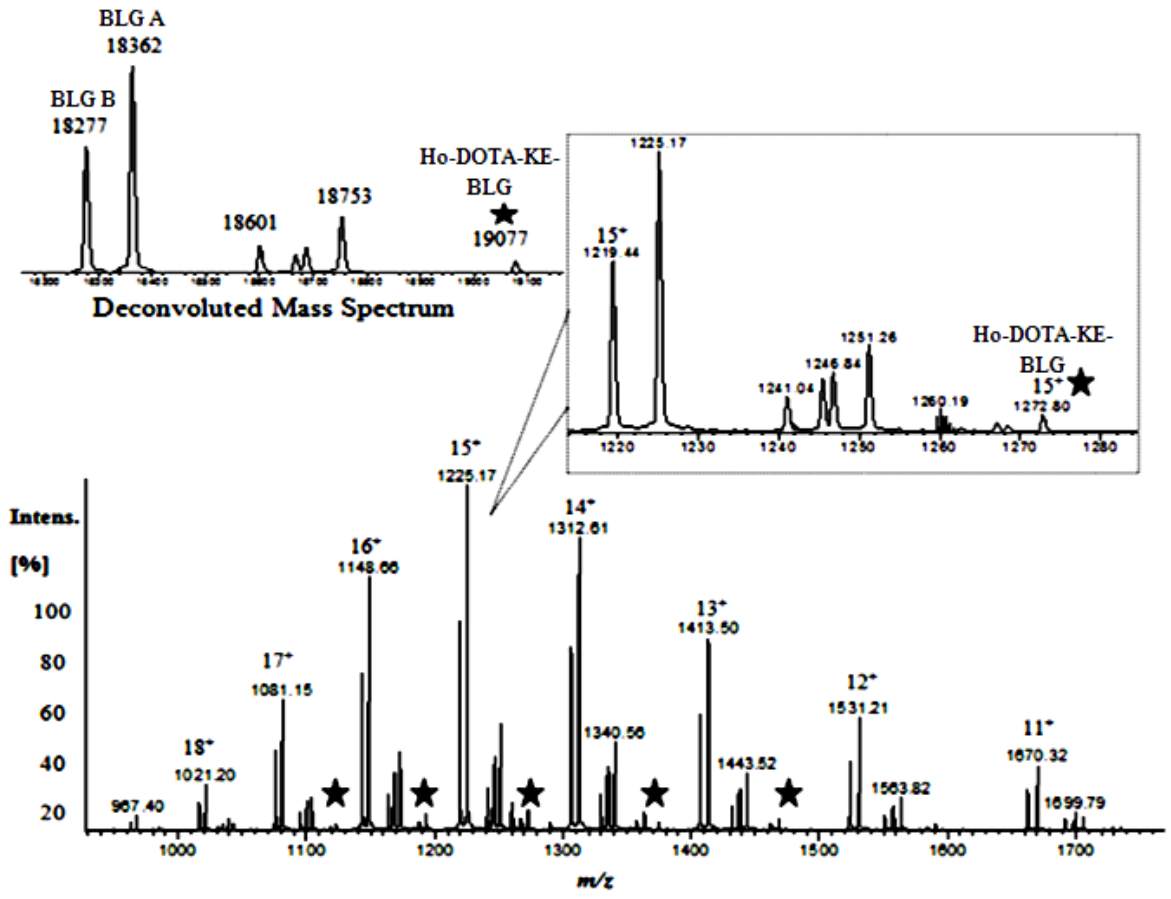

Figure 37. Mass spectrum obtained by ESI-q-TOF mass spectrometry for Ho-DOTA-KE-ß. lactoglobulin. Labelled SA residues are indicated with *stars*.

Table 3. Theoretical fragmentation pattern for ß-lactoglobulin and labelled SA in ß-lactoglobulin with Ho-DOTA-KE. Monoisotopic mass for labelling reagent (Ho-DOTA-KE) equals to 801.2170.

Charge	Fragmentation pattern of ß-lactoglobulin monoisotopic mass	Fragmentation pattern of Ho-DOTA-KE- ß-lactoglobulin monoisotopic mass
12^+	1523.45	1590.22
13^+	1406.34	1467.97
14^+	1305.96	1363.19
15^+	1218.96	1272.38
16^+	1142.84	1192.92
17^+	1075.67	1122.80

Finally, SEC-ICP-MS signal was used for the monitoring of Ho in the labelling reaction of SA in BLG. Figure 38 shows the elution time for the labelled SA with Ho-DOTA-KE (Figure 38-A) where two peaks are present corresponding to the labelling of A and B variants of BLG. Figure 38-B represents the excess of the labelling reagent.

Whereas SA detection with the relatively small BLG was possible, further labelling and quantification for SA was conducted with human serum albumin (HSA).

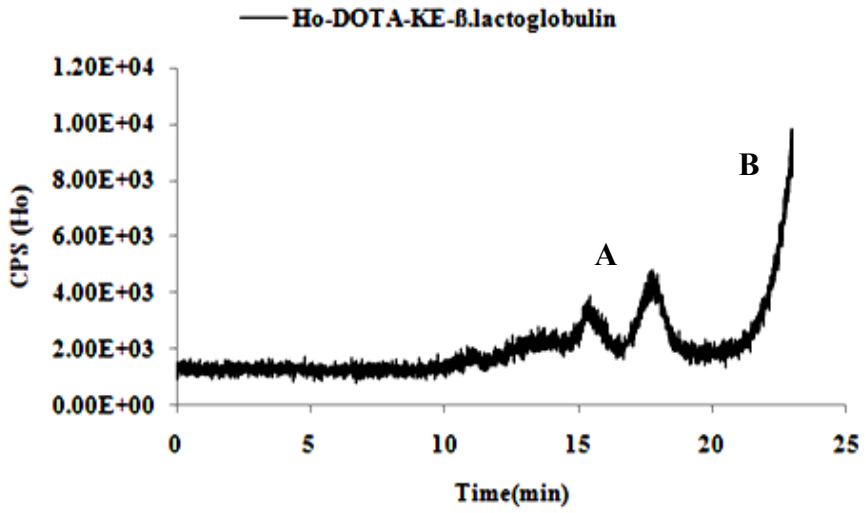

Figure 38. SEC-ICP-MS chromatogram obtained for Ho-DOTA-KE-ß-lactoglobulin labelling. A- represents the elution of the labelled species with Ho-DOTA-KE and B- represents the elution for the excess of the labelling reagent. Used column for separation Superdex peptide 10/300 GL.

Evaluation of SA labelling in albumin standards and serum samples

Albumin contains 35 cysteines forming 17 disulfide bridges (-S-S-) with only one free thiol, Cys-34, which comprises 80% of the total free thiols in the plasma and can follow the smallest change in the redox environment of the biological system [121]. A human serum albumin standard was prepared and analyzed using ESI-MS to evaluate the different forms of the protein and potential post-translational modifications. The ESI-MS spectrum provided the multiple charge profile of albumin (Figure 39) and the deconvolution of the spectrum resulted on a calculated molecular mass of 66557 Da.

This corresponds mainly to the form of cysteinylated albumin (covalently bound cysteine residue).Since only cysteine that is not forming disulfide bridges and is susceptible to form SA for subsequent labelling with the Ln-DOTA-KE, Cys-34, can be affected by this modification, the treatment with a reducing agent is considered necessary to reduce the proportions of the existing disulfides. However, the use of reducing agents (such as ß-mercaptoethanol or TCEP) will affect as well the other internal disulfide bridges present in albumin[97,121].

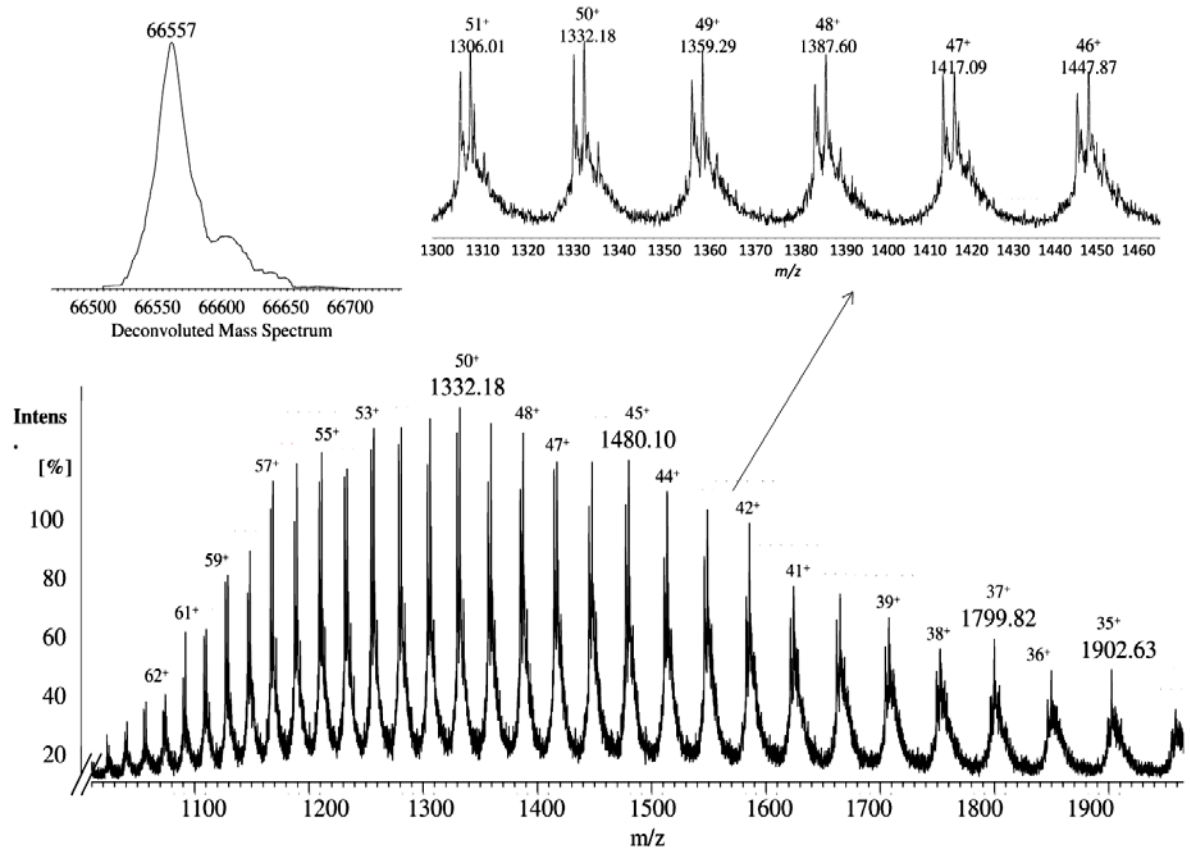

Figure 39. Mass spectrum obtained by ESI-q-TOF mass spectrometry for HSA obtained from the commercial standard.

Therefore, labelling was attempted directly in albumin from serum, expecting the presence of some traces of the native form of the protein. For this aim, albumin was first separated from the rest of the serum components using the HiTrap^{TM} Blue HP affinity column and the elution profiles were monitored by UV/VIS. The chromatogram is shown in Figure 40 in which two separated peaks correspond to plasma proteins (fraction A) and albumin (fraction B). The fractions were collected, purified and the products monitored using gel electrophoresis (10 % SDS-PAGE). As can be seen in the inset of Figure 40, the results obtained for fraction A showed bands that corresponds to α, ß, and ϒ- globulins among others and fraction B exhibited mainly the band corresponding to the purified albumin which

appeared at around 70 KDa, confirming the successful isolation of HSA with the proposed set-up.

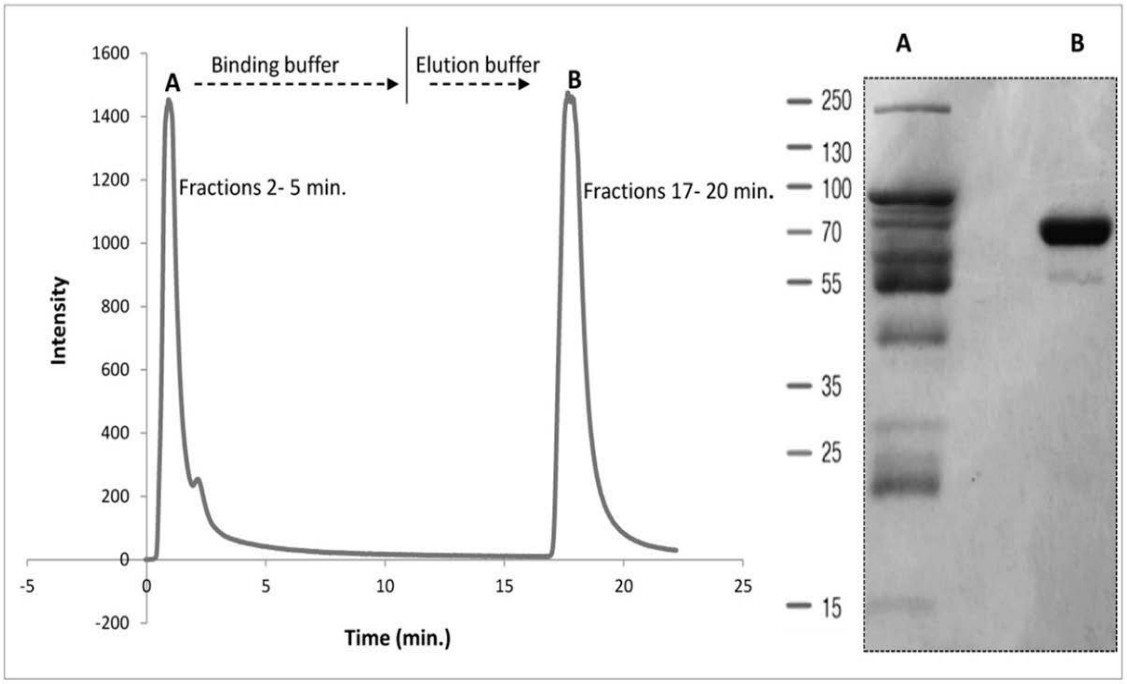

Figure 40. HPLC chromatogram for albumin purification from human serum with HiTrap™ Blue HP column, used binding buffer was 50 mM KH_2PO_4 (pH 7.00) and elution buffer was 50 mM KH_2PO_4 + 1.5 M KCl (pH 7.00). Signal was monitored at 280 nm, 10 µg of collected fractions A (plasma proteins) and B (albumin) were monitored by 10 % SDS- PAGE, band of purified albumin (fraction B) appeared at around 70 KDa in the inset.

The collected albumin (Figure 40- fraction B) was also analyzed using ESI-MS and in this case, the single chain of 585 amino acids of albumin (check Appendix Figure 5) (unmodified) was obtained as can be seen in Figure 41 at m/z 66438.In this case, also different PTMs and variants such as cysteinylated (Cys-HSA) and glycated (Glc-HSA) forms corresponding to 66557 Da and 66598 Da, respectively.

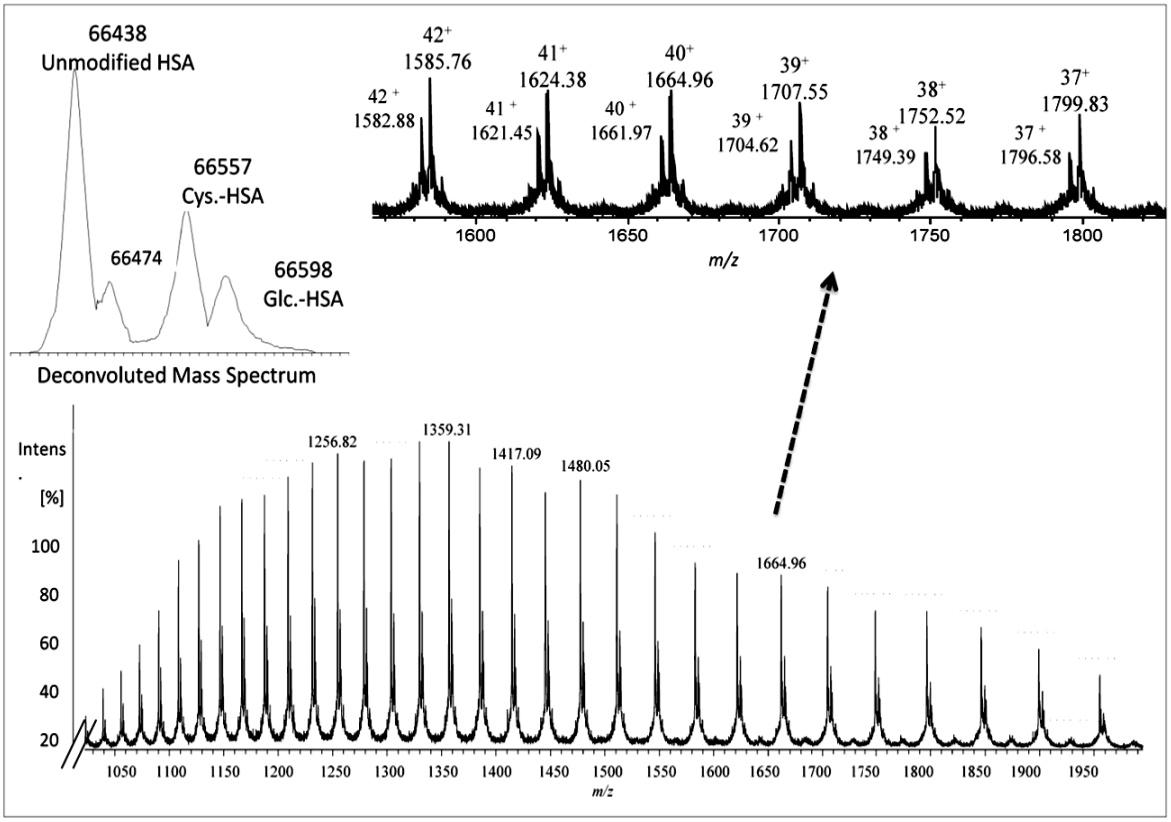

Figure 41. Mass spectrum obtained by ESI-q-TOF mass spectrometry for collected albumin from human serum. The deconvoluted mass spectrum represents different PTMs and variant average molecular weight of albumin in the range of 66438-66600 Da.

As before, urea was used for denaturating albumin and further labelling for SA was carried out in 100 mM of THAM buffer, pH= 8.4 using 30- fold excess of Nd-DOTA-KE to cysteine unit. Different oxidation conditions were tested and different fold excess of hydrogen peroxide (H_2O_2) (5mM) to Cys-34 were used to form the SA. The mixture was left for 4 h with gentle shaking at room temperature. The labelling reaction was monitored by ESI-MS and the results are shown in Figure 42. As can be observed, a mixture of labelled (marked with a *star*) and unlabelled HSA is obtained with a mass difference between both species

corresponding to the molecular mass of the used labelling reagent (Nd-DOTA-KE-HSA)which has 778.1945 u.

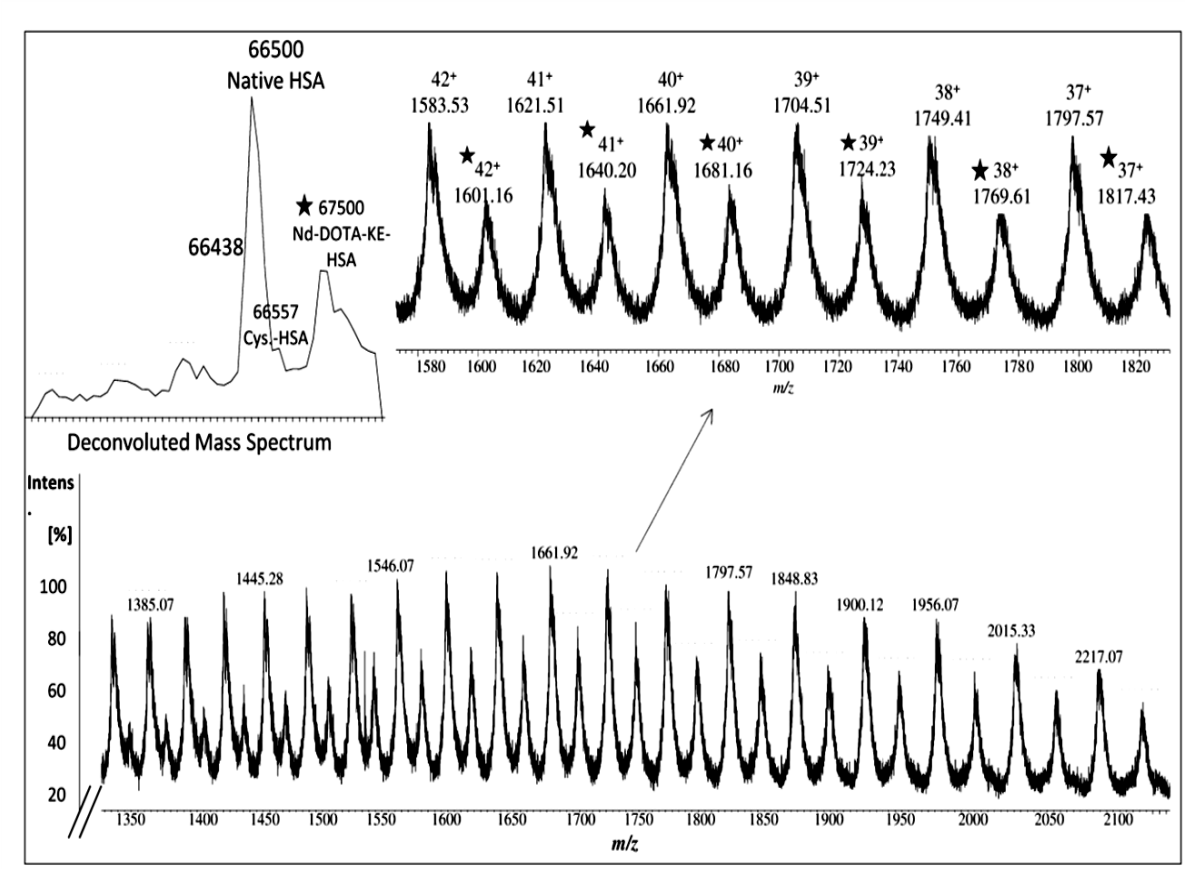

Figure 42. Mass spectrum obtained by ESI-q-TOF mass spectrometry for a labelled sulfenic acid (SA) in albumin with Nd-DOTA-KE. Labelled SA residues with Nd-DOTA-KE are indicated with *stars.* Deconvoluted mass spectrum represents different PTMs and average molecular weight of labelled albumin with Nd-DOTA-KE (67500 Da).

Results are summarized in Table 4. The deconvoluted mass spectrum showed high peak of native unlabelled HSA (66500 Da) with fractions of cysteinylated HSA, along the labelled HSA (67500 Da). Moreover, used labelling reagent (Nd-DOTA-KE) did not show any reactivity towards any amino acid residue other than SA [105].

Table 4.Theoretical fragmentation pattern for human serum albumin (HSA) and labelled SA in HSA with Nd-DOTA-KE. Monoisotopic mass for labelling reagent (Nd-DOTA-KE) equals to 778.1945.

Charge	Fragmentation pattern of albumin monoisotopic mass	Fragmentation pattern of Nd-DOTA-KE-albumin monoisotopic mass
42^+	1582.65	1601.18
41^+	1621.23	1640.21
40^+	1661.73	1681.18
39^+	1704.31	1724.27
38^+	1749.14	1769.62
37^+	1797.57	1817.42

The analysis of the samples by SDS-PAGE did not show any difference between the bands corresponding to the labelled and unlabelled compounds. As shown in Figure 43 the slight increase in albumin molecular weight band (C and D) can be attributed to the higher molecular weight resulting from the mixture of labelled and unlabelled albumin (slight differences in bands concentrations can be seen as all samples were filtered with 30KDa filters after labelling to remove the excess of reagent and the used denaturating agent).

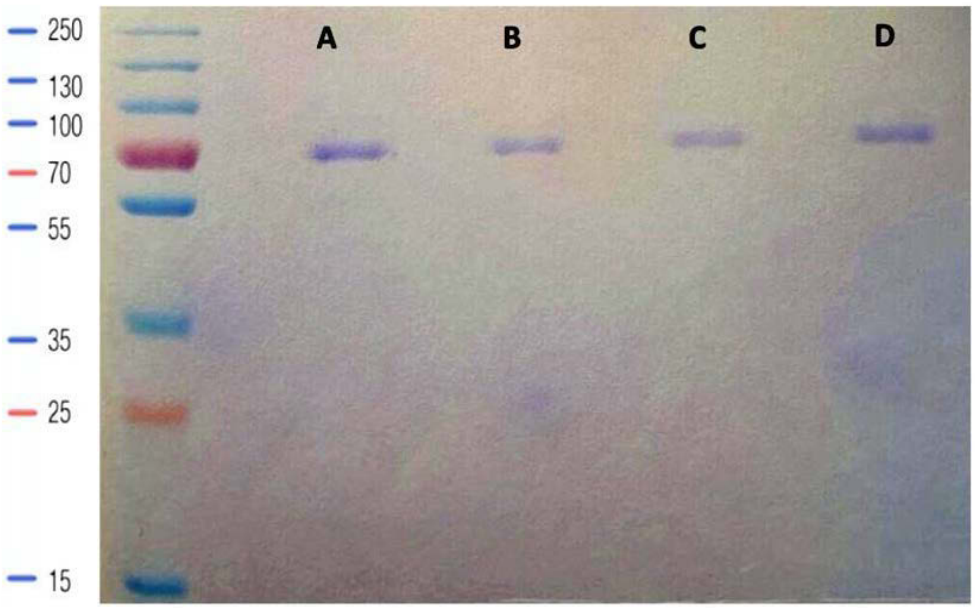

Figure 43. 10% SDS- PAGE for 3µg of albumin band is shown for: (A) human serum and (B) purified albumin from human serum (C) Nd-DOTA-KE-HSA with 8 excess H_2O_2 and (D) Nd-DOTA-KE-HSA with 5 excess H_2O_2 .

Finally, SEC-ICP-MS signal was used for the monitoring of both Nd and S simultaneously in the same peak. The instrument was used in the oxygen reaction mode in order to form the oxide of both species which has exhibited higher sensitivity in particular in the case of S analysis[122]. Figure 44 shows the elution time for the labelled SA with Nd-DOTA-KE (S and Nd signal) as well as the presence of the excess of the labelling compound.

It is noteworthy that the fist compound (peak A) shows the corresponding S signal for labelled and unlabelled HSA since they cannot be separated under these conditions. However, since the Nd concentration is proportional to the labelled species and the sensitivity of this element in ICP-MS is substantially higher, the quantification by the Nd signal will be very advantageous.

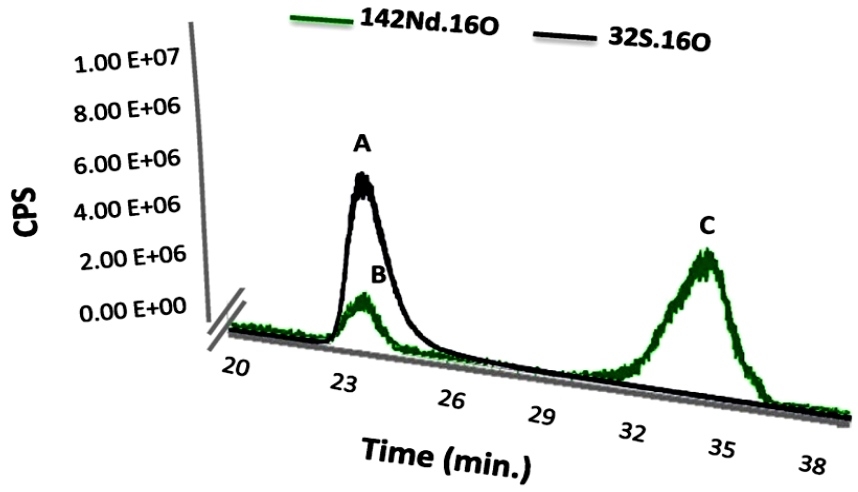

Figure 44. Chromatograms obtained by SEC-ICP-MS for labelled SA in HSA with Nd-DOTA-KE. Monitored isotopes were ^{142}Nd and ^{32} S where both were measured with oxygen reaction mode. Monitored $^{32}S^{16}O$ represented in peak A is related to the total HSA in the sample, where monitored $^{142}Nd^{16}O$ represented in peak B is related to the labelled HSA with Nd-DOTA-KE, and finally peak C represents the excess of the labelling reagent. Used SEC column for separation was Superdex 200 10/300 GL.

Quantification of the labelled SA by IDA-SEC-ICP-MS

Since the labelling reagent (Nd-DOTA-KE) is aimed to be used for quantitative labelling of SA in albumin, its concentration must be determined. For this purpose, ICP-MS analysis of Nd by flow injection analysis (FIA) of the purified Nd-DOTA-KE was carried out followed by a calibration curve of the metal measured under the same conditions (FIA-ICP-MS).

By knowing the stoichiometry Nd: complex (1:1), the obtained Nd concentration can be transformed into Nd-DOTA-KE concentration. Thus, the final concentration of the synthetic labelling reagent turned out to be 30.3mM which is in good agreement with the calculated concentration (32 mM). As expected, all Nd in the Nd-DOTA-KE solution is the metal in the complex and no free Nd is present in the solution.

To achieve the best precision for the ratio measurements, the theoretical optimum for spiking samples has to be identified. The error propagated by this factor alters as moving away from the theoretical optimum. Error propagation factor can be calculated from the measured isotopic system and is dependent on the isotopic abundances in the natural sample and the isotopically enriched (spike/tracer) material[100].

$$f_m = \frac{R_m(1-R_t.R_s)}{(R_m-R_t)(1-R_mR_s)}$$

f_m: error- propagation factor

R_m: measurement of isotope ratio

R_t:measured tracer isotope ratio

R_s:measured standard isotope ratio

Quantification for the labelled SA with Nd-DOTA-KE has been done using an isotopically enriched ^{145}Nd isotopic standard. Optimum ratio between ^{142}Nd standard and ^{145}Nd spike was experimentally determined (R_m) ^{142}Nd/^{145}Nd in order to achieve the best precision for the measurement (Figure 45).

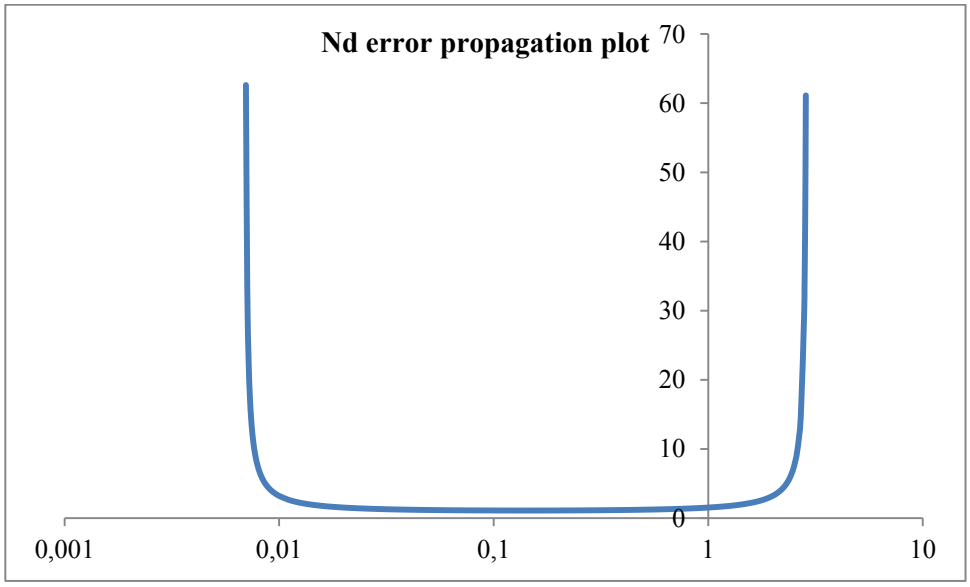

Figure 45. Error propagation plot for the standard ^{142}Nd and the spiking solution of ^{145}Nd. The error propagation plot represents the theoretical optimum ratio (R_m) that should present between the ^{145}Nd spiking solution and the samples with the standard ^{142}Nd in order to achieve the best precision for the measurement, where it was shown to be within 0.01 - 1.

Calculated R_m ratios (Table 5) were between 0.01-1. Post-column isotope dilution analysis of Nd (ID-ICP-MS) was carried out. For this purpose a continuous flow of a ^{145}Nd solution (5 ng/mL) was constantly pumped (0.1 ml min^{-1}) and mixed with the eluent of the chromatography. The mixed solution was then introduced into the ICP-MS.

Table 5.Calculated ratio (R_m) between ^{145}Nd spike solution (5 ppb) and ^{142}Nd in Nd-DOTA-KE-HSA samples with different excess of oxidizing agent H_2O_2.

Excess of H_2O_2 to free Cys-34	R_m
Control	0.054
2 excess	0.046
5 excess	0.372
8 excess	0.545
10 excess	0.078

Figure 46 shows the chromatogram obtained by SEC-ICP-MS for HSA labelling with Nd-DOTA-KE. Two peaks were eluted representing the labelled albumin with Nd-DOTA-KE

(peak A) and the excess of the labelling reagent (Nd-DOTA-KE) (peak B). This set-up was used for the evaluation of the labelled SA where the online isotopic dilution analysis using ^{145}Nd spike is shown.

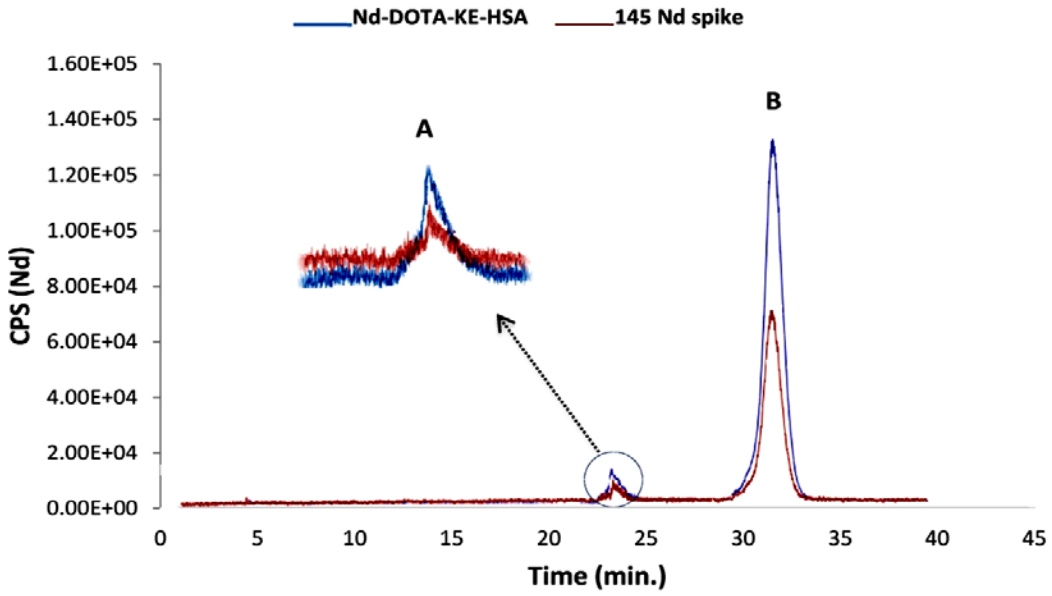

Figure 46. Chromatograms obtained by SEC-ICP-MS for labelled SA in HSA with Nd-DOTA-KE. Isotopic dilution analysis (IDA) was performed to quantify the labelled SA, monitored isotopes were natural ^{142}Nd in sample and ^{145}Nd in spike. Peak A represents the labelled HSA with Nd-DOTA-KE and peak B represents the excess of the labelling reagent. Used SEC column for separation was superdex 200 10/300 GL

Figure 47 shows the quantitative results of the SA formation upon exposure of90 µM of albumin to0 (control), 0.18 mM, 0.45 mM, 0.72 mM and 0.9 mMH_2O_2which corresponded to 0, 2-fold, 5-fold, 8-fold and 10-fold excess with respect to the -SH. Labelling percentages were found to be 2.6%, 2.2 %, 22.8 %, 39.8 % and 4.1 %, respectively.

As a relatively stable SA can be spontaneously formed in HSA [121],the control sample (without H_2O_2 addition) indicated some minor labelling percentage for SA. A similar percentage for SA labelling with Nd-DOTA-KE was detected for the 2-fold excess of H_2O_2,

which might indicate that this concentration is too low for any further formation of SA above the spontaneously existing amount.

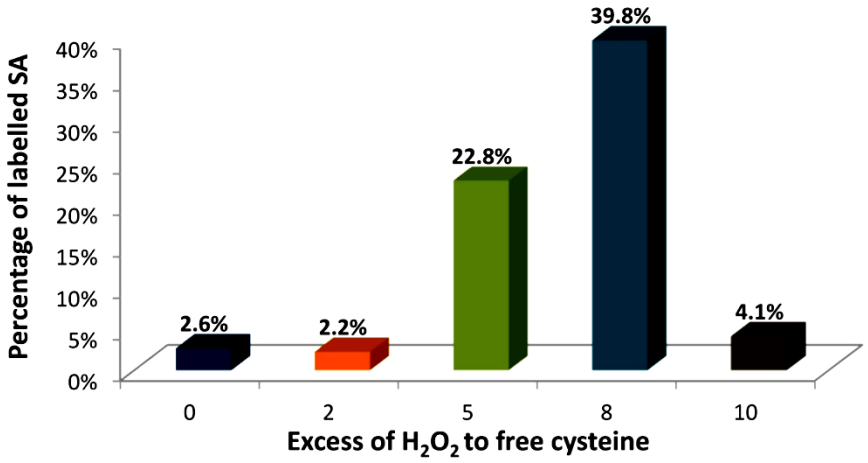

Figure 47.Percentage of labelled SA in HSA with Nd-DOTA-KE with different excess of H_2O_2 to free cysteine. Labelling was carried out with 90µM of HSA, 8M urea, and 30 excess of Nd-DOTA-KE in Tris buffer, pH 8.4 for 4 hours at room temperature.

Higher labelling percentages were detected upon the addition of 5-fold and 8-fold excess of H_2O_2, whereas with 10 excess of H_2O_2 only 4 % of SA was detected. This could be ascribed to the excessive oxidation and the formation of higher oxidation states such as sulfinic ($-SO_2H$) and sulfonic ($-SO_3H$) acids that cannot be labelled under the studied conditions. Therefore,8-fold excess of H_2O_2 was found to be optimum for producing sufficient SA residues.

5. Conclusions

In this work we presented a new method for the efficient labelling of SA in model peptides and proteins. Alkyne β - ketoester has been utilized for the effective labelling of SA in a new form where it was coupled to Ln-azide-DOTA. Elemental and molecular MS techniques have been used using the new synthesized reagent (Ln-DOTA-KE) in a complementary way. The new synthesized reagent allows the quantification and the detection of SA in peptides and proteins, using the advantage of the high sensitivity for ICP-MS, where the structure independent response of ICP-MS forms an absolute quantification for desired detected species.

SA labelling and quantification in human serum albumin (HSA) has also been carried out. Using a poly-isotopic Ln, the prepared Ln-DOTA-KE allowed the quantification of the detected SA using isotopic dilution analysis (IDA-ICP-MS) where an enriched tracer was used for the absolute quantification for labelled SA.

The new synthesized reagent (Ln- DOTA- KE) permits to capture SA and detect it by ESI- MS with good sensitivity. This improved sensitivity might allow the determination of the smaller available quantities of SA, even those spontaneously oxidized upon exposure to atmospheric oxygen. The new synthesized reagent did not induce accumulation for the sulfinic ($-SO_2H$) and sulfonic ($-SO_3H$) acids, and showed efficient labelling comparable to KE alone. The new reagent shows improved reactivity at higher pH (8.00- 8.50) compared to restricted reactivity of dimedone at pH 7.40.

Thestraight forward methodology and the specificity of the prepared reagent for SA detection, suggest a promising future for the specific quantification of SA in real samples and tissues.

6. References

1 Horgan, R. P. and Kenny, L. C. SAC review 'Omics' technologies: genomics, transcriptomics, proteomics and metabolomics. *The Obstetrician & Gynaecologist*, 13 (2011), 189-195.

2 Anderson, N. L. and Anderson, N. G. Proteome and Proteomics : new technologies, new concepts, and new words. *Electrophoresis* , 19 (1998), 1853-1861.

3 Pandey, A. and Mann, M. Proteomics to study genes and genomes. *Nature* , 405 (2000), 837-846.

4 Picotti, P., Bodenmiller, B., and Aebersold, R. Proteomics meets the scientific method. *Nat. Methods*, 10 (2013), 24-27.

5 Wasinger, V. C., Cordwell, S. J., Cerpa-Poljak, A., Yan, J. X., Gooley, A. A., and Wilkins, M. R. Progress with gene-product mapping of the Mollicutes: Mycoplasma genitalium. *Electrophoresis* , 16 (1995), 1090-1094.

6 Persidis, A. Proteomics. *Nat. Biotechnol.*, 16 (1998), 393-394.

7 Prusiner, S. B. Prion disease and the BSE crisis. *Science*, 278 (1997), 245-251.

8 Prusiner, S. B. Prions. *Proc. Natl. Acad. Sci. USA*, 95 (1998), 13363-13383.

9 Prusiner, S. B., Scott, M. R., De Armond, S. J., and Cohen, F. E. Prion protien biology. *Cell.*, 93 (1998), 337-348.

10 C., International Human Genome Sequencing. Finishing the euchromatic sequence of the human genome. *Nature* , 431 (2004), 931-945.

11 Jensen, O. N. Modification-specific proteomics: characterization of post-translational modifications by mass spectrometry. *Curr. Opin. Chem. Biol.*, 8 (2004), 33-41.

12 Mann, M. and Jensen, O. N. Proteomic analysis of post-translational modifications. *Nat. Biotechnol.*, 21 (2003), 255-261.

13 Prabakaran, S., Lippens, G., Steen, H., and Gunawardena, J. Post-translational modifications: nature's escape from genetic imprisonment and the basis for synamic information encoding. *Wiley Interdiscip Rev Syst Biol Med*, 4 (2012), 565-583.

14 Zhao, Y. and Jensen, O. N. Modification-specific proteomics: stratigies for characterization of post-translational modifications using enrichment techniques. *Proteomics* , 9 (2009), 4632-4641.

15 Brosnan, J. T. and Brosnan, M. E. The sulfur-containing amino acids:an overview. *J. Nutr.*, 136 (2006), 1636S-1640S.

16 Rodney, L. L., Jackob, M., and Earl, R. S. Oxidation of methionine in proteins: Roles in Antioxidant defense and cellualr regulation. *IUBMB life* , 50 (2000), 301-307.

17 Trifonov, E. N. The triple code from first principles. *J. Biomol. Struct. Dyn.*, 22 (2004), 1-11.

18 Bradsaw, R. A. and Dennis, E. A. *Handbook of cell signaling*. Academic Press , San Diego, California, 2003.

19 Eaton, P. Protein thiol oxidation in health and disease: Techniques for measuring disulfides and related modifications in complex protein mixtures. *Free Radic. Biol. Med.*, 40 (2006), 1889-1899.

20 Flohe, L. Changing paradigms in thiology from antioxidatiant defense toward redox reglation. *Methods Enzymol*, 473 (2010), 1-39.

21 Charles, R. L., Schröder, E., May, G. et al. Protein sulfenation as a redox sensor: proteomics studies using a novel Biotinylated Dimedone Analgue. *Mol. Cell Proteomics*, 6 (2007), 1473-1484.

22 Roos, G. and Messens, J. Protein sulfenic acid formation: From cellular damage to redox regulation. *Free Radiac. Biol. Med.*, 51 (2011), 314-326.

23 Kohen, R. and Nyska, A. Oxidation of biological systerm: oxidative stress phenomena, antioxidants,redox reactions, and methods for their quantification. *Toxicol Pathol* , 30 (2002), 650-650.

24 Pryor, W. A., Houk, K. N., Foote, C. S., Fukuto, J. M., Ignarro, L. J., Squadrito, G. L., and Davies, K. J. Free radical biology and medicine: it's a gas, man! *Am. J. Physiol. Regul. Integr. Comp. Physiol.*, 291 (2006), R491-511.

25 Slater, T. F. Free-redical mechanisms in tissue injury. *Biochem J.*, 222 (1984), 1-15.

26 Valko, M., Izakovic, M., Mazur, M., Rhodes, C. J., and Telser, J. Role of oxygen radicals in DNA damage and cancer incidence. *Mol. Cell. Biochem.*, 266 (2004), 37-56.

27 Roberts, R. A., Laskin, D. L., Smith, C. V., Robertson, F. M., Allen, E. M.G., Doom, J.

A., and Slikkerk, W. Nitrative and oxidative stress in toxicology and disease. *Toxicol. Sci.*, 112 (2009), 4-16.

28 Kelly, F. Oxidative stress:its role in air pollution and adverse health effects. *Occup. Environ. Med.*, 60 (2003), 612-616.

29 Imlay, J. A. Cellular defenses against superoxide and hydrogen peroxide. *Annu. Rev. Biochem.* , 77 (2008), 755-776.

30 Dominy Jr., J. E., Hwang, J., and Stipanuk, M. H. Overexpression of cysteine dioxygenase reduces intracellular cysteine and glutathione pools in HepG2/C3A cells. *Am. J. Physiol Endocrinol Metab*, 293 (2007), E62-E69.

31 Laemmli, U. K. Cleavage of structural proteins during the assembly of the head of bacteriophage T4. *Nature*, 227 (1970), 680-685.

32 Dayton, W. R. Protein separation techniques. *American Meat Science Association*, 36 (1983), 98-102.

33 Dunbar, B. S. *Two dimensional electrophoresis and immunological techniques*. Plenum Press, NewYork,USA, 1987.

34 Gresten, D. M. *Gel electrophoresis (Essential techniques series)*. Wiley, NewYork, USA, 1996.

35 Berg, J. M., Tymoczko, J. L., and Stryer, L. *Biochemistry*. WH Freeman, NewYork,USA, 2002.

36 Hegyi, G., Kardos, J., Kovács, M. et al. *Introduction to Pratical Biochemistry*. McGraw-Hill, NewYork, USA, 2013.

37 Ritchie, C. Protein purification. *Mater methods*, 2 (2012), 134.

38 Woodbury, R., Hardy, S., and Randall, L. Complex behavior in solution of homodimeric SecA. *Protein Sci.*, 11 (2002), 875-82.

39 Corbett, R. and Roche, R. Use of high-speed size-exclusion chromatography for the study of protein folding and stability. *Biochemistry* , 23 (1984), 1888-94.

40 Wilchek, M. and Chaiken, I. An overview of affinity chromatography. *Methods Mol. Biol.*, 147 (2000), 1-6.

41 Hewick, R. M., Hunkapiller, M. W., Hood, L. E., and Dreyer, W. J. A gas-liquid solid phase peptide and protein sequenator. *J. Biol. Chem.*, 256 (1981), 7990-7997.

42 Matsudaira, P. Sequence from picomole quantities of proteins electroblotted onto polyvinylidene difluoride membranes. *J. Biol. Chem.*, 262 (1987), 10035-10038.

43 Pappin, D. J. C., Rahman, D., Hansen, H. F., Bartlet- Jones, M., Jeffery, W., and Bleasby, A. J. *Chemistry, Mass Spectrometry and peptide-mass databases: Evolution of methods for the rapid identification and mapping of cellualr proteins*. Humana Press, New York, USA, 1996.

44 Westermeier, R., Naven, T., and Höpker, H. R. *Proteomics in practice: a guide to successful experimental design*. Weinheim Chichester: Wiley-VCH, Berlin, Germany, 2008.

45 Fenn, J. B., Mann, M., Meng, C. K., Wong, S. F., and Whitehouse, C. M. Electrospray ionization for mass spectrometry of large biomolecules. *Science* , 246 (1989), 64-71.

46 Aebersold, R. and Goodlett, D. R. Mass spectrometry in proteomics. *Chem. Rev.*, 101 (2001), 269-295.

47 Fenn, J. B. Electrospray wings for molecular elephants (Noble lecture). *Angew. Chem. Int. Ed. Engl.*, 42 (2003), 3871-3894.

48 Talyor, G. Disintegration of water drops in an electric field.. *Proceedings of the Royal society of London.Series A. Mathematical and physical sciences.* , 280 (1964), 383-397.

49 Canas, B., Loppez-Ferrer, D., Ramos-Fernandez, A., Camafeita, E., and Calvo, E. Mass spectrometry technologies for proteomics. *Brief Funt Genomic Proteomic.*, 4 (2006), 295-320.

50 Houk, R. S., Fassel, V. A., Flesch, G. D., Svec, H. J., Gray, A. L., and Taylor, C. E. Inductevily coupled argon plasma as an ion source for mass spectrometric determination of trace elements. *Anal. Chem.*, 52 (1980), 2283-2289.

51 Beauchemin, D. Inductively coupled plasma mass spectrometry. *Anal. Chem.*, 82 (2010), 4786-4810.

52 Date, A. R. and Gray, A. L. Plasma source mass spectrometry using an Inductively coupled plasma and a high resolution Quadrupole Mass filter. *Analyst.*, 106 (1981), 1255-1267.

53 Montaser, A. *Inductively Coupled Plasma Mass Spectrometry*. Wiley-VCH, NewJersey, 1998.

54 Thomas, R. *Practical guide to ICP-MS: A Tutorial fro Beginners*. CRC Press, Boca Raton, USA, 2008.

55 Wendt, R. H. and Fassel, V. A. Inductively coupled plasma spectrometric excitation source. *Anal. Chem.*, 37 (1965), 920-922.

56 Bettmer, J. Application of isotope dilution ICP-MS techniques to quantitative proteomics. *Anal. Bioanal. Chem.*, 397 (2010), 3495-3502.

57 Lobinski, R., Schaumloffel, D., and Szpunar, J. Mass spectrometry in bioinorganic analytical chemistry. *Mass Spectrom Rev.*, 25 (2006), 255-289.

58 Wind, M. and Lehmann, W. D. Elemental and molecualr mass spectrometry - an emerging analytcal dream team in the life sciences. *J. Anal. At. Spectrom.*, 19 (2004), 20-25.

59 Schlag, E. W. *Time-of-Flight mass spectrometry and its application*. Elsevier science , NewYork, USA, 1994.

60 Dawson, P. H. *Quadrupole mass spectrometry and its applications*. Elsevier, NewJersey,USA, 1976.

61 Sugiyama, N. and Shikamori, Y. Removal of spectral interferences on noble metal elements using MS/MS reaction cell mode of a triple quadrupole ICP-MS . *J. Anal. At. Spectrom.*, 30 (2015), 2481-2487.

62 Balcean, L., Woods, G., Resano, M., and Vanhaecle, F. Accurate determination of S in organic materices using isotope dilution ICP-MS/MS. *J. Anal. At. Spectrom.*, 28 (2013), 33-39.

63 Bandura, D. R., Baranov, V. I., and Tanner, S. D. Detection of ultratrace phosphorous and sulfur by quadrupole ICPMS with dynamic reaction cell. *Anal. Chem.*, 74 (2002), 1497-1502.

64 Bantscheff, M., Schirle, M., Sweetman, G., Rick, J., and Kuster, B. Qunatitative mass spectrometry in proteomics: a critical review. *Anal. Bioanal. Chem.*, 389 (2007), 1017-1031.

65 Aebersold, R. and Mann, M. Mass spectrometry- based proteomics. *Nature*, 422 (2003), 198-207.

66 Prange, A. and Profrock, D. Chemical labels and natural element tags for the quantitative analysis of bio-molecules. *J. Anal. At. Spectrom.*, 23 (2008), 432-459.

67 Mirgorodskaya, O. A., Kozmin, Y. P., Titov, M. I., Korner, R., Sonksen, C. P., and Roepstroff, P. Quantification of peptides and proteins by matrix-laser desorption/ionization mass spectrometry using (18) O-labeled internal standards. *Rapid*

Commin. Mass Spectrom., 14 (2000), 1226-1232.

68 Szpunar, J., Lobinski, R., and Prange, A. Hyphenated techniques for elemental speciation in biological systems. *Appl. Spectrosc.*, 57 (2003), 102A-112A.

69 Searle, P. F., Davison, B. L., Stuart, G. W., Wikie, T. M., Norstedt, G., and Palmiter, R. D. Regulation, linkage, and sequence of mouse metallothionein I and II genes. *Mol. Cell Biol.*, 4 (1984), 1221-30.

70 Blume-Jensen, P. and Hunter, T. Oncogenic kinase signalling. *Nature*, 411 (2001), 355-365.

71 Janek, K., Wenschuh, H., Bienert, M., and Krause, E. Phosphopeptide analysis by positive and negative ion matrix-assisted laser desorption/ionization mass spectrometry. *Rapid Commun.*, 15 (2001), 1593-1599.

72 Lee, K. A., Craven, K. B., Niemi, G. A., and Hurley, J. B. Mass spectrometric analysis of the kinetics of in vivo rhodopsin phosphorylation. *Protein Science.*, 11 (2002), 862-874.

73 Navaza, P., Encinar, J. R., Carrascal, M., Abian, J., and Sanz-Medel, A. Absolute and site-specific quantification of protein phosphorylation using integrated elemental and molecular mass spectrometry: its potential to assess phosphopeptide enrichment procedures. *Anal. Chem.*, 80 (2008), 1777-1787.

74 Wind, M., Edler, M., Jakubowski, N., Linscheid, M., Wesch, H., and Lehmann, W. D. Analysis of protein phosphorylation by capillary liquid chromatography coupled to element mass spectrometry with 31P detection and to electrospray mass spectrometry. *proteomics.*, 73 (2001), 29-35.

75 Wind, M., Wegener, A., Eisenmenger, A., Kellner, R., and Lehmann, W. D. Sulfur as the key element for quantitative protein analysis by capillary liquid chromatography coupled to element mass spectrometry. *Angew. Chem. Int. Ed.*, 42 (2003), 34256-3427.

76 Brigelius-Floche, R., Banning, A., and Schnurr, K. Selenium-dependent enzymes in endothelial cell function. *Antioxid. Redox Signal.*, 5 (2003), 205-215.

77 Gartner, R., Gasnier, B. C., Dietrich, J. W., Krebs, B., and Angstwurm, M. W. Selenium supplementation in patients with autoimmune thyroiditis decreases thyroid peroxidase antibodies concentrations. *Metab.*, 87 (2002), 1687-1691.

78 Chitta, K. R., Landero-Figueroa, J. A., Kodali, P., Caruso, J. A., and Merino, E. J. Identification of selenium-containing proteins in HEK 293 kidney cells using multiple chromatographies, LC-ICPMS and nano-LC-ESIMS. *Talanta.*, 114 (2013), 25-31.

79 Anan, Y., Nakajima, G., and Ogra, Y. Complementary Use of LC-ICP-MS and LC-ESI-Q-TOF-MS for Selenium Speciation. *Anal. Sci.*, 31 (2015), 561-564.

80 Kápolna, E., Hillestrøm, P. R., Laursen, K. H., Husted, S., and Larsen, E. H. Effect of foliar application of selenium on its uptake and speciation in carrot. *Food Chemistry* , 115 (2009), 1357-1363.

81 Aureli, F., Querdane, L., Bierla, K., Szpunar, J., Prakash, N. T., and Cubadda, F. Identification of selenosugars and other low-molecular weight selenium metabolites in high-selenium cereal crops. *Metallomics*, 4 (2012), 968-978.

82 Ouerdane, L., Aureli, F., Flis, P., Bierla, K., Preud'homme, H., Cubadda, F., and Szpunar, J. Comprehensive speciation of low-molecular weight selenium metabolites in mustard seeds using HPLC - electrospray linear trap/orbitrap tandem mass spectrometry. *Metallomics*, 5 (2013), 1294-1304.

83 Prange, A. and Schaumlöffel, D. Hyphenated techniques for the characterization and quantification of metallothionein isoforms. *Anal. Bioanal. Chem.*, 373 (2002), 441-53.

84 Coufalíková, K., Benešová, I., Vaculovič, T., Kanický, V., and Preisler, J. LC coupled to ESI, MALDI and ICP MS - A multiple hyphenation for metalloproteomic studies. *Analytica Chimica Acta.*, 968 (2017), 58-65.

85 Nischwitz, V., Michalke, B., and Kettrup, A. Identification and quantification of metallothionein isoforms and superoxide dismutase in spiked liver extracts using HPLC-ESI-MS offline coupling and HPLC-ICP-MS online coupling. *Anal. Bioanal. Chem.*, 375 (2003), 145-456.

86 Infante, H. G., Cuyckens, F., Campenhout, K. V., Blust, R., Claeys, M., Vaeck, L. V., and Adams, F. C. Characterization of metal complexes with metallothioneins in the liver of the carp Cyprinus carpio by reversed-phase HPLC with ICP-MS and electrospray ionization (ESI)-MS. *J. Anal. At. Spectrum.*, 19 (2004), 159-166.

87 Guo, Y., Xu, M., Yang, L., and Wang, Q. Strategy for absolute quantification of proteins: CH3Hg+labeling integrated molecular and elemental mass spectrometry. *J. Anal. At. Spectrom.*, 24 (2009), 1184-1187.

88 Espina, J. G., Montes-Bayón, M., Blanco-González, E., and Sanz-Medel, A. Determination of Reduced Homocysteine in Human Serum by Elemental Labelling and Liquid Chromatography With ICP-MS and ESI-MS Detection. *Anal. Bioanal. Chem.*, 407 (2015), 7899-7906.

89 Camp, C. L., Moustafa, E. M., Reid, H. J., Sharp, B. L., and Shoeib, T. An ICP-MS, ESI-MS and molecular modelling investigation of homogeneous gallium affinity tagging

(HMAT) of phosphopeptides. *Int. J. Mass Spectrom.*, 18-27 (2013), 341-342.

90 Krüger, R., Braun, K., Pipkornc, R., and Lehmann, W. D. Characterization of a gadolinium-tagged modular contrast agent by element and molecular mass spectrometry. *J. Anal. At. Spectrom.*, 19 (2004), 852-857.

91 Yan, X., Li, Z., Liang, Y., Yang, L., Zhang, B., and Wang, Q. A chemical "hub" for absolute quantification of a targeted protein: orthogonal integration of elemental and molecular mass spectrometry. *Chem. Commun.*, 50 (2014), 6578-6581.

92 He, Y., Esteban- Fernández, D., and Linscheid, M. W. Novel approach for labeling of biopolymers with DOTA complexes using in situ click chemistry for quantification. *Talanta.*, 136 (2016), 68-76.

93 He, Y., Esteban- Fernández, D., Neumann, B., Bergmann, U., Bierkandt, F., and Linscheid, M. w. Application of MeCAT-Click labeling for protein abundance characterization of E. coli after heat shock experiments. *J. Proteomics*, 136 (2016), 68-76.

94 Vančo, J., Trávníček, Z., Kozák, O., and Boča, R. Structural, Magnetic and Luminescent Properties of Lanthanide. *Int. J. Mol. Sci.*, 16 (2015), 9520-9539.

95 Bergmann, U., Ahrends, R., Neumann, B., Scheler, C., and Linscheid, M. W. Application of Metal-Coded Affinity Tags (MeCAT): Absolute Protein Quantification With Top-Down and Bottom-Up Workflows by Metal-Coded Tagging. *Anal. Chem.*, 84 (2012), 5268-5275.

96 Schwarz, G., Mueller, L., Beck, S., and Linscheid, M. W. DOTA based metal labels for peotein quantification: a review. *J. Anal. At. Spectrom.*, 29 (2014), 221-233.

97 El-khatib, A. H., Esteban-Fernández, D., and Linscheid, M. W. Inductively Coupled Plasma Mass Spectrometry-Based Method for the Specific Quantification of Sulfenic Acid in Peptides and Proteins. *Anal. Chem.*, 86 (2014), 1943-1948.

98 Vuojola, J. and Soukka, T. Luminescent lanthanide reporters: new concepts for use in bioanalytical applications. *Methods Appl. Fluoresc.*, 2 (2014), 1-28.

99 Viola-Villegas, N., Rabideau, A. E., Bartholoma, M., Zubieta, J., and Doyle, R. P. Targeting the cubilin receptor through the vitamin B(12) uptake pathway:cytotoxicity and mechanistic insight through flourescent Re(I) delivery. *J. Med. Chem.*, 52 (2009), 5253-5261.

100 Alonso, J. and Gonzalez, P. Isotope dilution mass spectrometry. RSC publications,

Cambridge , 2013.

101 Calvete, J. J., Petras, D., Calderón-Celis, F., Lomonte, B., Encinar, J. R., and Sanz-Medel, A. Protein-species quantitative venomics: looking through a crystal ball. *Journal of Venomous Animals and Toxins including Tropical Diseases*, 23 (2017), 1-9.

102 Wang, M., Feng, W., Lu, W. et al. Quantitative analysis of proteins via sulfur determination by HPLC coupled to isotope dilution ICP-MS with a Hexapole collision cell. *Anal. Chem.*, 79 (2007), 9128-9134.

103 Giusti, P., Schaumloeffel, D., Ruiz Encinar, J., and Szpunar, J. Interfacing reversed phase nanoHPLC with ICP-MS and On-line isotope dilution analysis for the accurate quantification of selenuim--containing peptides in protein tryptic digests. *J. Anal. At. Spectrom.*, 20 (2005), 1101-1107.

104 Kretschy, D., Koellensperger, G., and Hann, S. Elemental labelling combined with liquid chromatography inductively coupled plasma mass spectrometry for quantification of biomolecules. A review. *Anal. Chim. Acta.*, 750 (2012), 98-100.

105 Qian, J., Wani, R., Klomsiri, C., Poole, L. B., Tsang, A. W., and Furdui, C. M. A simple and effective strategy for labeling cysteine sulfenic acid in proteins by utilization of ß-Ketoesters as cleavable probes. *Chemm. Commun.*, 48 (2012), 4091-4093.

106 Yadav, J. S., Reddy, B.V. S., Krishna, A. D., Suresh Reddy, Ch., and Narsaiah, A. V. Triphenylphosphine: An efficient catalyst for transesterification of β -Ketoesters. *J. Mol. Cata. A: Chem.*, 261 (2007), 93-97.

107 Hong, V., Presolski, S. I., Ma, C., and Finn, M. G. Analysis and optimization of copper-catalyzed azide- alkyne cycloaddition for bio-conjugation. *Angew. Chem. Int. Ed. Engl.*, 48 (2009), 9879-9883.

108 Presolski, S. I., Phong Hong, V., and Finn, M. G. Copper- catalyzed azide- alkyne click chemistry for bioconjugation. *Curr. Protoc. Chem. Biol.*, 3 (2011), 153-162.

109 Fassett, J. D. and Paulsen, P. J. Isotope dilution mass spectrometry for accurate elemental analysis. *Anal. Chem.*, 61 (1989), 643A-649A.

110 Gupta, V. and Carroll, K. S. Sulfenic acid chemistry, detection and cellular lifetime. *Biochimica et Biophysica Acta.*, 1840 (2014), 847-875.

111 Esteban-Fernández, D., Scheler, C., and Linscheid, M. W. Absolute protein quantification by LC-ICP-MS using MeCAT peptide labeling. *Anal Bioanal Chem.*, 401 (2011), 657-666.

112 Housecroft, C. and Sharpe, A. G. *Inorganic chemistry*. Prentice hall , NewJersey,USA, 2004.

113 Drahos, B., Kubicek, V., Bonnet, C., Hermann, P., Lukes, I., and Tóth, E. Dissociation kinetics of Mn2+ complexes of NOTA and DOTA. *Dalton Trans.*, 40 (2011), 1945-51.

114 Huisgen, R. 1,3-Dipolar cycloadditions. Past and future. *Angew Chem Int Ed Engl.*, 2 (1963), 565-598.

115 Wang, Q., Chan, T. R., Hilgraf, R., Fokin, V. V., Sharpless, K. B., and Finn, M. G. Bioconjugation by copper(I)-catalyzed azide-alkyne [3+2] cycloaddition. *J. Am. Chem. Soc.*, 125 (2003), 3192-3.

116 Hong, V., Udit, A. K., Evans, R. A., and Finn, M. G. Electrochemically protected copper(II)-catalyzed azide-alkyne cysloaddition. *Chembiochem.*, 9 (2008), 1481-6.

117 Liu, P. Y., Jiang, N., Zhang, J., Wei, X., Lin, H. H., and Yu, X. Q. The oxidative damage of plasmid DNA by ascorbic acid derivatives in vitro:the first research on the relationship between the structure of ascorbic acid and the oxidative damage of plasmid DNA. *Chem Biodivers.*, 3 (2006), 958-67.

118 Carr, S. A. and Biemann, K. Identification of posttranslationally modified amino acids in proteins by mass spectrometry. *Methods Enzymol.*, 106 (1984), 29-58.

119 McKenzie, H. A. and Sawyer, W. H. *B-Lactoglobulins. In Milk proteins: Chemistry and molecular biology*. Academic press, NewYork,USA, 1971.

120 Tanford, C., Bunnville, L. G., and Nozaki, Y. The reversible transformation of B-lactoglobulin at pH 7.5. *J. Am. Chem. Soc.*, 81 (1959), 4032-4036.

121 Alvarez, B. and Carballal, L. Formation and Reactions of Sulfenic Acid in Human Serum Albumin. *Methods Enzymol.*, 473 (2010), 117-136.

122 Fernández, S. D., Sugishama, N., Encinar, J. R., and Sanz-Medel, A. Triple Quad ICPMS (ICPQQQ) as a New Tool for Absolute Quantitative Proteomics and Phosphoproteomics. *Anal. Chem.*, 84 (2012), 5851-5857.

123 Aguilar, M. I. and Hearn, M.T. W. High resolution reversed phase high performance liquid chromatography of peptides and proteins. *Meth. Enzymol.*, 270 (1996), 3-26.

124 Arseneault, M., Wafer, C., and Morin, J.- F. Recent Advances in Click Chemistry Applied to Dendrimer Synthesis. *Molecules.*, 20 (2015), 9263-9294.

7. Abbreviations

BLG	ß-Lactoglobulin
CuAAC	Copper-(I)-catalyzed azide-alkyne cycloaddition
DOTA	1,4,7,10-tetraazacyclododecane-*N,N′,N″,N‴*-tetraacetic acid
EIC	Extracted ion chromatogram
ESI	Electrospray ionization
FIA	Flow injection analysis
HPLC	High performance liquid chromatography
HSA	Human serum albumin
IA	Iodoacetamide
ICP	Inductively coupled plasma
IDA	Isotopic dilution analysis
KE	Alkyne ß-keto ester
LC	Liquid chromatography
Ln	Lanthanides
LOD	Limit of detection
MeCAT	Metal- coded affinity tag
MS	Mass spectrometry
NHS	*N*- hydroxysuccinimide
PTMs	Post- translational modifications
Q	Quadrupole
RP-HPLC	Reversedphase liquid chromatography
SA	Sulfenic acid
SDS-PAGE	Sodium dodecyl sulphate polyacrylamide gel electrophoresis
TCEP	Tris (2- carboxyethyl)-phosphine
TEAA	Triethylammonium acetate
TOF	Time of flight

Appendix

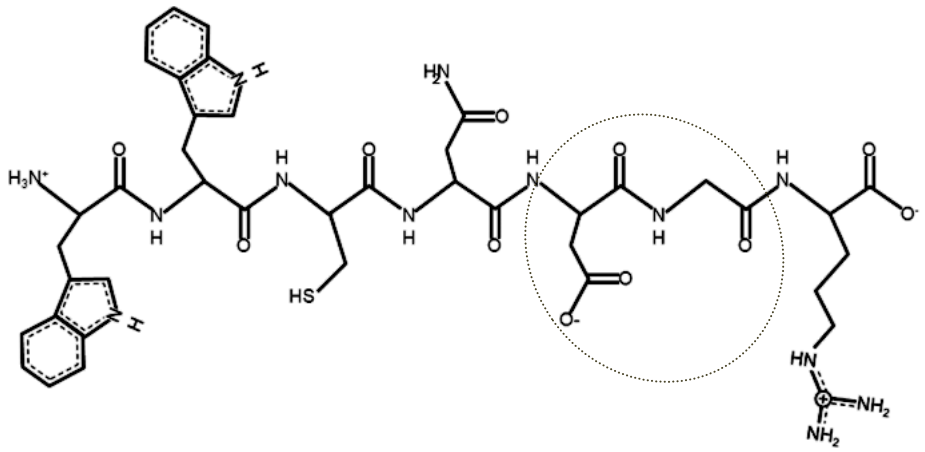

Figure 1: Structure of peptide sequence WWCNDGR .Iso-aspartate can be formed due to the presence of aspartic acid (D) and glycine(G) (pointed out witch a circle).

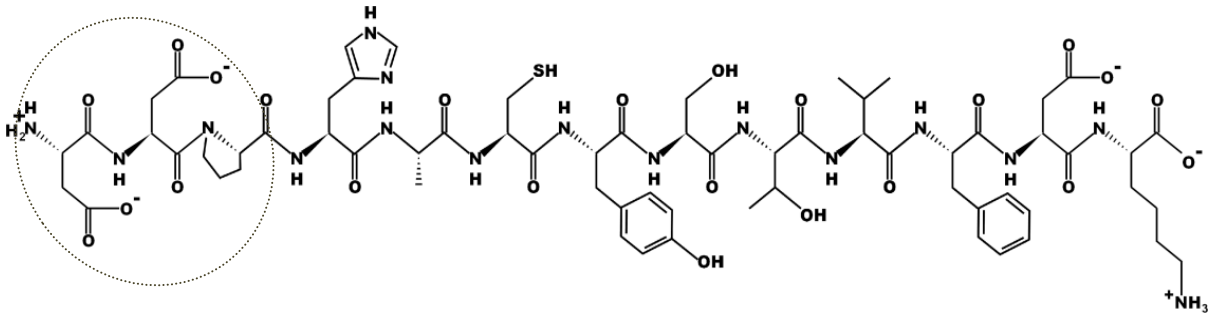

Figure 2: Structure of peptide sequence DDPHACYSTVFDK. Loss of aspartic acid units (pointed out witch a circle) was observed.

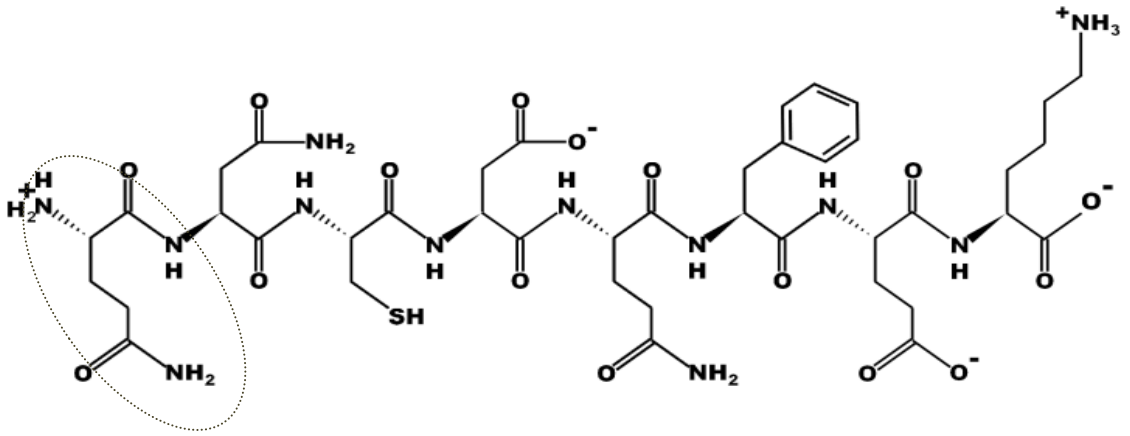

Figure3: Structure of peptide sequence QNCDQFEK . N- terminal glutamine residue (pointed out with a circle) can readily cyclize to the pyroglutamyl derivative.

```
  10         20         30         40         50
MKCLLLALAL TCGAQALIVT QTMKGLDIQK VAGTWYSLAM AASDISLLDA
        60         70         80         90        100
QSAPLRVYVE ELKPTPEGDL EILLQKWENG ECAQKKIIAE KTKIPAVFKI
       110        120        130        140        150
DALNENKVLV LDTDYKKYLL FCMENSAEPE QSLACQCLVR TPEVDDEALE
       160        170
KFDKALKALP MHIRLSFNPT QLEEQCHI
```

Figure 4: ß-lactoglobulinsingle chain of 162 amino acids. ß-lactoglobulincomprises 5 cysteines where 4 disulfide bridges are formed and one free cysteine is left (cys-121). Source: UniProt, ß-lactoglobulin, Bostaurus P02754. PTM processing 17-178 position.

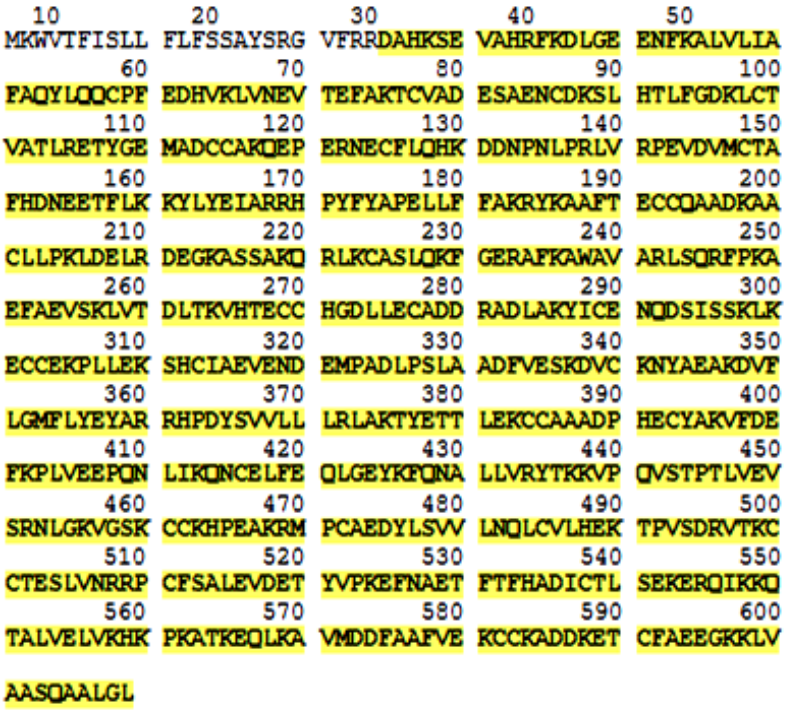

Figure 5: Human serum albumin (HSA) single chain of 585 amino acids. HSAcomprises 35 cysteines where 17 disulfide bridges are formed and one free cysteine is left (cys-34). Source: UniProt, Serum albumin, Homo sapiens P02768. PTM processing 25-609 position.

Konferenzbeiträge und **Vorträge**

Mona Sharar, Maria Montes- Bayón, Michael W. Linscheid, *Elemental labelling and mass spectrometry for the specific detection of sulfenic acid groups in model peptides and proteins*, Metallomics 2017: The 6th international symposium on Metallomics, University of Vienna, Austria (August/ 2017), Oral presentation.

Publikationsliste

Sharar M., Saied E.M., Rodriguez M.C., Arenz C., Montes- Bayón M., Linscheid M.W., Elemental labelling and mass spectrometry for the specific detection of sulfenic acid groups in model peptides: a proof of concept. ***Anal.Bioanal. Chem***. 2017, 409, 8, 2015-2027.

Sharar M., Rodriguez-SoIIa H., Linscheid M.W., Montes- Bayón M., Detection of sulfenic acid in intact proteins by Mass Spectrometric techniques: application to serum samples. ***RCS Advances***. 2017,7,44162-44168.

Montes- Bayón M., **Sharar M.**, Rodriguez M.C., Trends on (Elemental and Molecular) Mass Spectrometry based strategies for Speciation and Metallomics.***TrAC, Trends Anal. Chem.*** https://doi.org/10.1016/j.trac.2017.09.025.